4

Laboratory for Manufacturing and Productivity

School of Engineering

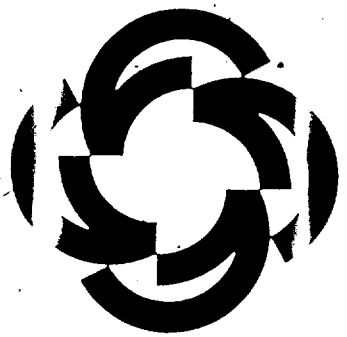

Massachusetts Institute of Technology

(4)

THE TRIBOLOGY OF UNDULATED SURFACES

(ONR Contract No. N00014-86-K-0269)

by

N. Saka, H. Tian, S. T. Oktay and D. E. Kim

May 1989

Unclassified
SECURITY CLASSIFICATION OF THIS PAGE

REPORT DOCUMENTATION PAGE

1a. REPORT SECURITY CLASSIFICATION: Unclassified	1b RESTRICTIVE MARKINGS: None
2a. SECURITY CLASSIFICATION AUTHORITY: ------	3 DISTRIBUTION / AVAILABILITY OF REPORT: Unlimited
2b. DECLASSIFICATION / DOWNGRADING SCHEDULE:	
4 PERFORMING ORGANIZATION REPORT NUMBER(S): -----	5. MONITORING ORGANIZATION REPORT NUMBER(S): -----
6a. NAME OF PERFORMING ORGANIZATION: Massachusetts Institute of Technology; 6b. OFFICE SYMBOL (If applicable): --	7a. NAME OF MONITORING ORGANIZATION: Office of Naval Research
6c. ADDRESS (City, State, and ZIP Code): 77 Massachusetts Avenue, Cambridge, MA 02139	7b ADDRESS (City, State, and ZIP Code): 800 North Quincy Street, Arlington, VA 22217-5000
8a. NAME OF FUNDING / SPONSORING ORGANIZATION: Office of Naval Research; 8b. OFFICE SYMBOL (If applicable): ---	9. PROCUREMENT INSTRUMENT IDENTIFICATION NUMBER: ---
8c. ADDRESS (City, State, and ZIP Code): 800 North Quincy Street, Arlington, VA 22217-5000	10. SOURCE OF FUNDING NUMBERS

PROGRAM ELEMENT NO.	PROJECT NO.	TASK NO.	WORK UNIT ACCESSION NO
N00014	-86-K-	0269	4316008

11. TITLE (Include Security Classification)

Tribology Undulated Surfaces

12. PERSONAL AUTHOR(S) Nannaji Saka, Hong Tian, Turker Oktay and Dae Eun Kim

13a. TYPE OF REPORT	13b. TIME COVERED	14. DATE OF REPORT (Year, Month, Day)	15. PAGE COUNT
Final	FROM 2/1/86 TO 1/31/89	5/30/89	120

16. SUPPLEMENTARY NOTATION ------

17. COSATI CODES			18. SUBJECT TERMS (Continue on reverse if necessary and identify by block number)
FIELD	GROUP	SUB-GROUP	

19. ABSTRACT (Continue on reverse if necessary and identify by block number)

The objective of this research has been to investigate the friction, wear and lubrication characteristics of undulating metallic surfaces. Both dry and lubricated sliding experiments have been conducted to evaluate the tribological behavior of metallic surfaces. In addition, analytical studies have been carried out on the friction and wear behavior of the undulated surfaces, and practical applications of the undulated surfaces have also been explored.

20. DISTRIBUTION / AVAILABILITY OF ABSTRACT	21. ABSTRACT SECURITY CLASSIFICATION
☒ UNCLASSIFIED/UNLIMITED ☐ SAME AS RPT ☐ DTIC USERS	Unclassified

22a. NAME OF RESPONSIBLE INDIVIDUAL	22b. TELEPHONE (Include Area Code)	22c. OFFICE SYMBOL
Dr. Nannaji Saka	(617) 253-2227	

DD FORM 1473, 84 MAR — 83 APR edition may be used until exhausted. All other editions are obsolete.

SECURITY CLASSIFICATION OF THIS PAGE
Unclassified

TRIBOLOGY OF UNDULATED SURFACES

Final Technical Report to
The Office of Naval Research

Contract No. N00014-86-K-0269

Nannaji Saka
Hong Tian
S. Turker Oktay
Dae Eun Kim

Tribology Research Program
Laboratory for Manufacturing and Productivity
School of Engineering
Massachusetts Institute of Technology
Cambridge, MA 02139

May 1989

Table of Contents

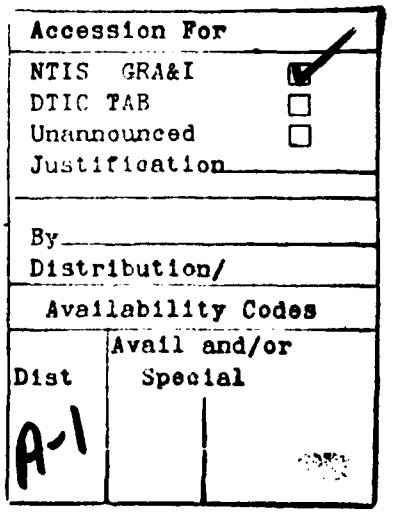

BOUNDARY LUBRICATION STUDIES ON UNDULATED TITANIUM SURFACES

SUMMARY

It is customary in tribological research, and especially in practice, to employ smooth surfaces, for it is generally believed that smooth surfaces should have low sliding friction. However the wear particles produced during sliding get trapped at the interfaces, and plowing by the wear particles becomes the principal mechanism of friction. Through experimental and theoretical investigations, it is shown that the plowing friction component can be substantially reduced by means of surface undulations. Steel-titanium and titanium-titanium pairs were tested to investigate the role of surface undulations in boundary lubricated sliding. Compared with the experimental results of flat titanium surfaces, friction coefficient and wear rate were considerably reduced with the undulated titanium surfaces, especially when lubricants considered ineffective for titanium were used. In addition, the effects of pad width and cavity volume fraction of the undulated surface were also investigated. A plowing model proposed for boundary lubricated sliding is in good agreement with experimental results. It is suggested, furthermore, that the undulated surfaces provide an effective means of investigating many important effects of lubricants which are masked by the wear particles.

I. INTRODUCTION

One of the earliest models of friction in boundary lubricated sliding is that of Bowden et al. [1, 2]. In this model, friction between lubricated sliding surfaces is attributed to adhesion at solid-to-solid contacts, and to shearing of the lubricant film wherever a thin film separates the contacting asperities. As a result, the early boundary lubrication research focused primarily on the physico-chemical properties of lubricant films, physisorption and chemisorption, and a variety of tribochemical reactions which occur on sliding surfaces [3, 4]. On the basis of the above model, attempts have also been made to create adsorbed layers, soft and hard films on sliding surfaces by incorporating appropriate additives in lubricants. Boundary lubrication with various anti-wear additives has been recently reviewd by Kapsa et al. [5].

Surprisingly, however, plowing by wear particles during sliding, an important factor in the genesis of friction, has been essentially ignored until recently. It has become increasingly apparent in recent years that plowing plays a dominant role in both dry and lubricated sliding. For example, Suh and Sin [6] have proposed that the friction coefficient in dry sliding is comprised of three components: adhesion, asperity deformation, and plowing by wear particles entrapped between sliding surfaces and by hard asperities. Furthermore, plowing was shown to be the dominant mechanism of friction in dry sliding. Following that proposition, undulated surfaces with cavities to trap wear particles have been successfully used to essentially eliminate plowing in dry sliding [7, 8]. More recently, Komvopoulos et al. [9] have investigated the primary friction mechanisms in boundary lubricated sliding and they too have confirmed that plowing is the key mechanism of friction, while adhesion between asperities and shearing of lubricant films are generally of secondary importance.

The purpose of this investigation is to examine the mechanisms of friction and the effect of surface undulations on plowing in boundary lubricated sliding. Titanium was chosen for investigation, for it is generally hard to lubricate. Rabinowicz [10] has shown, for example, that the common liquid lubricants are essentially ineffective for titanium, and that only a few lubricants, such as halogenated hydrocarbon oil 11-14 and methylene iodide, are effective. In this investigation, the undulated surfaces are used to eliminate, or at least minimize, the plowing component of friction so that titanium can be effectively lubricated even with the common lubricants.

II. EXPERIMENTAL

A. Materials and Lubricants

Commercially pure titanium (99.99%) disks with flat and undulated surfaces, and flat pins (6.35 mm in diameter) of AISI 52100 steel and titanium were used for study. Several kinds of lubricants were investigated. They include mineral oil, a long-chain fatty acid (oleic acid), jet engine oil (turbo oil Mil-1-23699c), and a synthetic long-chain compound (silicone oil). In addition, halogenated hydrocarbons (halocarbon oil 11-14 and methylene iodide), the well-known lubricants for titanium, were also tested. The experimental materials and the lubricants are listed in Table 1.

B. Preparation of the Undulated Surfaces

In an earlier study on the Oxygen Free High Conductivity (OFHC) copper [8], the undulated surfaces were produced by lithography and electrochemical etching processes. Although this technique provides finer resolution and smaller undulations, it is not well-suited for many engineering materials. In the present investigation, the undulated surfaces were prepared by machining (at a moderate cutting speed) with a shaper, using high-speed steel cutting tools and a lubricant. Machining debris and burrs were removed by lightly abrading the machined surfaces on silicon carbide abrasive papers followed by polishing with 0.3 μm alumina suspension in water. The pins were also polished with 0.3 μm alumina. The undulated surface is characterized by the parameters shown in Figure 1. The pad width of the undulated surfaces, a, was 20-550 μm, the depth of the undulations was 50-800 μm, and the distance between the pads, c, was 80-1000 μm.

C. Apparatus and Experimental Procedures

The experimental setup is shown schematically in Figure 2. The titanium disks were mounted on a small cart which was driven back and forth at a speed of 1.1 cm/s by an electric motor. The stroke length was about 30 mm and the normal load was 5 N. The pin was held stationary in a holder which was attached to a strain ring. The friction force was measured by the strain gages mouned on the strain ring and was recorded continuously. The lubricant was kept in an aluminum container. The disks and the pins were cleaned by isopropyl alcohol and by acetone, and dried before experiments. After the tests, the specimens were cleaned with acetone in an ultrasonic cleaner for a few minutes and then observed in optical and scanning electron microscopes. The wear volume of flat titanium surfaces were calculated from the profiles of the wear tracks, and the wear volume of the undulated titanium surfaces was calculated by comparing the pad widths before and after tests. All tests were conducted at room temperature in a laboratory environment.

Table 1. Experimental materials and lubricants

Material		Hardness (MPa)
Titanium (99.99%)		2352± 90
AISI 52100 steel		7957± 112
Lubricant	**Type or formula**	**Viscosity (cSt @310 K)**
Mineral oil	Naphthenic hydrocarbon	74
Oleic acid	$C_{18}H_{34}O_2$	--
Turbo oil	Mil-L-23699c	25
Silicone oil	DC550	45
Halogenated hydrocarbon	Series 11-14	--
Methylene iodide	CH_2I_2	--

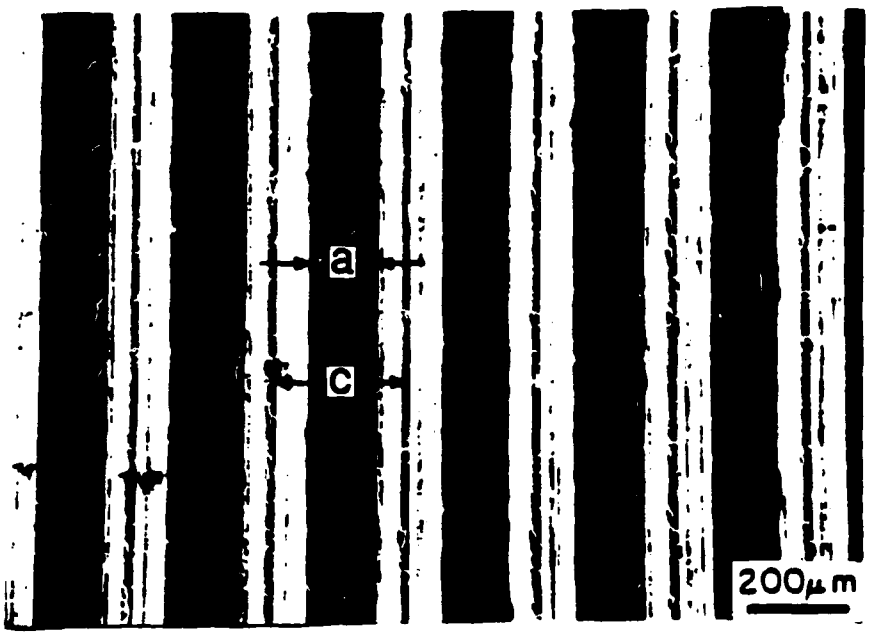

Figure 1. Micrographic illustration of the undulated surface
a: 15 μm -- 700μm
c: 0.15 mm -- 1 mm

a. load
b. strain gages
c. pin
d. disk specimen
e. container
f. motor
g. lubricant
h. bearings
i. flexible plate
j. counter weight

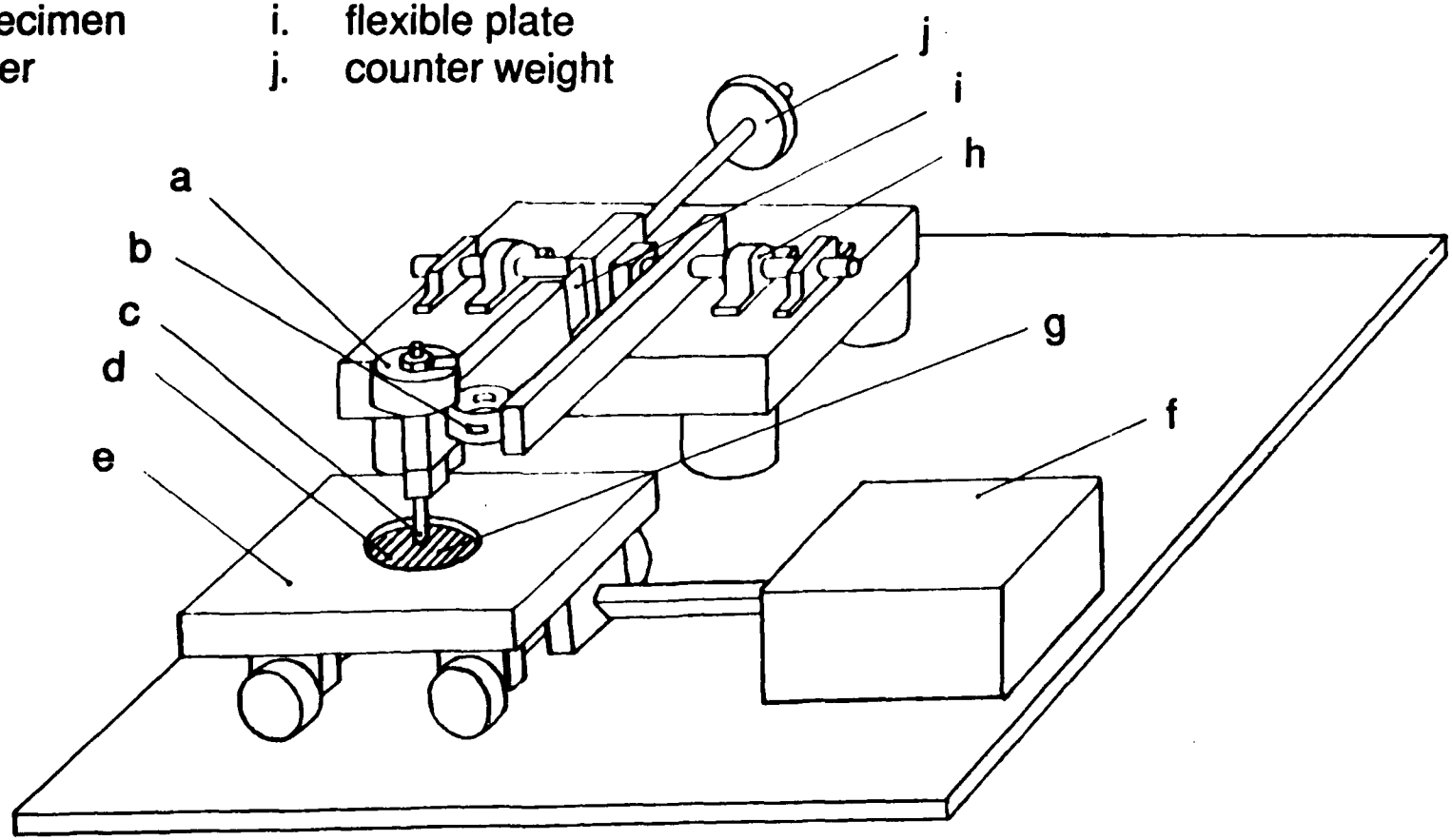

Figure 2. Experimental apparatus

III. RESULTS

A. AISI 52100 Steel on Titanium

Friction coefficients of the AISI 52100 steel pins slid on titanium disks with different lubricants are shown in Figure 3. By comparing the friction coefficients of the undulated titanium surfaces with those of the flat titanium surfaces, the substantial reduction in friction is apparent even with marginal lubricants. It is important to note, however, that the extent of reduction in friction coefficient was different for different lubricants (mineral oil: from 0.60 to 0.38, oleic acid: from 0.48 to 0.12, silicone oil: from 0.47 to 0.24 and turbo oil: from 0.47 to 0.17). It is also interesting to note that the undulated surface had little effect on the friction coefficient when halocarbon oil 11-14 and methylene iodide were used.

Reduction in friction was accompanied by reduction in wear in many cases. Table 2 lists the wear values of flat and undulated titanium disks. The wear of the AISI 52100 steel pins was negligible, and the wear rates and the wear coefficients of the titanium disks were reduced by an order of magnitude when the undulated surfaces were used.

B. Titanium on Titanium

Although mineral oil, oleic acid, turbo oil and silicone oil are ineffective for lubricating titanium, they are generally found to be good for steels. Therefore titanium-on-titanium tests were conducted to further emphasize the effect of the undulated surfaces in reducing friction. Again, the same lubricants were tested and the results are summarized in Table 3. It is evident that low friction coefficients can be obtained in boundary lubrication of undulated titanium surfaces even when the so-called poor lubricants (for titanium) are used.

C. Effects of Undulation geometry

Figure 4 shows that large wear particles have formed deep and wide plowing grooves on the flat titanium surfaces with different lubricants. The micrographs in Figure 5 depict the effect of pad width of the undulated surfaces in reducing plowing. With large pads, some wear particles still stayed on the surface and formed plowing grooves (Figure 5a), and the corresponding friction coefficient was 0.45. By contrast, with small pads wear particle were very small and were trapped in the cavities. The plowing grooves were correspondingly finer (Figure 5d), and the friction coefficient was 0.38. In general, the friction coefficient decreased as the pad width decreased (Figure 6).

Profiles of the flat and undulated worn surfaces are shown in Figure 7. In the case of flat surfaces, the width and depth of plowing grooves were 20-60 μm and 5-15 μm, respectively. Profiles of the wear tracks on the undulated surfaces show that the width and depth of plowing grooves were significantly reduced (width: 2-10 μm, depth: 0.5-2 μm). Smaller pad widths resulted in finer plowing grooves (Figure 7c).

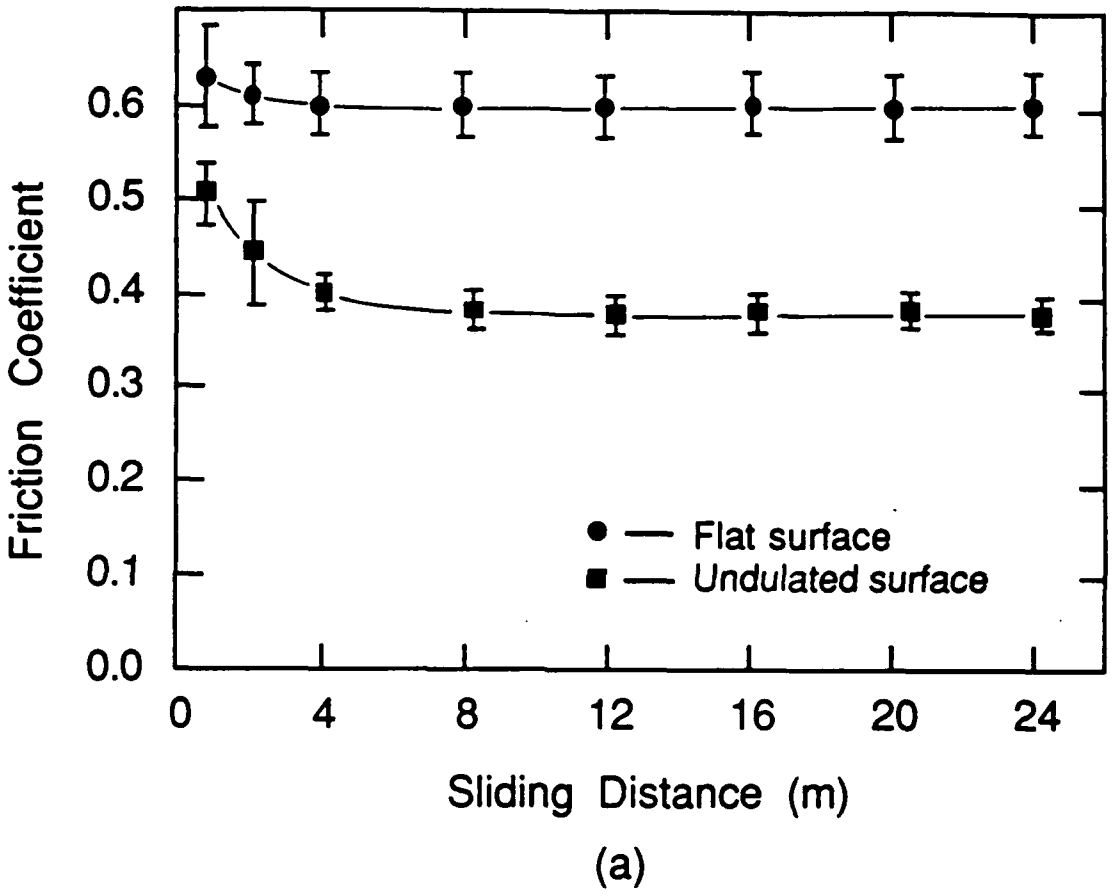

Fig. 3 Friction coefficients of AISI 52100 steel on flat and undulated titanium surfaces with various lubricants: (a) mineral oil

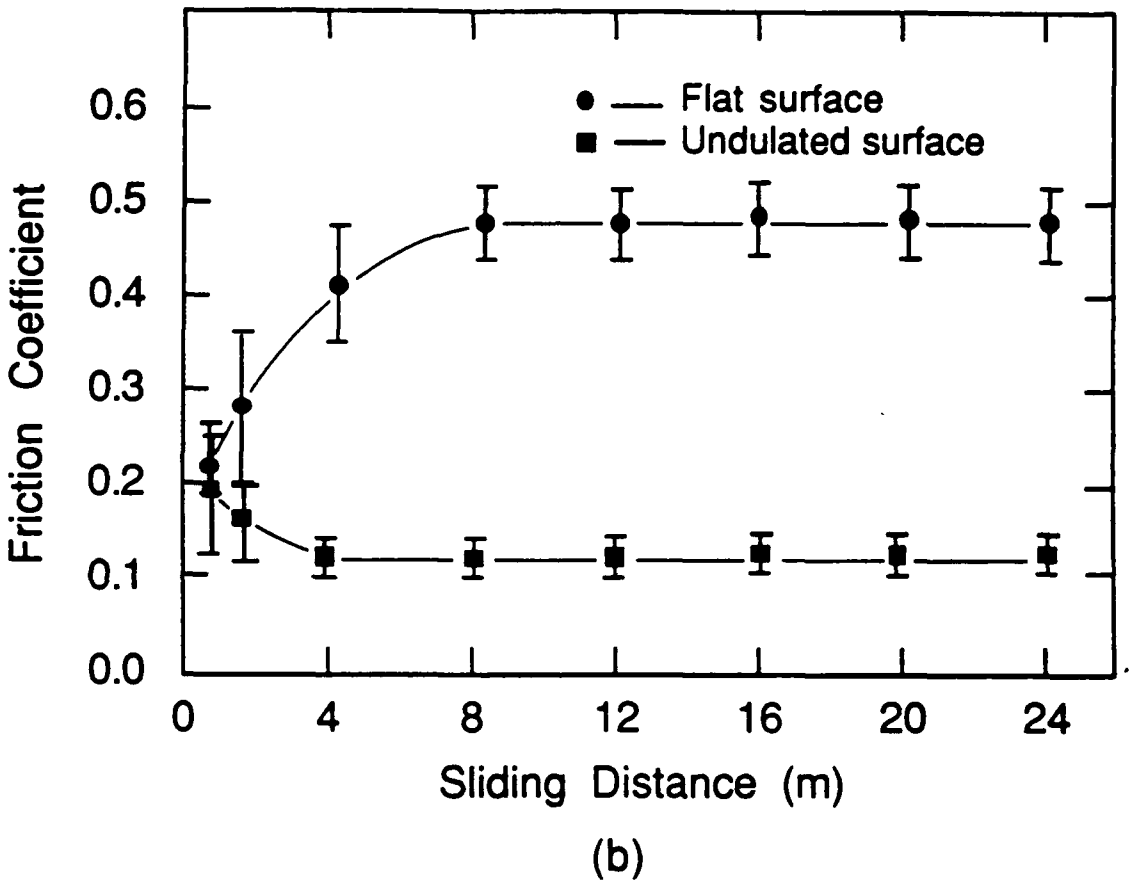

Fig. 3 Friction coefficients of AISI 52100 steel on flat and undulated titanium surfaces with various lubricants: (b) oleic acid

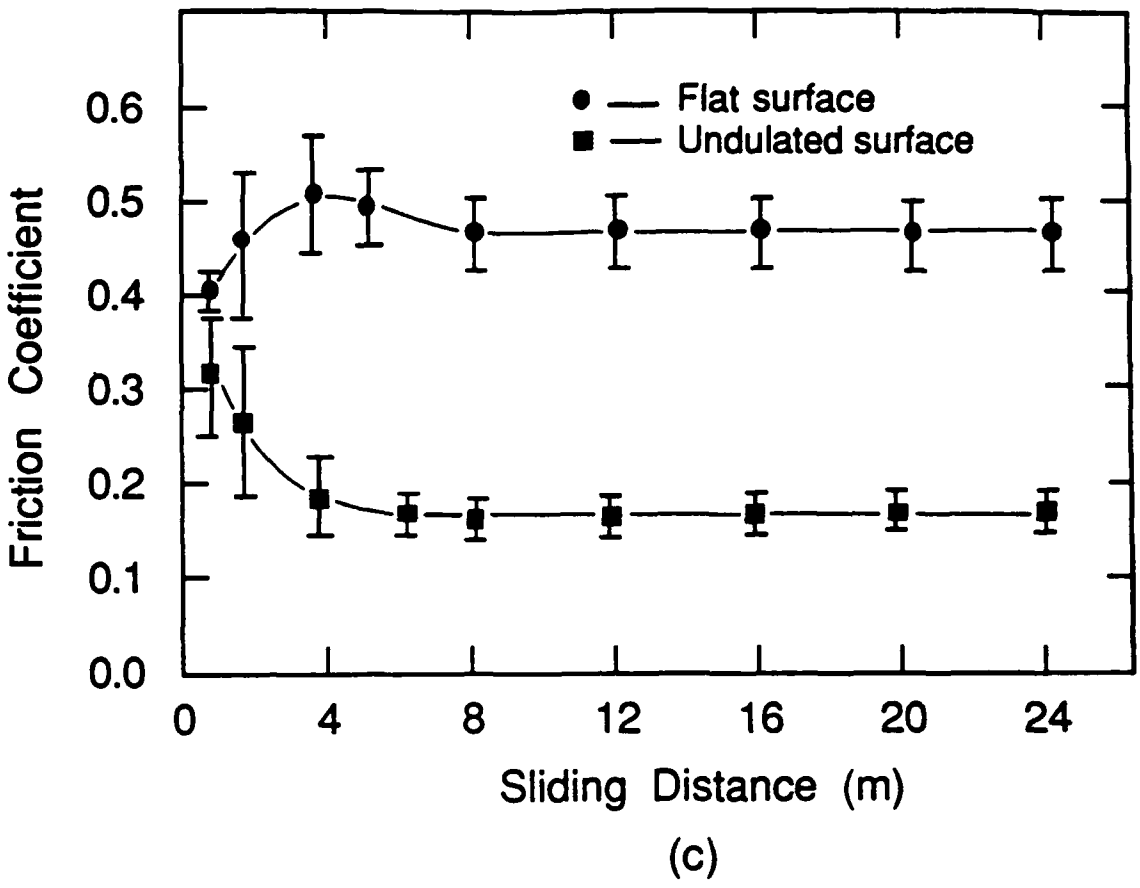

Fig. 3 Friction coefficients of AISI 52100 steel on flat and undulated titanium surfaces with various lubricants: (c) turbo oil

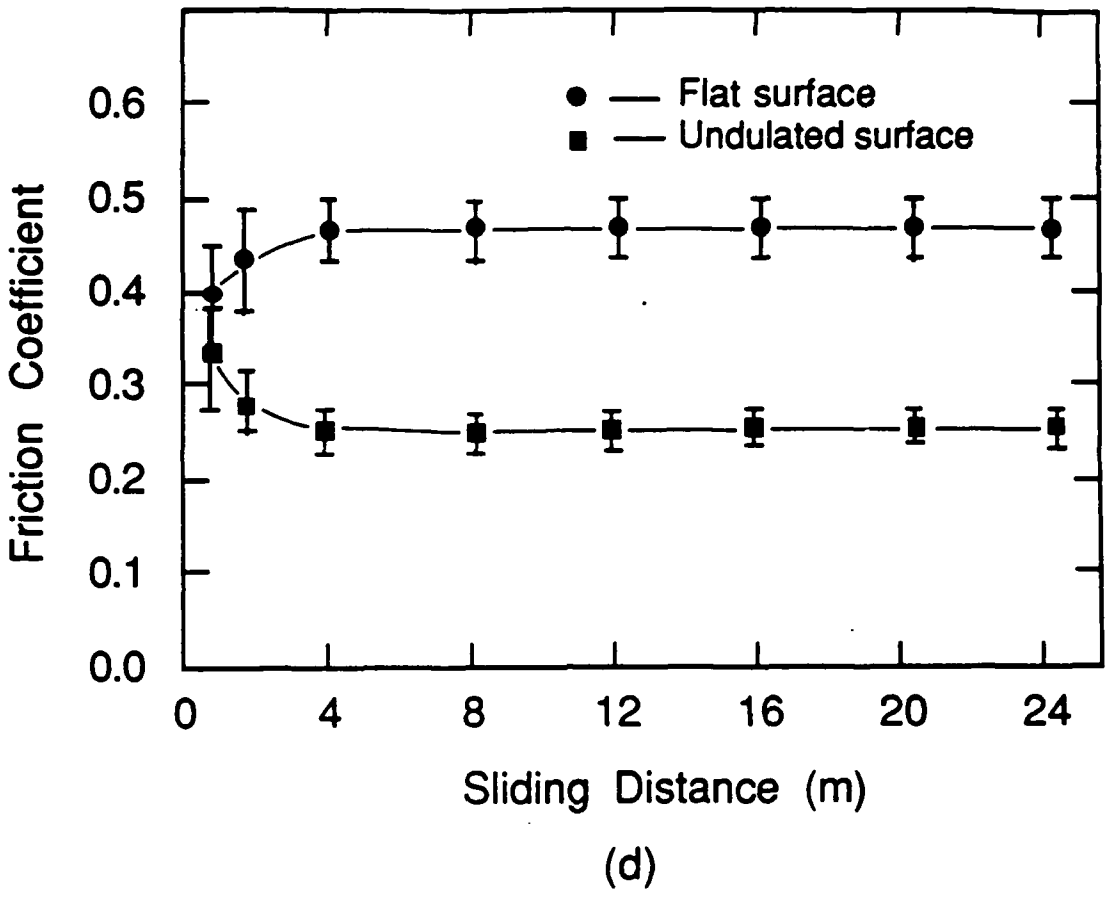

Fig. 3 Friction coefficients of AISI 52100 steel on flat and undulated titanium surfaces with various lubricants: (d) silicone oil

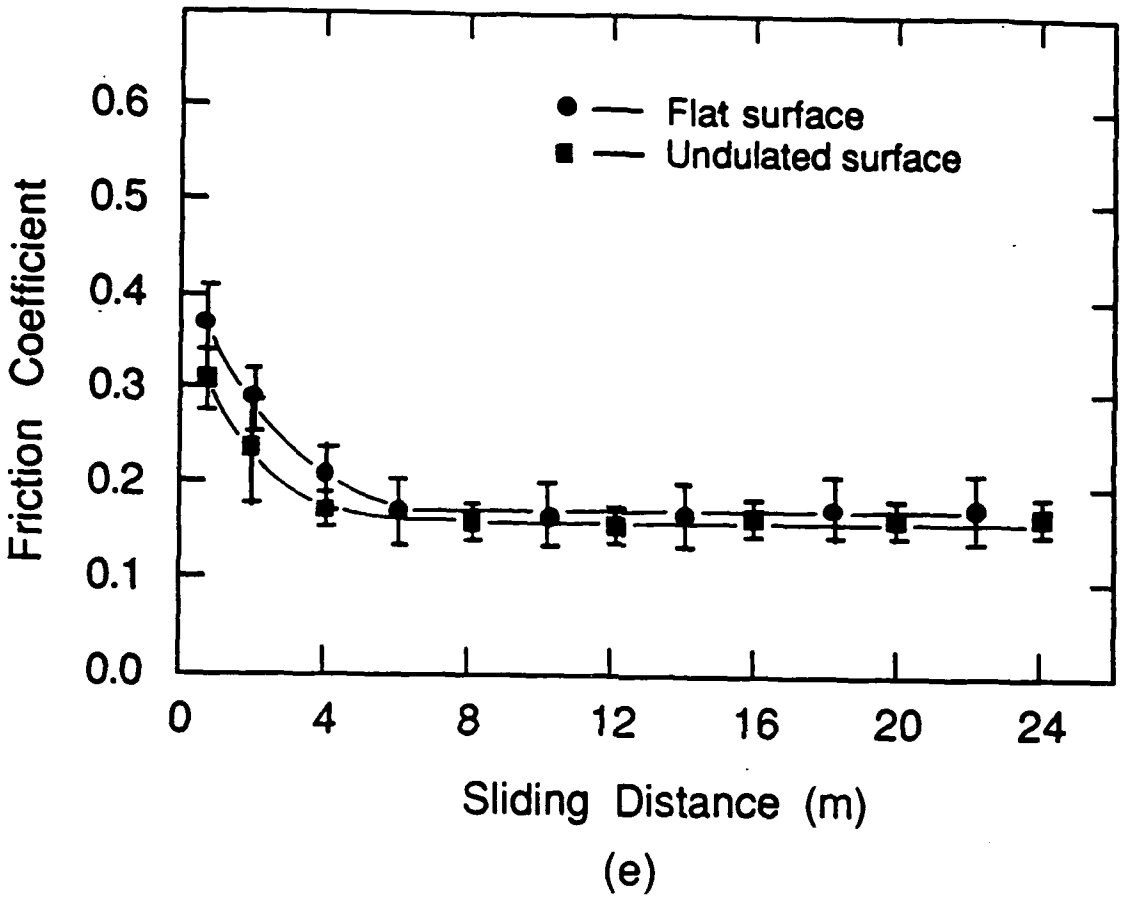

Fig. 3 Friction coefficients of AISI 52100 steel on flat and undulated titanium surfaces with various lubricants: (e) halocarbon oil

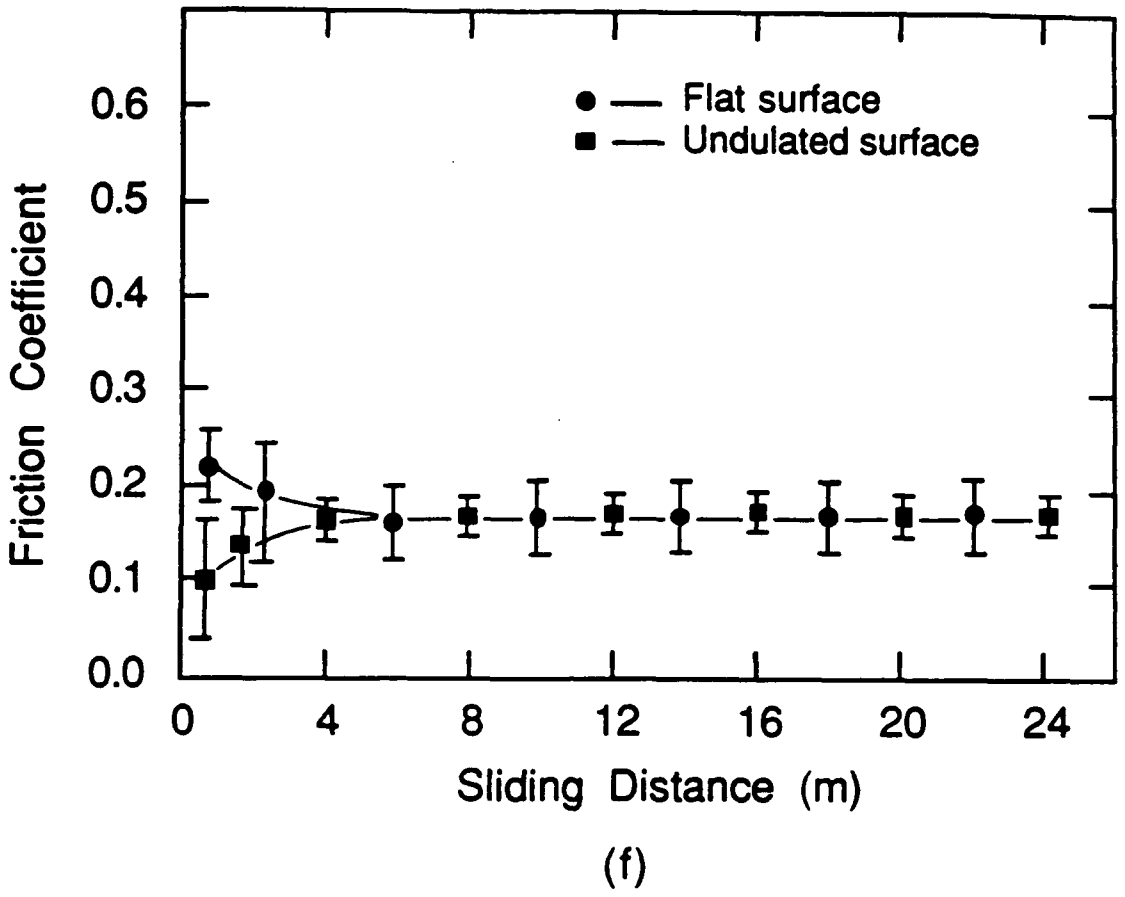

Fig. 3 Friction coefficients of AISI 52100 steel on flat and undulated titanium surfaces with various lubricants: (f) methylene iodide

Table 2. Friction and wear values of flat and undulated titanium surfaces

Lubricant	Friction coefficient		Wear rate * $(m^3/m)\ 10^{-12}$		Wear coefficient (10^{-3})	
	Flat	Undulated	Flat	Undulated	Flat	Undulated
Mineral oil	0.60	0.38	13.9	0.807	6.73	0.388
Oleic acid	0.49	0.12	9.19	0.846	4.42	0.407
Turbo oil	0.47	0.17	8.53	0.624	4.10	0.301
Silicone oil	0.47	0.24	8.01	0.437	3.85	0.211
Halocarbon oil	0.17	0.16	very small		very small	
Methylene iodide	0.17	0.16	very small		very small	

* Normal load: 0.5 kgf Slider: AISI 52100 steel

Table 3. Friction coefficients of titanium slid on titanium with different lubricants

Lubricant	Friction coefficient	
	Flat surfaces	Undulated surfaces
Mineral oil	0.50	0.45
Oleic acid	0.45	0.24
Turbo oil	0.48	0.20
Silicone oil	0.50	0.24
Halocarbon oil	0.18	0.16
Methylene iodide	0.17	0.16

Normal load: 0.5 kgf

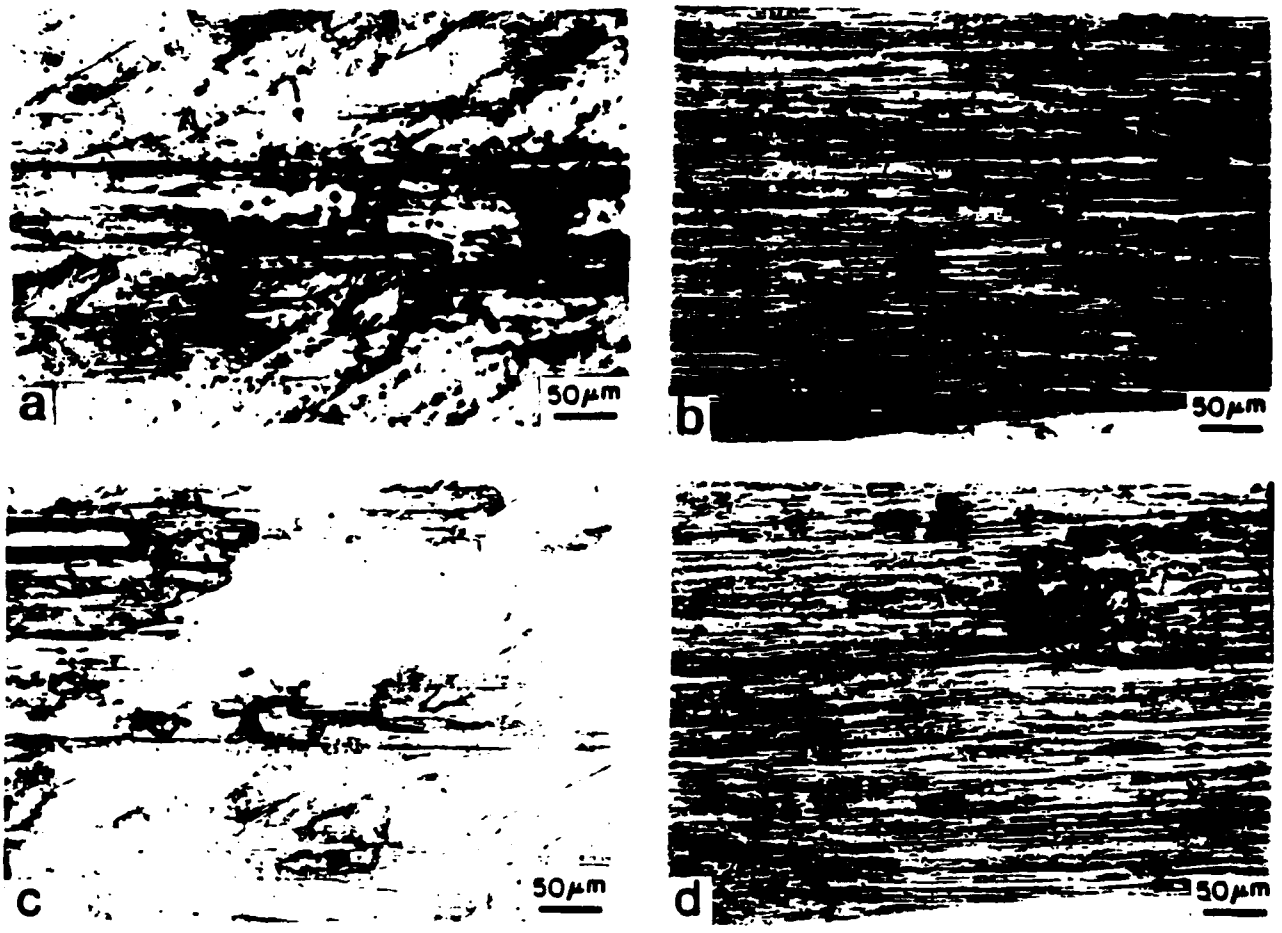

Figure 4. Worn flat titanium surfaces: (a) AISI 52100 steel on titanium with mineral oil, (b) AISI 52100 steel on titanium with oleic acid, (c) titanium on titanium with turbo oil, and (d) titanium on titanium with silicone oil

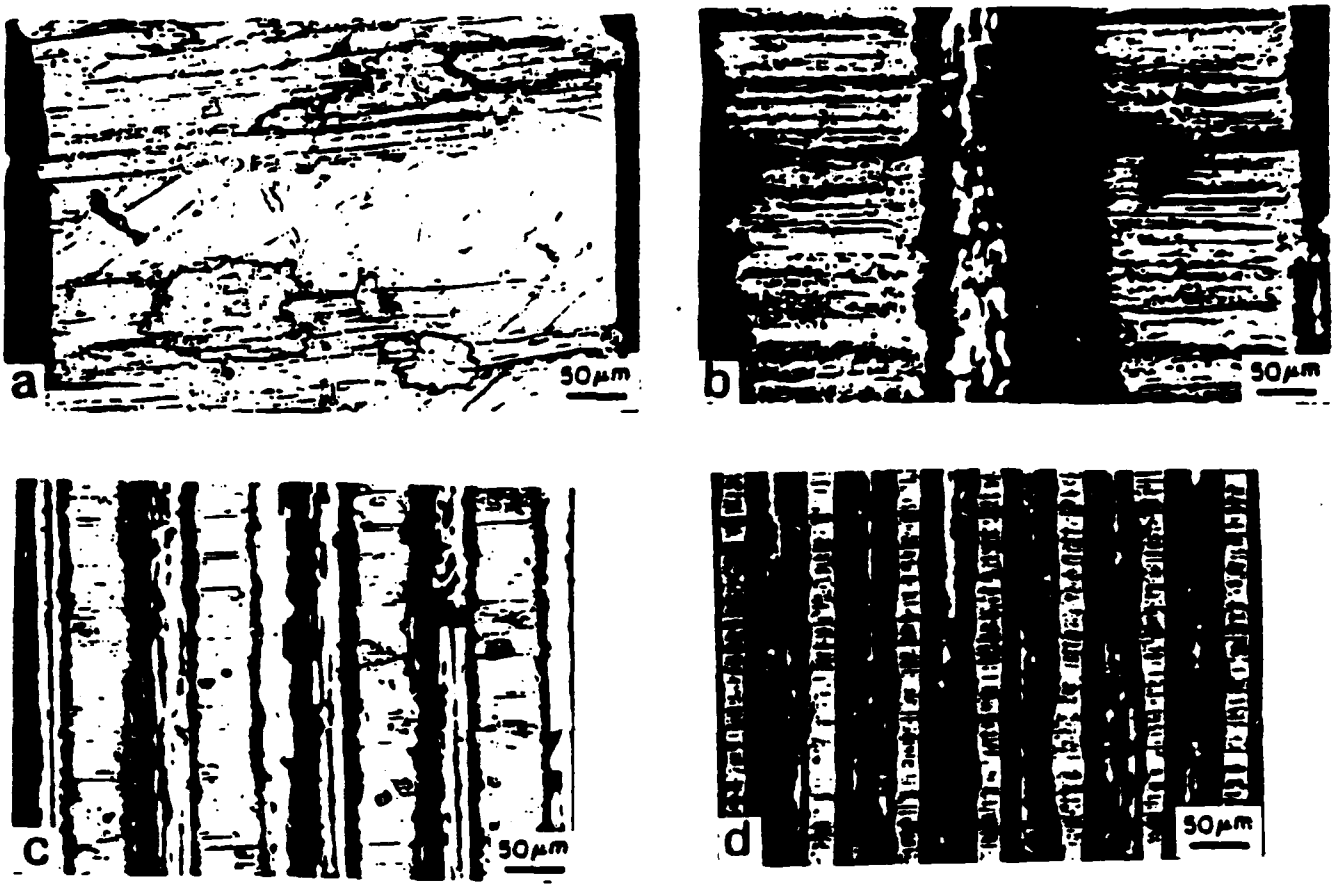

Figure 5 Micrographs of undulated surfaces for AISI 52100 steel on titanium with mineral oil: (a) extra-large pads, (b) large pads, (c) medium pads, and (d) small pads

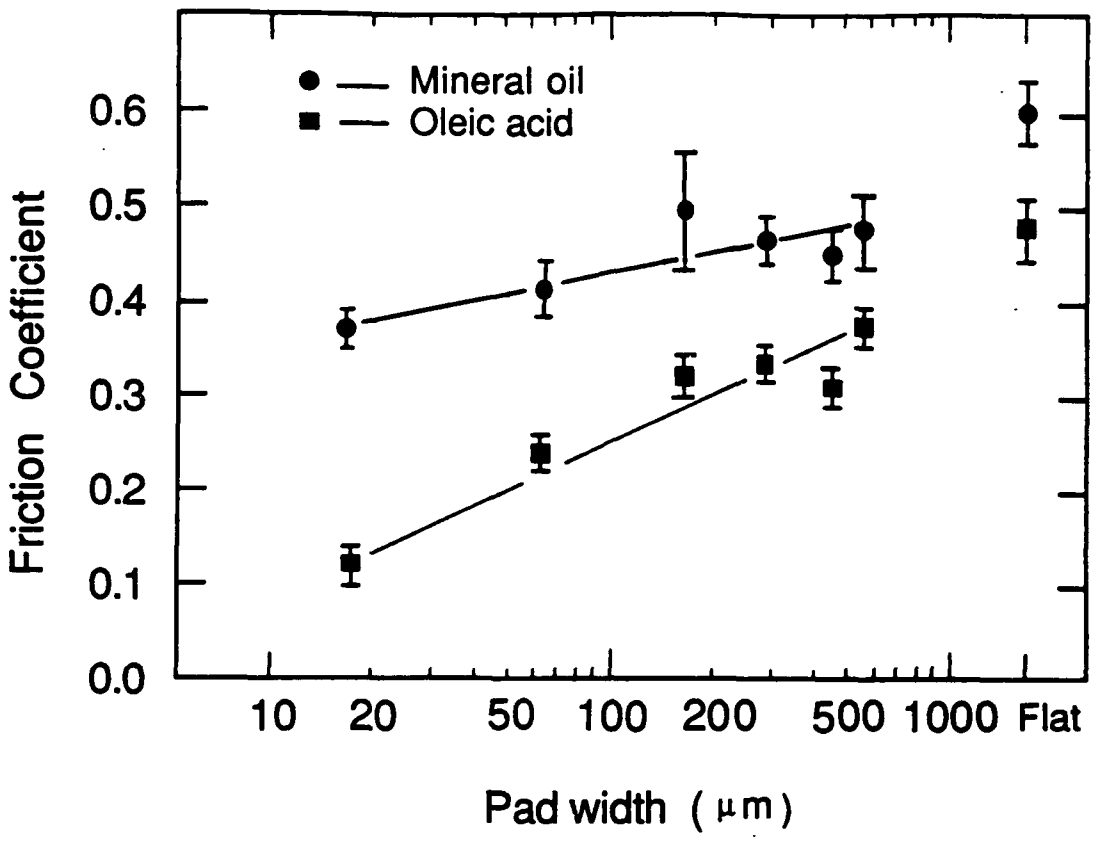

Figure 6: Friction coefficient versus pad width of undulated surfaces

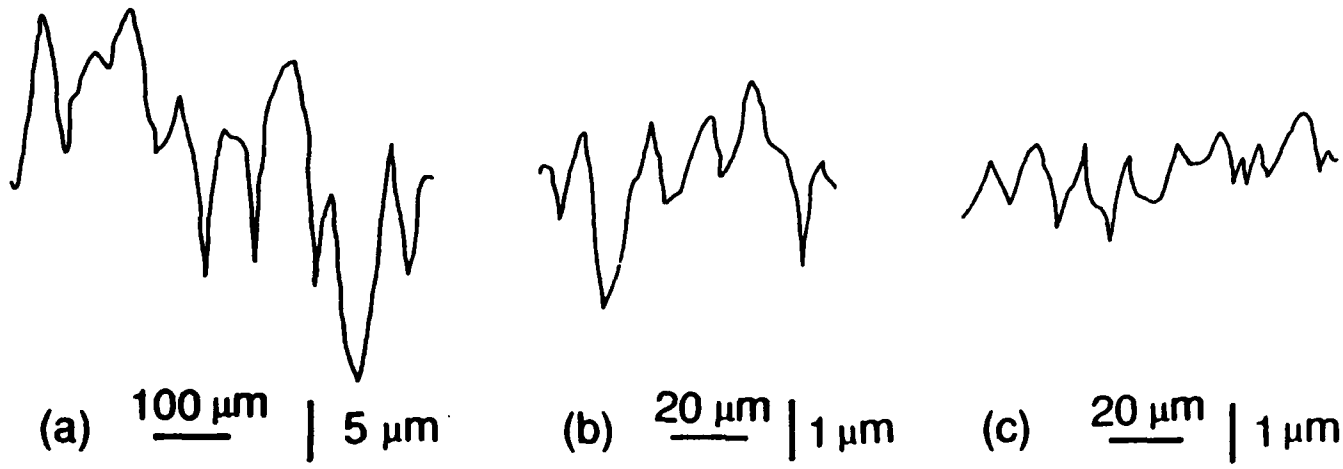

Figure 7 Profiles of worn surfaces: (a) flat surface with mineral oil, (b) undulated surface of large pads with mineral oil, (c) undulated surface of small pads with mineral oil. In all cases, the slider was AISI 52100 steel.

Supposing that the pad width is a, and that the wave length of undulation is c, the "cavity volume fraction" of the undulated surface V_c is given by 0.5 (1-a/c) (Figure 8). The undulated titanium surfaces which had different cavity volume fractions, but of the same pad width (a is about 100 μm), were tested using mineral oil and oleic acid as lubricants. Figure 9 shows that friction coefficients decrease monotonically as the cavity volume fraction increases until it is greater than 0.1, for both mineral oil and oleic acid tests. Beyond this value, the friction coefficients are low and independent of cavity volume volume fraction.

Above all, the sliding direction is important when undulated surfaces are used. When sliding was along the direction in which the grooves were cut, wear particles still formed long plowing grooves on the surfaces (Figure 10) and the coresponding friction coefficient was almost the same as that of a flat surface. This result clearly supports the hypothesis that wear particles are trapped in the cavities if the sliding direction is normal to the grooving direction and that the friction force will be reduced.

C. Effects of Undulated Geometry

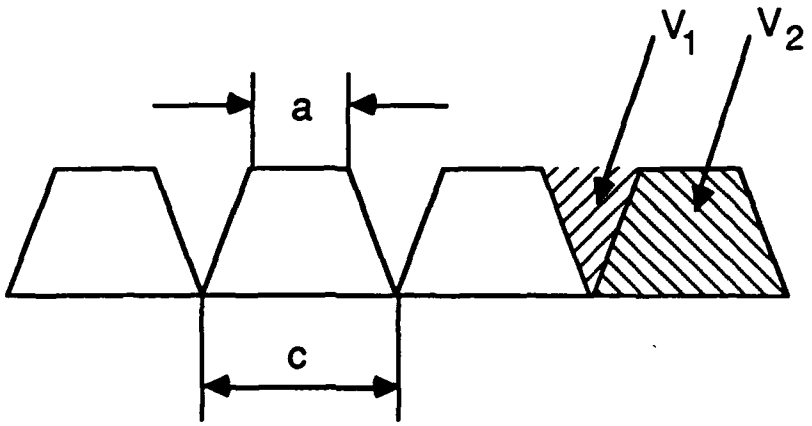

$$V_c = \frac{V_1}{(V_2 + V_1)} = \frac{1}{2}\left[1 - \frac{a}{c}\right]$$

Fig. 8 Geometry for calculating cavity volume fraction

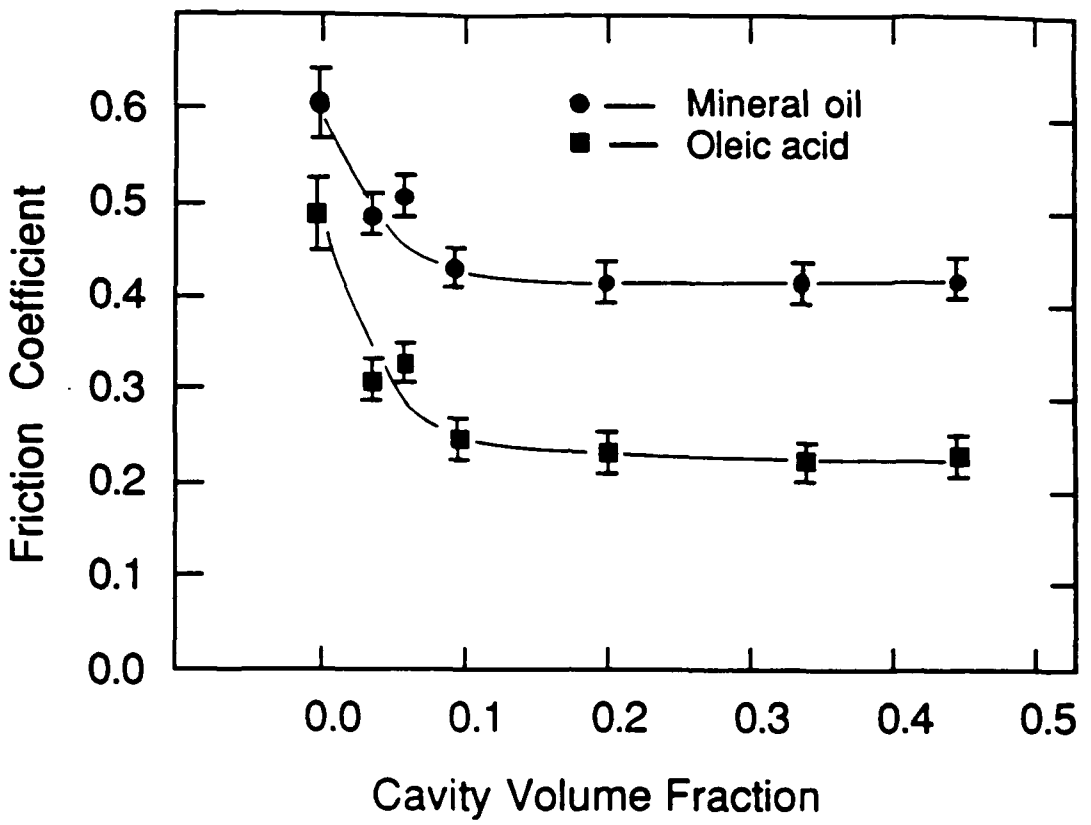

Fig. 9 The relation between friction coefficients and cavity volume fraction of undulated surfaces

Figure 10 Plowing grooves of worn undulated titanium surface on which AISI 52100 steel slid with mineral oil

IV. DISCUSSION

The experimental results of this investigation clearly confirm the significance of plowing in the boundary lubricated sliding of flat titanium surfaces when the common lubricants are used. The substantial reduction of friction and the differences in the topography of the worn surfaces emphasize the effectiveness of surface undulations in minimizing plowing. Nevertheless, some fine plowing grooves have still appeared on the undulated surfaces. In order to quantitatively analyze the contribution of plowing to friction in boundary lubricated sliding, therefore, in what follows a simple plowing model is presented and the plowing component of friction is estimated.

A. The plowing model

In the past, a good deal of effort was devoted to developing models of plowing friction in dry and lubricated sliding [11-14]. Theoretical estimates of friction coefficients are usually obtained from a model of wear particle or hard asperity of a well-defined geometry. On real sliding surfaces, however, the wear particles and asperities are of different sizes (and shapes) and follow a statistical distribution. Friction force due to plowing should then take into account the contribution of the entire population of wear particles and hard asperities.

Consider a conical wear particle (or a conical hard asperity) which has an indentation diameter, w, penetration depth, h, and plowing angle, θ (Figure 11). The elemental normal load, dL, and the elemental friction force, dF, acting on an elemental area dA at radius r of this wear particle are:

$$\begin{aligned} dL &= p \cos\theta \, dA \\ &= p \cos\theta \sec\theta \, r \, dr \, d\gamma \\ &= p \, r \, dr \, d\gamma \end{aligned} \qquad (1)$$

$$\begin{aligned} dF &= p \sin\theta \cos\gamma \, dA + s \sin\gamma \, dA \\ &= p \tan\theta \cos\gamma \, r \, dr \, d\gamma + s \sec\theta \sin\gamma \, r \, dr \, d\gamma \end{aligned} \qquad (2)$$

where p and s are the interfacial normal pressure and shear stress. The plowing angle θ is defined by

$$\theta = \cot^{-1}\left(\frac{w}{2h}\right) \qquad (3)$$

Integrating Equations (1) and (2) over the front half of the conical surface gives the normal load, L, and the friction force, F, as:

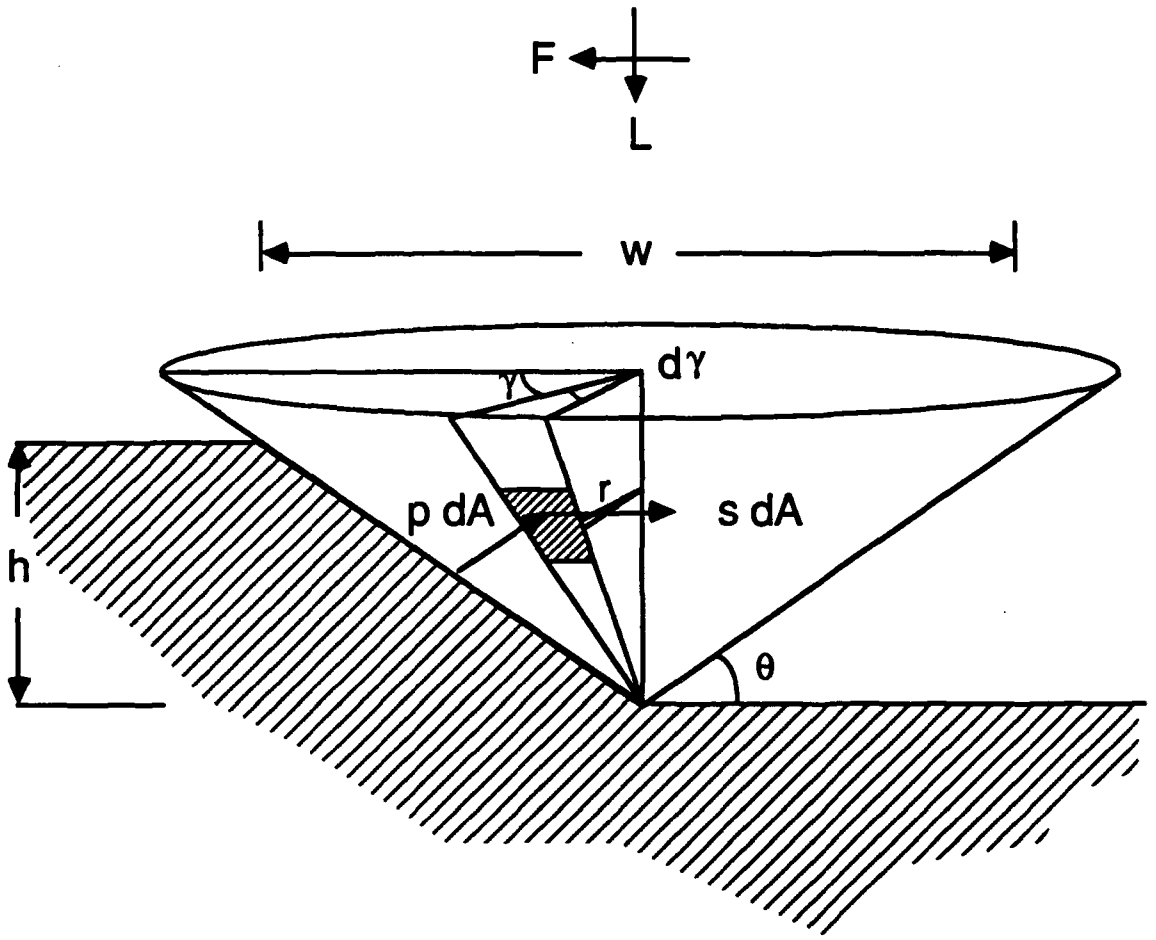

Figure 11 The plowing model for boundary lubrication

$$L = \frac{\pi}{2} p h^2 \cot^2\theta \qquad (4)$$

$$F = p h^2 \cot^2\theta \left[\tan\theta + \frac{s}{p} \sec\theta \right] \qquad (5)$$

If $\sigma(\theta)$ and $\varphi(h)$ are the frequency distribution functions of the plowing angle θ and the penetration depth h, respectively, the total normal load, L_t, and the total friciton force, F_t, are given by

$$L_t = \int_0^{h_{max}} \int_0^{\theta_{max}} L\, \sigma(\theta)\, \varphi(h)\, d\theta\, dh \qquad (6)$$

$$F_t = \int_0^{h_{max}} \int_0^{\theta_{max}} F\, \sigma(\theta)\, \varphi(h)\, d\theta\, dh \qquad (7)$$

where h_{max} and θ_{max} are the *maximum* values of penetration depth and plowing angle, respectively. Assuming that $\sigma(\theta)$ and $\varphi(h)$ are independent of each otherand and substituting Equations (4) and (5) into Equations (6) and (7),

$$L_t = A \int_0^{h_{max}} h^2\, \varphi(h)\, dh \qquad (8)$$

$$F_t = B \int_0^{h_{max}} h^2\, \varphi(h)\, dh \qquad (9)$$

where

$$A = \frac{\pi}{2} p \int_0^{\theta_{max}} \cot^2\theta\, \sigma(\theta)\, d\theta \qquad (10)$$

$$B = p \int_0^{\theta_{max}} \cot^2\theta \left[\tan\theta + \frac{s}{p} \sec\theta \right] \sigma(\theta)\, d\theta \qquad (11)$$

Thus the friciton coefficient, μ, is given by

$$\mu = \frac{F_t}{L_t} = \frac{B}{A} \qquad (12)$$

From Equations (10), (11) and (12), the friction coefficient can be written as

$$\mu = \frac{2 \int_0^{\theta_{max}} \left[\cot\theta + \frac{s}{p} \sec\theta \cot^2\theta \right] \sigma(\theta)\, d\theta}{\pi \int_0^{\theta_{max}} \cot^2\theta\, \sigma(\theta)\, d\theta} \qquad (13)$$

From Equation (13), the friction coefficient is dependent only on the frequency distribution function of the plowing angle, $\sigma(\theta)$, and independent of the frequency distribution function of the penetration depth, $\varphi(h)$. For a given distribution of the plowing angle, Equation (13) gives the friction coefficient due to all of the wear particles and hard asperities which plow the sliding surfaces. In practice, however, it is not possible to determine an exact mathematical expression for $\sigma(\theta)$ from the measurement of surface profiles. Thus supposing that n measurements of the plowing angle are taken (denoted by θ_i, i=1..... n), Equation (13) can be approximately written as

$$\mu = \frac{2 \sum_{i=1}^{n} \left[\cot\theta_i + \frac{s}{p} \sec\theta_i \cot^2\theta_i \right]}{\pi \sum_{i=1}^{n} \cot^2\theta_i} \qquad (14)$$

As $n \to \infty$, of course, Equation (14) will be equivalent to Equation (13). Assuming further that the normal pressure p is approximately equal to the hardness of the soft material (i.e., the material being plowed), which in turn is equal to six times the shear strength, s_m, then Equation (14) becomes

$$\mu = \frac{2\sum_{i=1}^{n}\left[\cot\theta_i + \frac{s}{6s_m}\sec\theta_i \cot^2\theta_i\right]}{\pi\sum_{i=1}^{n}\cot^2\theta_i} \qquad (15)$$

where the ratio s/s_m represents the interfacial friction condition. For "ideal" boundary lubricated sliding the ratio approaches zero, and for dry sliding the interfacial shear stress approaches the shear strength and the ratio will be close to unity.

When $s/s_m = 0$, Equation (15) represents the friction coefficient due to pure plowing. Therefore, Equation (15) can be further separated into the two terms, i.e.,

$$\mu = \mu_p + \mu_s \qquad (16)$$

where

$$\mu_p = \frac{2\sum_{i=1}^{n}\cot\theta_i}{\pi\sum_{i=1}^{n}\cot^2\theta_i} \qquad (17)$$

$$\mu_s = \frac{2\sum_{i=1}^{n}\frac{s}{6s_m}\sec\theta_i \cot^2\theta_i}{\pi\sum_{i=1}^{n}\cot^2\theta_i} \qquad (18)$$

where μ_p represents the friction coefficient due to pure plowing and μ_s the friction coefficient due to the adhesive interaction between the wear particles and the surface being plowed.

The surface roughness may be defined in different ways. According to one definition it is the peak-to-trough distance, i.e., the penetration depth, h. Another is the roughness angle which is the same as the plowing angle if the asperities and wear particles are conical. It is interesting to note that the peak-to-trough distance does not appear in Equation (13), though it contributes both to normal load and friction force individually in Equations (8) and (9). The friction coefficient depends only on the roughness angle, i.e., the plowing angle. Thus as far as friction is concerned,

the roughness angle is a more meaningful mearsure of plowing friction than the peak-to-trough distance.

B. The mechanism of friction

The indentation diameter w and penetration depth h are determined by measuring the width and depth of plowing grooves on a profilometer using low scanning speed and small scanning distances, and the plowing angle θ is calculated from Equation (3). For each specimen, twelve measurements of w and h are taken from the surface profile. Then substituting the twelve plowing angles calculated from Equation (3) into Equation (17), the plowing friction coefficient, μ_p, is obtained. Then from Equation (16), μ_s is obtained by substracting plowing friction coefficient μ_p from the experimental friction coefficient, μ_{exp}. Finally, the ratio s/s_m is calculated from Equation (18). All theses items are listed in Table 4 for different sliders and lubricants.

It can be seen from column of μ_p/μ_{exp} in Table 4 that plowing contributes about 80 percent of the total friction coefficient of flat titanium surfaces when the common lubricants are used. When undulated surfaces are used, plowing accounts for about 32-80 percent of the total friction coefficient, although the average plowing angles, θ_m, and plowing friction coefficinets, μ_p, are substantially reduced. Thus, plowing due to wear particles is eliminated by using undulated surfaces, but plowing due to hard asperities is still significant when the common lubricants are used. It is also noted that when undulated surfaces are used, the friction coefficients due to shearing of lubricant films and adhesion between asperities are essentially unchanged, and so is the ratio s/s_m. The ratio s/s_m is about 0.6-0.9, which explains the ineffectiveness of the common lubricants.

Since no wear particles are generated at the very biginning of sliding, undulated surfaces should not have any effect on friction. The true effect of lubricants is thus reflected in terms of the initial friction coefficient. When sliding reaches a steady state, however, plowing due to wear particles and hard asperities makes almost the same fractional contribution (about 80 percent) to the total friction coefficient of flat titanium surfaces with different common lubricants. The contribution of shearing of lubricant films and adhesion between asperities in all tests is about 20 percent for all lubricants. Thus the true effect of lubricants at the steady state is masked by the dominant plowing friction. When the undulated surfaces are used, however, plowing due to wear particles is eliminated, and plowing due to hard asperities contributes 30-80 percent of the total friction coefficient, depending on the lubricants and sliders. The fractional contribution of plowing with AISI 52100 steel pins is always lower than that with titanium pins for the same lubricant when undulated titanium surfaces are used. For oleic acid, for example, the fractional contribution of plowing with AISI 52100 steel pins is about 30 percent, whereas that with titanium pins it is about 65 percent, and the friction coefficients are also different. Moreover, the friction coefficients with different lubricants were quite different in the tests of AISI 52100 steel on undulated titanium surfaces (0.38 for mineral oil, 0.12 for oleic acid, 0.24 for silicone oil and 0.17 for turbo oil). All these differences indirectly reflect the true effect of material combinations and lubricants in boundary

Table 4 Experimental and Theoretical Friction coefficients

Lubricant	μ_{exp}		μ_p		μ_p / μ_{exp}		μ_s		θ_m (degree)		s/s_m	
	flat	undulated	flat	undulated	flat	undulated	flat	undulated	flat	undulated	flat	undulated
Slider: AISI 52100												
1. mineral oil	0.60	0.38	0.485	0.275	0.808	0.724	0.115	0.105	37.8	23.6	0.87	0.90
2. oleic acid	0.48	0.12	0.397	0.039	0.827	0.325	0.083	0.081	32.5	6.54	0.67	0.75
3. silicone oil	0.49	0.24	0.407	0.159	0.831	0.663	0.083	0.081	33.3	16.7	0.65	0.72
4. turbo oil	0.47	0.17	0.384	0.081	0.817	0.476	0.086	0.089	31.5	10.6	0.72	0.83
Slider: Titanium												
1. mineral oil	0.50	0.45	0.419	0.367	0.838	0.815	0.081	0.083	33.8	31.2	0.63	0.68
2. oleic acid	0.45	0.24	0.362	0.156	0.804	0.650	0.088	0.084	30.0	14.0	0.73	0.75
3. silicone oil	0.50	0.24	0.414	0.164	0.828	0.683	0.086	0.076	33.7	15.1	0.67	0.68
4. turbo oil	0.48	0.20	0.388	0.107	0.808	0.563	0.092	0.093	31.6	11.2	0.72	0.75

lubricated sliding.

When halocarbon oil 11-14 and methylene iodide (the well-known lubricants for titanium) were used, adsorbed lubricant molecules may have effectively prevented asperity penetration. In such an event, shearing of the lubircant film and adhesion between asperities become the dominant components of sliding friction. Since the primary role of surface undulations is to eliminate plowing component by removing wear particles, the undulated surfaces did not have substantial effect in reducing friction when halocarbon oil and methylene iodide were used(Figures 3e,3f).

C. Geometrical effects of the undulated surfaces

The basic idea of using undulated surfaces in this study has two origins. First, the size of wear particle itself is reduced when the pad width of the undulated surfaces is sufficiently small. If the pad width is too large, the undulated surfaces will not reduce friction because they generate large wear particles and behave like flat surfaces. It was found in this investigation that the relation between the friction coefficient and the logarithm of pad width is approximately a straight line (Figure 6). The smaller the pad width, the smaller is the friction coefficient. Second, the wear particles produced during sliding are expected to be trapped in the surface cavities. When the cavities are filled with wear particles to the brim, even the undulated surfaces may behave like flat surfaces. But as long as the cavities have enough space for trapping the wear particles, there will be no difference between high and low cavity volume fraction. It is reasonable to assume, then, that the cavity volume fraction of the undulated surfaces has a critical value beyond which the friction coefficient will be low and constant. Moreover, reduction of plowing leads to concomitant reduction of wear, thus producing fewer wear particles which may never fill the cavities fully. The experimental results indeed substantiate this (Figure 9). The critical cavity volume fraction is about 0.1. This critical volume fraction depends, however, on the normal load and the sliding distance.

The primary purpose of this investigation was to eliminate plowing due to wear particles and to lubricate titanium with the common lubricants. But the undulated surfaces can be used to advantage for other reasons as well; for example, as built-in filters, as reservoirs of extremely viscous lubricants (such as greases) and as capillary passages for continuously supplying lubircants. Another possible beneficial effect of surface undulations is reducing friction in boundary lubricated sliding at elevated temperatures by continuously removing wear particles, even with additive-free lubricants.

V. CONCLUSIONS

(1) In the boundary lubricated sliding of titanium, plowing due to wear particles entrapped between sliding surfaces is the primary mechanism of friction, contributing about 80 percent to the total friction coefficient.

(2) The undulated surface geometry provides an alternative for effectively lubricating titanium surfaces even with lubricants considered ineffective for titanium. Pad width and cavity volume fraction are the two primary parameters of the undulated surfaces. Friction coefficient generally decreases as the pad width decreases and the cavity volume fraction increases.

(3) Even though plowing due to wear particles is eliminated by using the undulated surfaces, the plowing due to hard asperities is still significant when the common lubricants are used.

(4) The plowing model proposed for boundary lubricated sliding is in good agreement with experimental results.

(5) The undulated surfaces provide an effective alternative to study the true role of materials and lubricants in the steady state of boundary lubricated sliding.

REFERENCES

[1] Bowden, F.P., Gregory, J.N., and Tabor, D., "Lubrication of Metal Surfaces by Fatty Acids," *Nature*, **156**, pp97-101 (1945).

[2] Bowden, F.P., and Tabor, D., "Mechanism of Boundary Lubrication," Chap. X, *The Friction and Lubrication of Solids*, Clarendon Press, Oxford, pp119-227 (1958).

[3] Godfrey, D., "Boundary Lubrication," *Proceedings International Symposium on Lubrication and Wear*, ed. by Muster, D. and Sternlicht, B., Houston, Texas, pp285-306 (1963).

[4] Campbell, W.E., "Boundary Lubrication," *Boundary Lubrication: An Appraisal of World Literature*, ed. by Ling, F.F., Klaus, E.E. and Fein, R.S, ASME, New York, pp87-117 (1969).

[5] Kapsa, Ph., and Martin, J.M., "Boundary Lubricant Films: A Review," *Tribology International*, **15**, pp37-42 (1982).

[6] Suh, N.P., and Sin, H.-C., "The Genesis of Friction," *Wear*, **69**, pp91-114 (1981).

[7] Saka, N., Liou, M.J., and Suh, N.P., "The Role of Tribology in Electrical Contact Phenomena," *Wear*, **100**, pp77-105 (1984).

[8] Suh, N.P., and Saka, N., "Surface Engineering," *Annals of the CIRP*, **36**, pp403-408 (1987).

[9] Komvopoulos, K., Saka, N., and Suh, N.P., "The Mechanism of Friction in Boundary Lubrication," *Journal of Tribology, ASME Trans.*, **107**, pp452-462 (1985).

[10] Rabinowicz, E., "Boundary Lubrication of Titanium," *Proceedings of the Fifth World Petroleum Congress*, **6**, pp319-330 (1958).

[11] Bowden, F.P., Moore, A.J.W. and Tabor, D., "The Ploughing and Adhesion of Sliding Metals," *J. of Applied Physics*, **14**, pp80-91 (1943).

[12] Hisakado, T., "On the Mechanism of Contact between Solid Surfaces," *Bull. JSME*, **13**, No.55, pp129-139 (1970).

[13] Tzukizoe, T., and Sakamoto, T., "Friction in Scratching without Metal Transfer," *Bull. JSME*, **18**, No. 115, pp65-72 (1975).

[14] Komvopoulos, K., Saka, N., and Suh, N.P., "Plowing Friction in Dry and Lubricated metal Sliding," *Journal of Tribology, ASME Trans.*, **108**, pp301-313 (1986).

BOUNDARY LUBRICATION OF UNDULATED METAL SURFACES AT ELEVATED TEMPERATURES

SUMMARY

In the boundary lubricated sliding of metals, lubricant molecules desorb from metal surfaces as the interfacial temperature exceeds the transition temperature. As a consequence, numerous metallic contacts will be established, leading to adhesion and wear particle formation. The wear particles so formed plow the sliding surfaces, resulting in high friction and severe wear. In this paper, it is shown that friction can be reduced at elevated temperatures even with additive-free lubricants by using undulated surfaces. Flat and undulated OFHC copper surfaces were tested with various lubricants at different temperatures. Experimental results and theoretical analysis show that undulated surfaces minimize the plowing component of friction due to wear debris, thereby keeping the friction coefficient at a low value after the transition.

I. INTRODUCTION

The principal feature of the phenomenon of boundary lubrication is the formation of thin protective films on metal surfaces by such processes as physisorption, chemisorption, and chemical reactions [1]. The strongly adsorbed lubricant films inhibit metal-to-metal contact and thus reduce friction and wear. Unfortunately, however, most common lubricants strongly adsorb to metal surfaces only up to moderately high temperatures. When the temperature of the sliding surfaces exceeds a certain temperature, termed transition temperature, friction increases sharply and severe wear ensues [2, 3].

In general, the temperature effect in boundary lubrication reflects in two ways. On the one hand, high temperature can cause disorientation, desorption or decomposition of the physically adsorbed lubricant molecules. As a result, most lubricants cannot effectively prevent metal-to-metal contact at high temperatures. On the other hand, high temperature can provide the activation energy necessary for chemisorption and chemical reactions. For example, the transition temperature is greatly increased by incorporating additives into base lubricants, since the additives react with metal surfaces to form tenacious solid films [4-6]. These solid films prevent metal-to-metal contact at temperatures above the transition temperature of additive-free lubricants, and maintain low friction and wear. Even so, effective lubrication by additives is often at the expense of corrosive wear resistance [7, 8]. And the effectiveness of an additive is not only specific to a specific base lubricant but also to the metal surface. For example, titanium is unresponsive to most additives that are effective for bearing steels.

Almost all investigations to date on the temperature effect in boundary lubrication are empirical and the basic reasons for the transition are still not entirely clear. Nevertheless, experimental observations suggest that when the temperature at the asperity junctions exceeds the transition temperature, lubricant molecules desorb from metal surfaces, leading to numerous metal-to-metal contacts. As a result, plowing by hard asperities and wear particles contribute most to friction rise. Thus as the temperature increases, the mechanism of friction changes from small-scale plowing and shearing of the adsorbed lubricant films to full-fledged plowing, much as in dry sliding.

In a previous investigation by the authors [9], plowing was shown to be the key mechanism of friction in the boundary lubrication of titanium when common lubricants were used. The plowing contribution to friction was effectively reduced by using undulated surfaces. This result suggests the possibility of obtaining low friction in boundary lubricated sliding at elevated temperatures even with additive-free lubricants by using the undulated surfaces. The primary objective of this paper therefore is to investigate the effect of surface undulations on the transition temperature and the mechanism of friction in boundary lubricated sliding.

II . EXPERIMENTAL

A. Materials and lubricants

Oxygen Free High Conductivity (OFHC) copper disk specimens with flat and undulated surfaces were used in this study. The pad width of the surface undulations was about 50 μm, the depth of the undulations was about 130 μm and the distance between the pads was about 200 μm.The details of preparation of the undulated surfaces were given in a previous paper [9]. AISI 52100 steel pins with round ends, 6.35 mm in diameter, were used as sliders. Before each test, both the pins and the disk specimens were polished with 0.3 μm alumina suspension in water. Several lubricants were tested, including mineral oil, jet engine turbo oil, paraffin oil, and silicone oil. The materials and lubricants are listed in Table 1.

B. Apparatus and procedures

Figure 1 schematically illustrates the experimental apparatus. The set-up was enclosed in a thermally insulated chamber. The disk specimens were mounted in a cup which contained the lubricant. The cup was driven back and forth on wheels by an electric motor at an average velocity of 1 cm/s. The stroke length was about 18 mm and the normal load was 1 N. The pins were mounted in an insulated holder (for protecting strain gages from excessive heating) which in turn was attached to a strain ring. The friction force was measured by the strain gages mounted on the strain ring. The bulk temperature of the lubricant was controlled by a temperature controller. Three plate heaters (150 W each) were attached to the bottom of the cup. A thermocouple was immersed in the lubricant near the disk for temperature measurement and control. During the sliding tests, the temperature was raised step by step (10 to 30 °C a step, depending on the change in the friction coefficient) from room temperature up to 220-300 °C. The sliding distance at each temperature was about 5-10 meters. All the tests were conducted in a laboratory environment.

Table 1. Experimental materials and lubricants

Material		Hardness (MPa)
OFHC copper		784 ± 40
AISI 52100 steel		7957 ± 112
Lubricant	**Type**	**Viscosity (cSt @ 310 K)**
Mineral oil	Naphthenic hydrocarbon	74
paraffin oil	"BAKER"	70-75
Turbo 2380	Mil-L-23699c	25
Silicone oil	DC550	45

a. load
b. holder
c. lubricant
d. thermocouple
e. plate heater
f. motor
g. thermo-insulated box
h. disk specimen
i. pin
j. balance weight

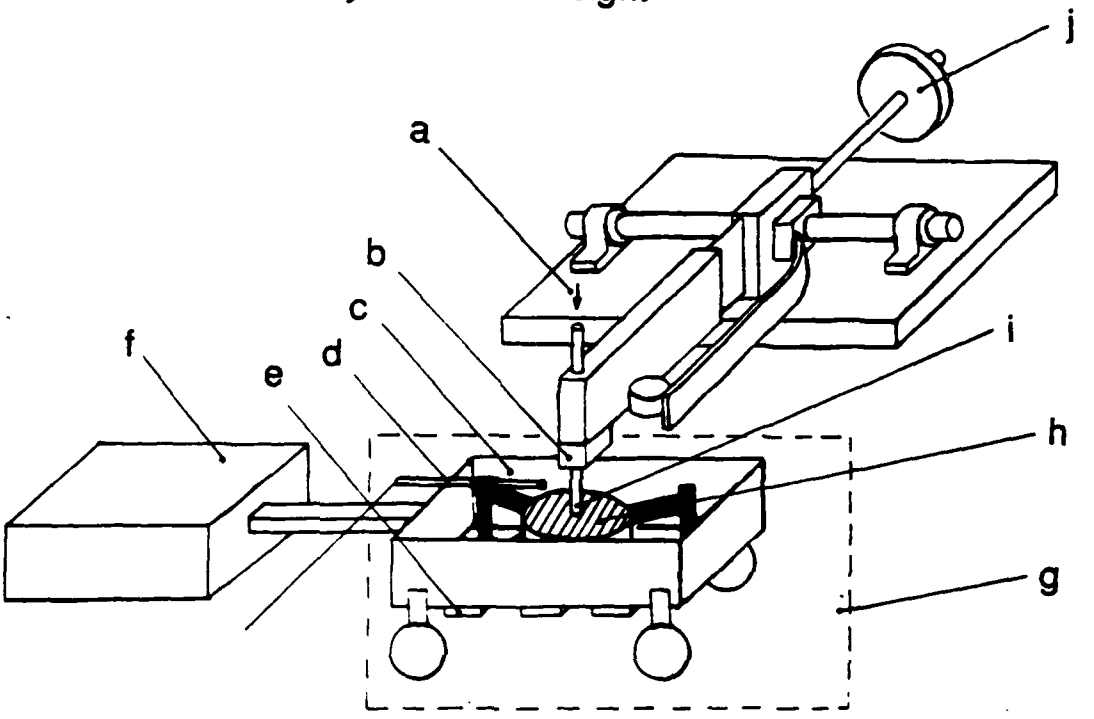

FIG. 1 Experimental apparatus

III. RESULTS

While the transition temperature may be defined as the temperature at which the friction coefficient increases sharply, in general the increase is gradual. The shape of the friction coefficient-temperature curve depends not only on the material combination and lubricants, but also on the scales used for plotting. Accordingly, in this paper, the transition temperature is defined as the interfacial temperature at which the friction coefficient increases by fifty percent of the total rise.

In Figure 2 the average friction coefficients and the standard deviations are plotted against the bulk temperature of the lubricant for the sliding pair AISI 52100 steel and OFHC copper with mineral oil as a lubricant. When the lubricant temperature was below 100 °C, the friction coefficients of both flat and undulated surfaces were almost the same, about 0.15. As the temperature of the lubricant was increased, however, the friction coefficient started increasing. With flat surfaces, the friction coefficient increased to 0.42 by 150 °C and then remained constant as the temperature was increased further. The transition temperature was about 135 °C. By contrast, the friction coefficient of the undulated copper surface remained essentially low as the temperature was raised. Even at 220 °C, the friction coefficient was only 0.22. The transition temperature was still about 135 °C.

When the AISI 52100 steel was slid on OFHC copper with the paraffin oil lubricant, the friction coefficients of both flat and undulated surfaces started increasing at 60 °C (Figure 3). The friction coefficient of the flat surface has increased to 0.42 by 220 °C, but that of the undulated surfaces to only 0.26. The transition temperature was about 130 °C for flat surfaces and 120 °C for undulated surfaces. The results of the sliding pair AISI 52100 steel and copper with silicone oil lubricant are shown in Figure 4. The shape of the two friction coefficient-temperature curves is almost the same except that the friction coefficient of the undulated surfaces was lower than that of the flat surfaces. These curves have two transitions instead of one. Figure 5 shows the results with turbo oil lubricant. The friction coefficients of both flat and undulated copper surfaces started increasing at the same temperature, about 100 °C. But the transition temperature of flat surfaces was about 250 °C, while that of the undulated surfaces was about 280 °C. This is the only case for which by using undulated surfaces, not only was the friction coefficient reduced but also the transition temperature was raised.

Figure 6 shows micrographs of the flat and undulated copper surfaces with the AISI 52100 steel as a slider and with the paraffin oil as a lubricant. At 60 °C, which was below the transition temperature (about 130 °C), the friction coefficients were about 0.16 on both the flat and the undulated surfaces, and a few plowing grooves were observed on the surfaces of the flat and undulated specimens. As the temperature was increased up to the transition temperature (130 °C), however, the lubricant no longer provided effective lubrication, and the plowing grooves produced by wear particles were observed on the flat copper surfaces, which account for the rise in friction (from 0.16 to 0.27 at 130 °C). On the undulated surfaces, by contrast, only fine grooves were

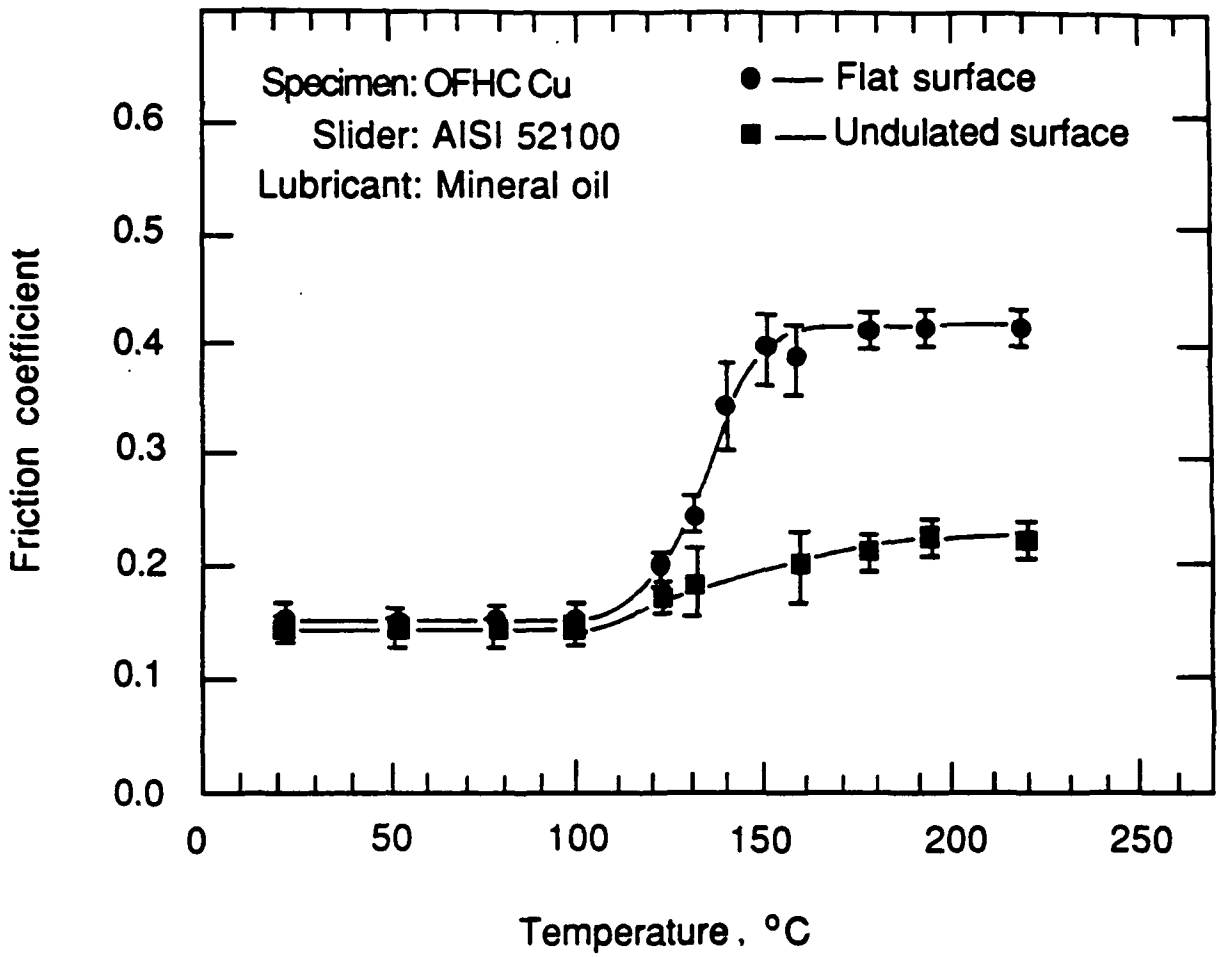

Figure 2 Friction coefficient versus temperature AISI 52100 steel on flat and undulated OFHC copper with mineral oil as lubricant

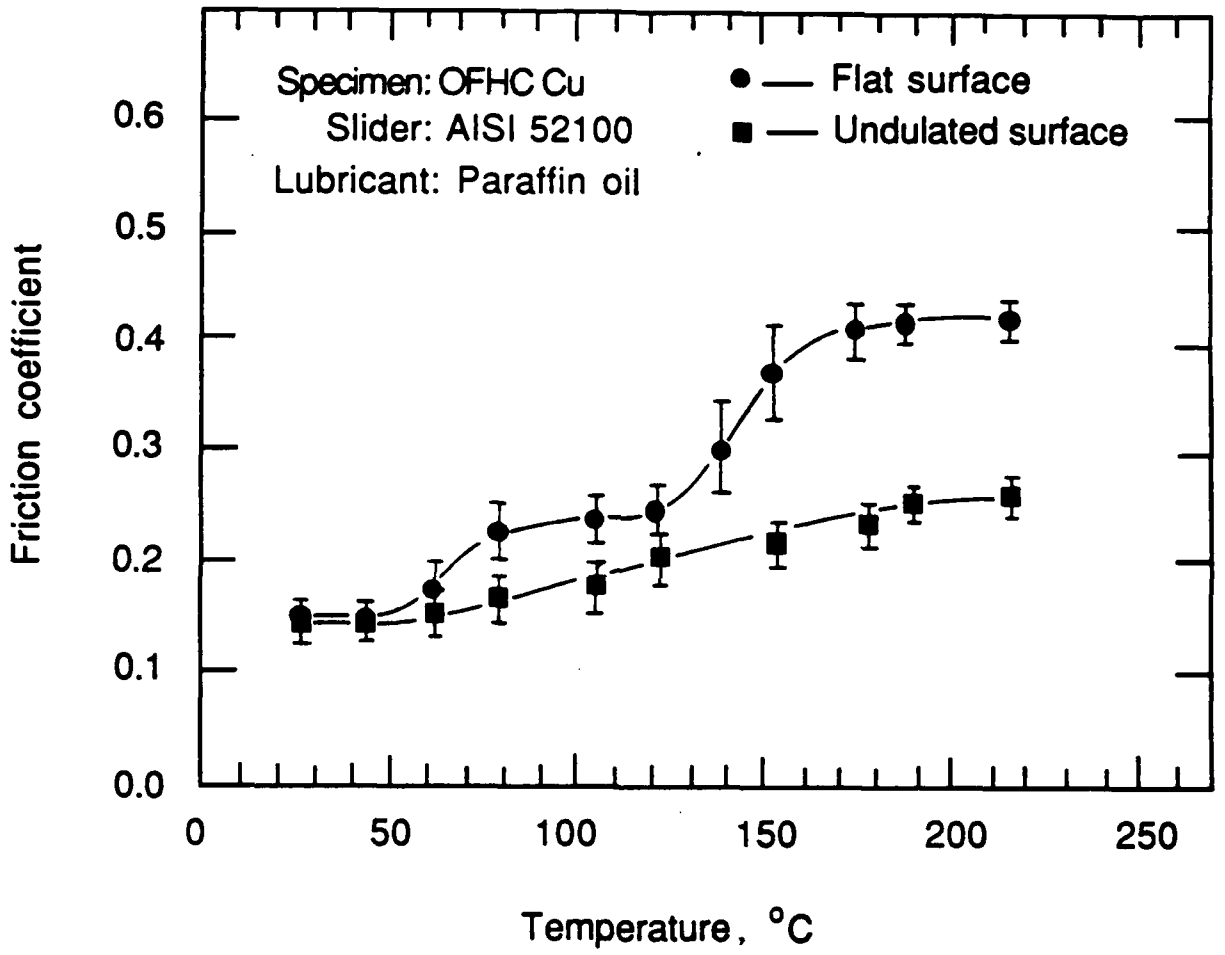

Figure 3 Friction coefficient versus temperature AISI 52100 steel on flat and undulated OFHC copper with paraffin oil as lubricant

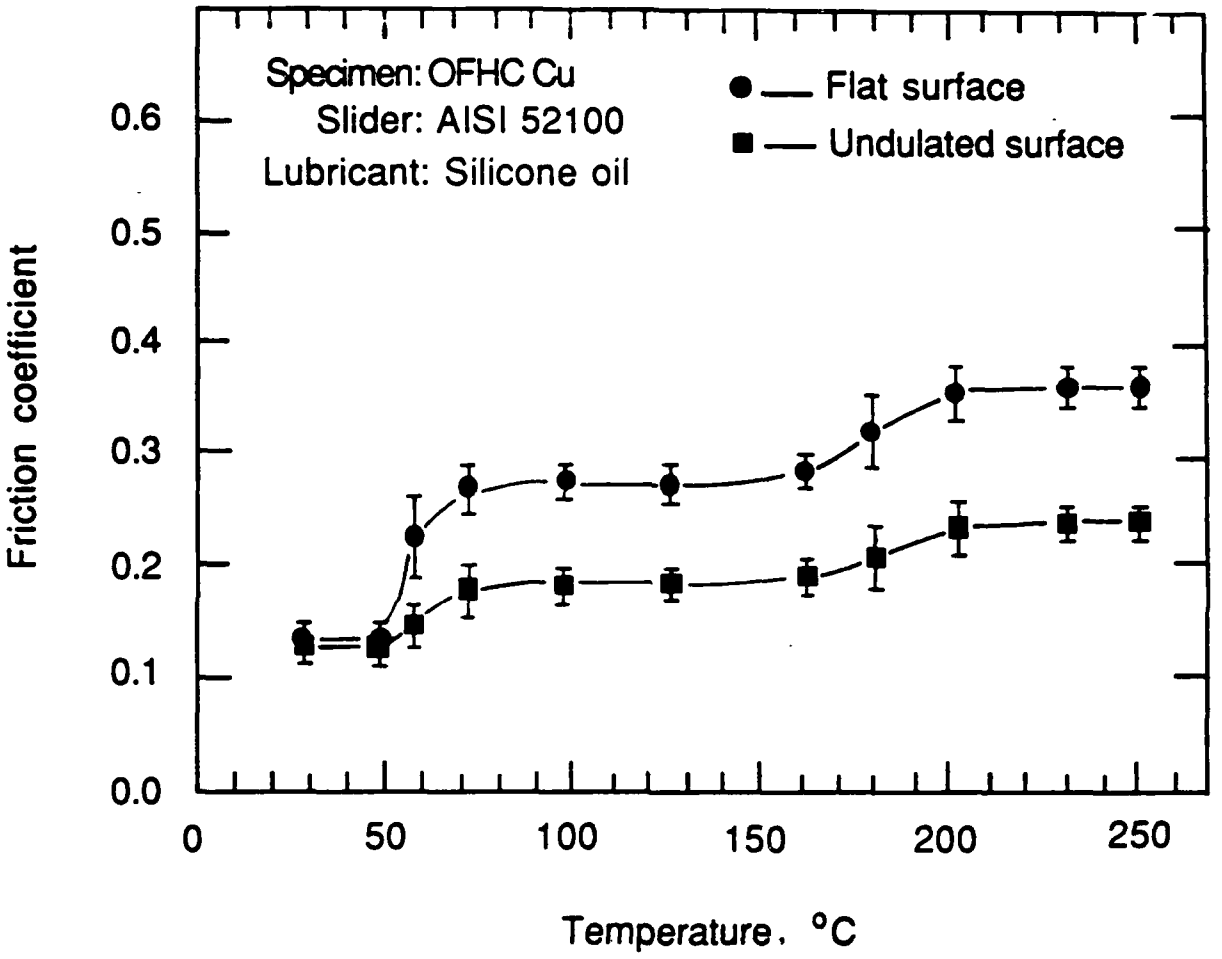

Figure 4 Friction coefficient versus temperature AISI 52100 steel on flat and undulated OFHC copper with silicone oil as lubricant

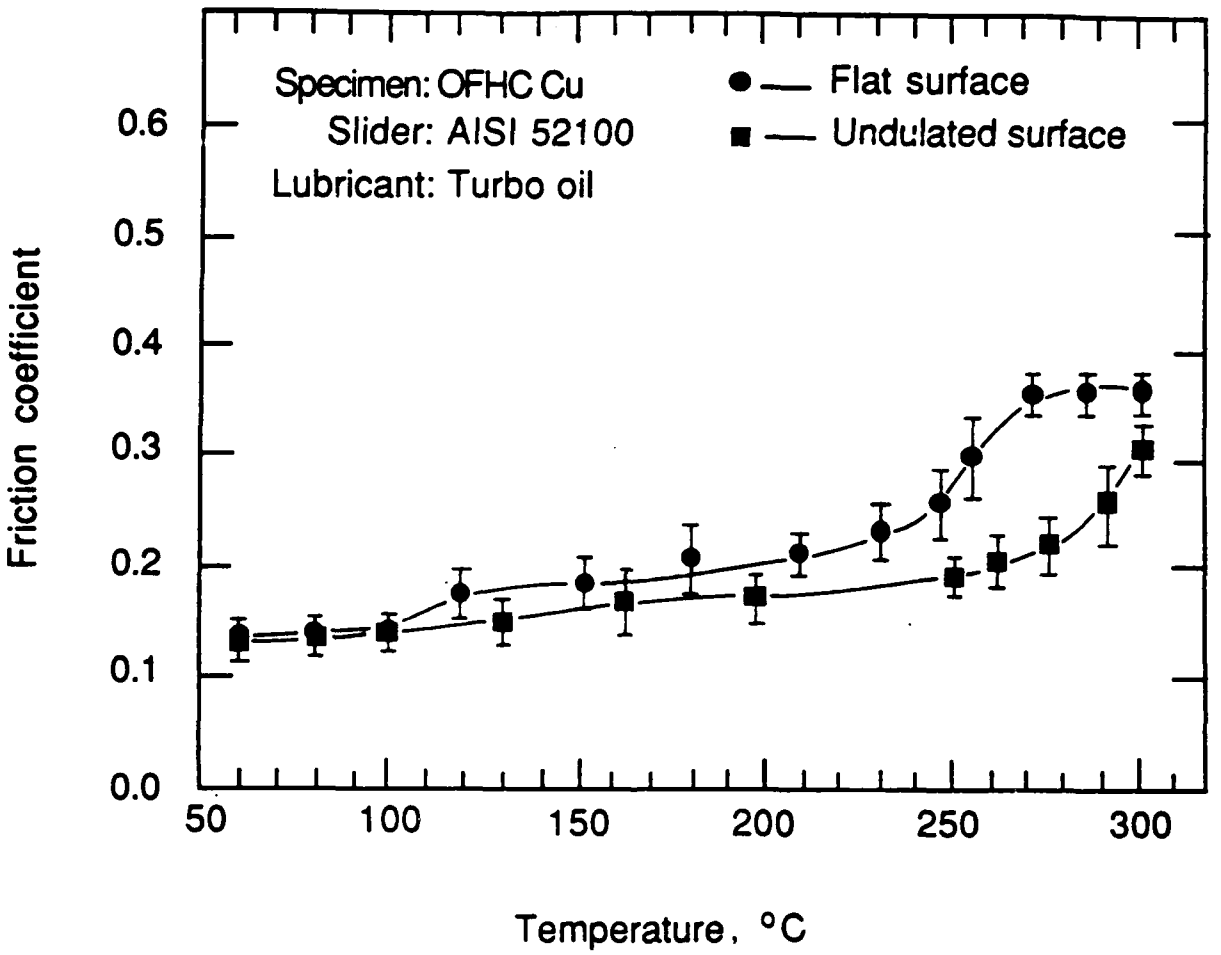

Figure 5 Friction coefficient versus temperature AISI 52100 steel on flat and undulated OFHC copper with turbo oil as lubricant

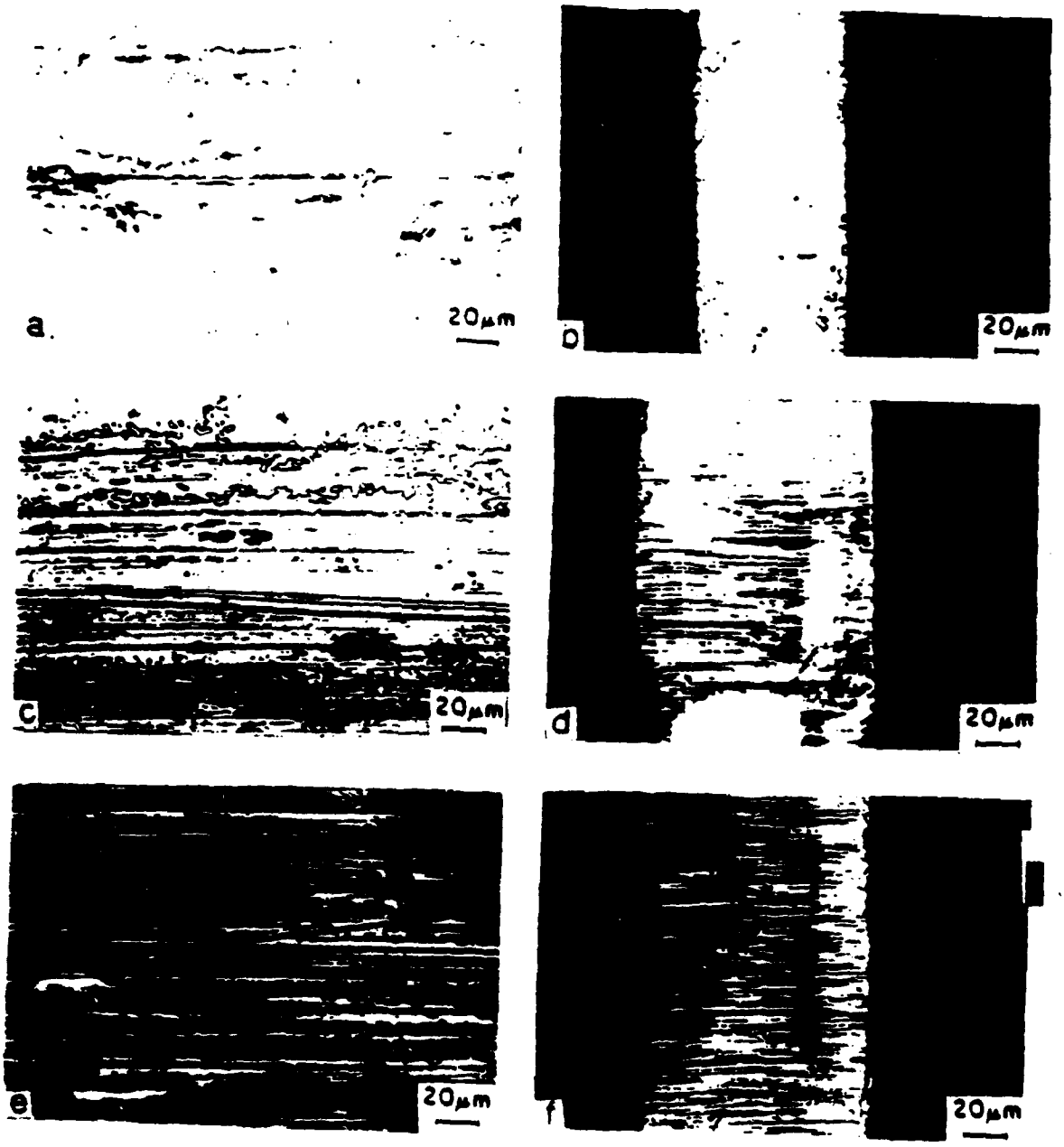

Figure 6. Micrographs of worn surfaces (slider: AISI 52100steel; lubricant: paraffin oil):
(a) flat copper surface at 60 °C
(b) undulated copper surface at 60 °C
(c) flat copper surface at 130 °C
(d) undulated copper surface at 130 °C
(e) flat copper surface at 220 °C
(f) undulated copper surface at 220 °C

observed, and the friction coefficient was low (0.20 at 130 °C). As the temperature was further increased to 220 °C, plowing grooves on the flat surfaces became wider and deeper, and the friction coefficient was increased to 0.42. While many fine grooves were observed on the undulated surfaces, the friction coefficient was only 0.26 at 220 °C.

The corresponding surface profiles are shown in Figure 7. Before the transition, the depth of plowing grooves was about 0.04 μm on both the flat and the undulated surfaces. At the transition temperature, the average depth of plowing grooves on the flat surfaces was 0.1 μm. At 220 °C, the depth of plowing grooves on the flat surfaces was about 0.3 μm. The profiles of the undulated surfaces (Figures 7b, 7d and 7f) show that as temperature increases, the number of plowing grooves increases but the depth of the plowing grooves is essentially unchanged. Before the transition temperature, the depth of plowing grooves on the undulated surfaces was 0.04 μm. After the transition, the depth of grooves was about 0.06μm.

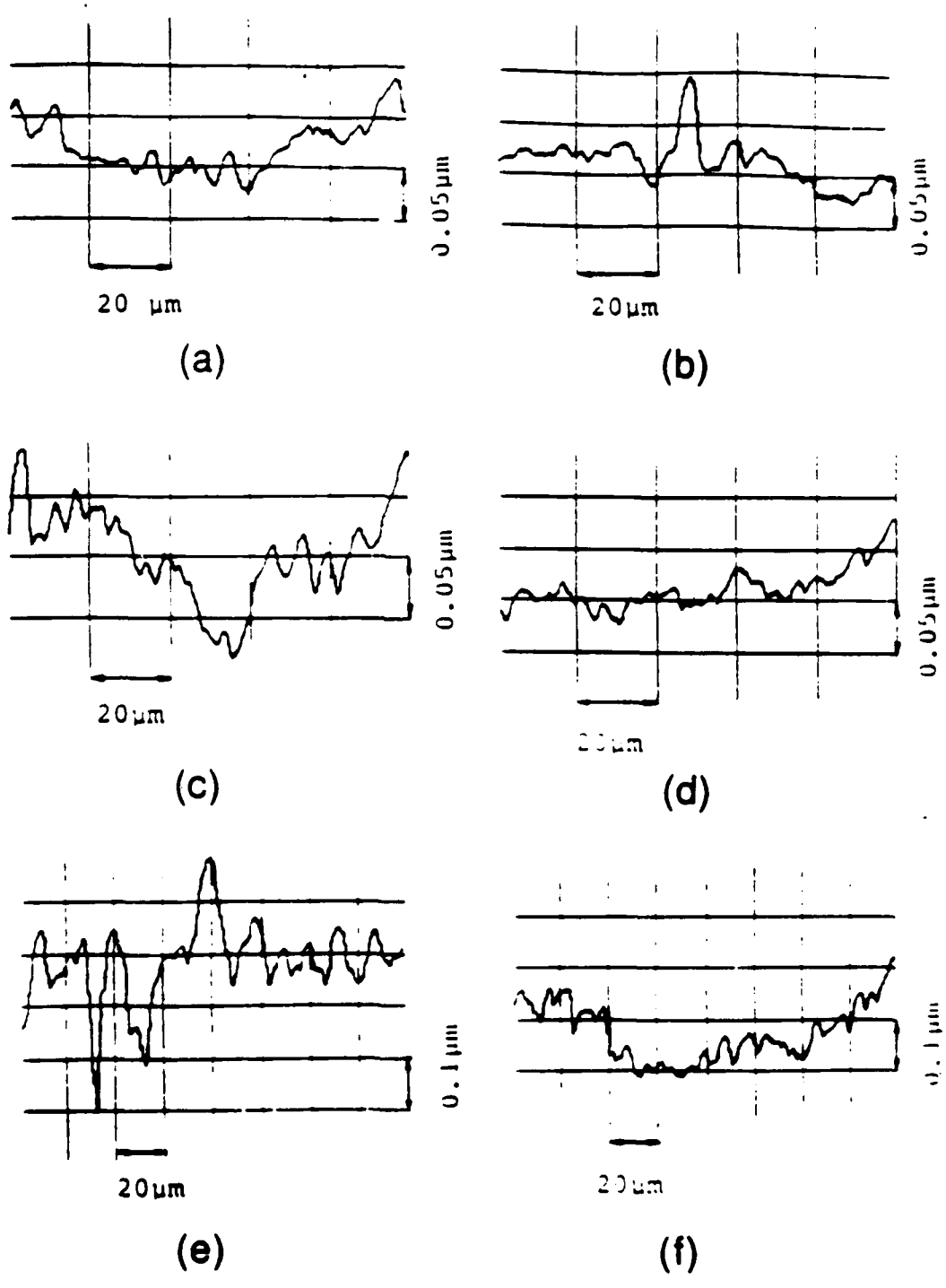

Figure 7. Profiles of worn surfaces (slider: AISI 52100steel; lubricant: paraffin oil):
(a) flat copper surface at 60 °C
(b) undulated copper surface at 60 °C
(c) flat copper surface at 130 °C
(d) undulated copper surface at 130 °C
(e) flat copper surface at 220 °C
(f) undulated copper surface at 220 °C

IV. DISCUSSION

A. Transition temperature

The interfacial temperature, T_i, is the sum of two parts: the bulk temperature of the lubricant, T_b, and the "flash" temperature rise, T_f. Thus

$$T_i = T_b + T_f \tag{1}$$

T_b can be measured and controlled, but T_f can only be estimated from theoretical models [10-13]. According to reference [13], a simple estimate of the flash temperature can be given as

$$T_f = \frac{\mu V}{4(k_1 + k_2)} \left[\frac{\pi p L}{n}\right]^{1/2} \tag{2}$$

where μ is the friction coefficient, V the sliding velocity, p the hardness of the softer material, L the normal load, and k_1 and k_2 are the thermal conductivities of the sliding pair, and n is the number of contacting asperities. Assuming that the radius of the contacting asperities is from 5 to 100 μm and that the real contact area is given by the relation $L=pA_r$ (A_r is the real contact area), the number of contacting asperities is 1-16. Substituting n=1 or 16, μ=0.3, L=0.98 N, V=0.01 m/s, p=784 MPa, k_{Cu}=386 J/msK and k_{Steel}=40 J/msK into Equation (2), the temperature rise is about 0.08 or 0.02 °C. The contribution from frictional heat to the interfacial temperature therefore is negligible in this study. The interfacial temperature is thus essentially the bulk temperature of the lubricant, and the transition temperature can be directly determined from the bulk temperature of the lubricant and the friction coefficient.

B. Mechanisms of friction

According to the classical boundary lubrication model, which is based in part on the adhesion theory of friction, the friction coefficient is assumed to be the weighted sum of the component due to lubricant shear and the component due to adhesion at "unlubricated" solid-solid contacts. Recent investigations suggest, however, that the contribution due to plowing by hard asperities and wear particles should not be ignored. For example, Komvopoulos et al. [14] have investigated the primary friction mechanisms in boundary lubricated sliding and have confirmed in fact that plowing is the key mechanism of friction. In the present investigation also, plowing grooves were observed on worn surfaces before and after the transition. In order to quantitatively analyze the plowing friction before and after the transition, therefore, an appropriate plowing model should be considered.

Assume that wear particles and hard asperities are spherical (see Figure 8). By following the

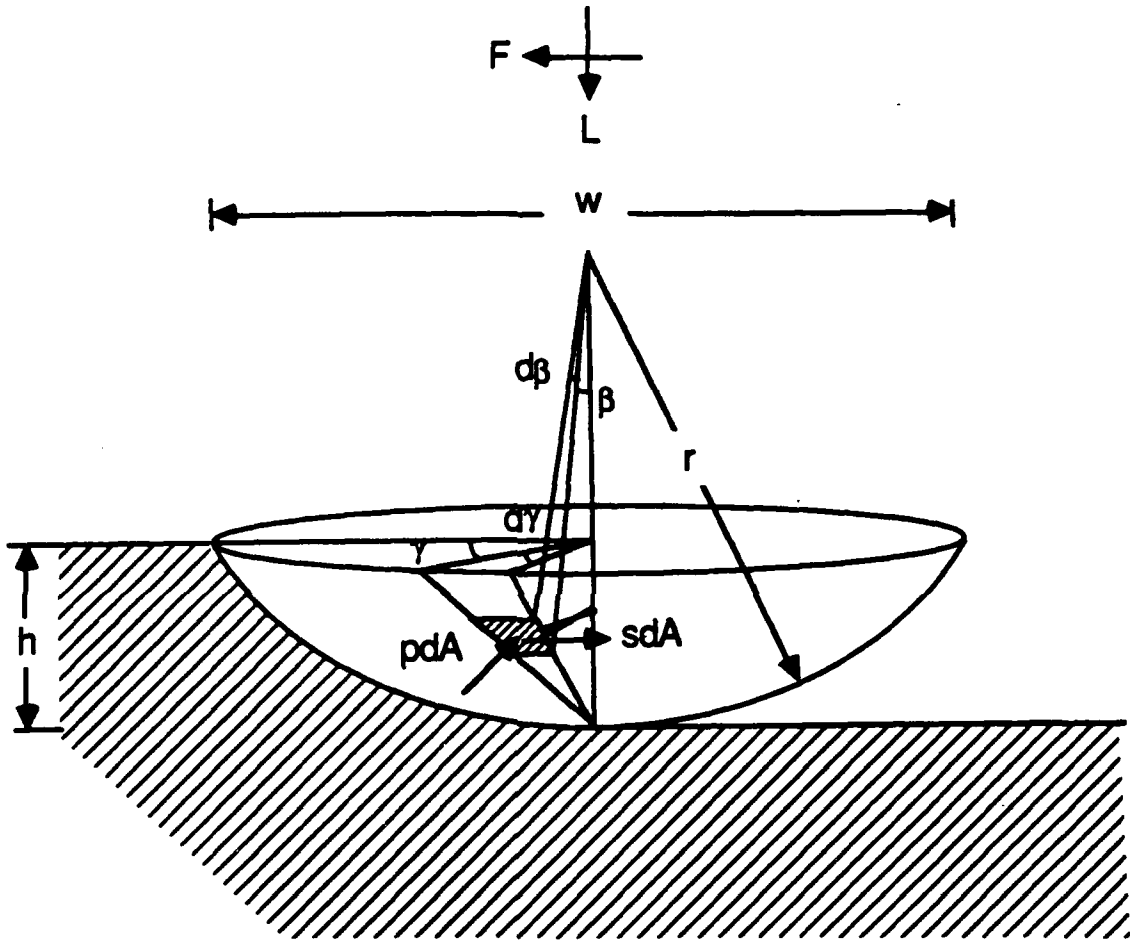

Figure 8. Plowing model for boundary lubricated sliding

procedure outlined in reference [9], the friction coefficient can be given as (see the Appendix)

$$\mu = \mu_p + \mu_s \tag{3}$$

where

$$\mu_p = \frac{2\sum_{i=1}^{N} \{\sin^{-1}[2(\frac{h}{r})_i - (\frac{h}{r})_i^2]^{1/2} - [2(\frac{h}{r})_i - (\frac{h}{r})_i^2]^{1/2}[1 - (\frac{h}{r})_i]\}}{\pi \sum_{i=1}^{N} [2(\frac{h}{r})_i - (\frac{h}{r})_i^2]^{1/2}} \tag{4}$$

$$\mu_s = \frac{2\sum_{i=1}^{N} \frac{s}{3s_m}(\frac{h}{r})_i}{\pi \sum_{i=1}^{N} [2(\frac{h}{r})_i - (\frac{h}{r})_i^2]^{1/2}} \tag{5}$$

The first term in Equation (3), μ_p, represents the friction coefficient due to pure plowing and the second term, μ_s, the friction coefficient due to the adhesive interactions between the wear particles and the surface being plowed. In Equations (4) and (5), N is the number of measurements, h the penetration depth, r the radius of the wear particle and the ratio s/s_m the interfacial friction condition. For "ideal" boundary lubrication this ratio approaches zero, and for dry sliding the interfacial shear stress approaches the shear strength and thus the ratio has a value close to unity.

For each specimen, twelve measurements of the indentation diameter, w, i.e., the width of the plowing grooves, and the penetration depth, h, are taken from the profiles of worn surfaces. All the twelve measurements were made on the same profile which was taken in the middle third of the stroke. Then by substituting the twelve values of h/r calculated from Equation (A18) into Equation (4), the plowing friction coefficient, μ_p, was obtained. The sliding component of friction, μ_s, was obtained from Equation (3) by substracting μ_p from the experimental friction coefficinet, μ_{exp}. Finally, the ratio s/s_m was determined from Equation (5). All these values for the flat surfaces with different lubricants are listed in Table 2.

At temperatures far below the transition temperature, lubricant molecules effectively adsorb on metal surfaces, and the ratio s/s_m calculated from Equation (5) is about 0.25-0.40, which is reasonably close to the value for boundary lubricated sliding. The friction coefficients due to shearing of lubricant films and adhesion between asperities, μ_s, are very small (less than 0.05), but

the plowing friction component, μ_p, is large and contributes about 80 percent to the total friction coefficients. As the temperature increases, the lubricant molecules desorb from the metal surfaces and more metal-to-metal contacts occur, leading to adhesion and wear particle formation. The wear particles so formed plow the sliding surfaces, which in turn results in high friction. It can be seen from Table 2 that after transition, the mean value of (h/r) increases and the calculated s/s_m ratio approaches very high values (0.64-0.93), as in dry sliding. This indicates that the interfacial friction conditions have changed from moderate but effective lubrication to ineffective lubrication as the temperature increases. The increases in μ_p, due to plowing by the wear particles, and in μ_s, due to desorption of lubricant molecules and to more metal-to-metal contacts, in turn result in a high friction coefficients at temperatures above the transition temperature. Plowing is the dominant component of friction, contributing about 85 percent to the totle friction coefficient.

C. Role of surface undulations

Similar calculations were performed for the undulated surfaces and are listed in Table 3. Before the transition, all the values in Table 3 are almost the same as those in Table 2. That is, surface undulations have little effect at temperatures below the transition temperature because the plowing friction at low temperatures is due perhaps to hard asperities. After the transition, desorption of lubricant molecules changes the interfacial friction conditions. The ratio s/s_m and friction component μ_s are increased to almost the same values as in the case of flat surfaces. However, the mean value of (h/r) and the plowing component of friction μ_p have been considerably reduced, which in turn results in low total friction even after the transition.

Desorption of lubricant molecules from metal surfaces depends on the properties of materials and lubricants, and especially on the temperature at the contacting asperities. When the interfacial temperature of the sliding surfaces reaches the transition temperature, the lubricants start to desorb physicochemically no matter whether the surfaces are flat or undulated. As a result the friction coefficients of both flat and undulated surfaces should start increasing at the same temperature. From Figures 2 to 5, the friction coefficients of both the flat and the undulated surfaces indeed start increasing at almost the same temperature. As the temperature is increased further, more and more metal-to-metal contacts generate wear particles. These wear particles plow the flat surfaces and the friction coefficients increase sharply. Even with the undulated surfaces more and more metal contacts generate wear particles. But these wear particles are trapped in the cavities of the undulations instead of contributing to severe plowing. Therefore at temperatures above the transition temperature, the friction coefficients of the undulated surfaces are lower than those of the flat surfaces due to the elimination of wear particles, but is somewhat higher than the friction coefficients at temperatures far below the transition temperature due to the desorption of lubricants.

Table 2 Experimental and Theoretical Friction Coefficients of Flat Surfaces *

Lubricant	Before transition						After transition					
	T (°C)	μ_{exp}	μ_p	μ_s	$(\frac{h}{r})_m \times 10^{-3}$	$\frac{s}{s_m}$	T (°C)	μ_{exp}	μ_p	μ_s	$(\frac{h}{r})_m \times 10^{-3}$	$\frac{s}{s_m}$
Mineral oil	90	0.15	0.133	0.017	2.11	0.30	220	0.42	0.367	0.053	62.8	0.85
Paraffin oil	90	0.14	0.119	0.021	0.57	0.40	220	0.42	0.362	0.058	55.6	0.92
Turbo oil	90	0.13	0.114	0.016	0.54	0.30	300	0.37	0.332	0.038	51.6	0.64
Silicone oil	60	0.13	0.116	0.047	1.10	0.25	250	0.37	0.312	0.058	99.6	0.93

* Slider: AISI 52100 steel Disk: OFHC copper Load: 100g

Table 3 Experimental and Theoretical Friction Coefficients of Undulated Surfaces *

Lubricant	Before transition						After transition					
	T (^{o}C)	μ_{exp}	μ_p	μ_s	$\left(\frac{h}{r}\right)_m \times 10^{-3}$	$\frac{s}{s_m}$	T (^{o}C)	μ_{exp}	μ_p	μ_s	$\left(\frac{h}{r}\right)_m \times 10^{-3}$	$\frac{s}{s_m}$
Mineral oil	90	0.14	0.126	0.014	1.25	0.28	220	0.22	0.169	0.051	11.2	0.91
Paraffin oil	90	0.14	0.120	0.020	0.92	0.41	220	0.26	0.212	0.048	23.8	0.87
Turbo oil	90	0.12	0.107	0.013	0.36	0.27	300	0.31	0.267	0.043	24.0	0.75
Silicone oil	60	0.12	0.105	0.015	1.05	0.26	250	0.24	0.186	0.054	14.4	0.95

* Slider: AISI 52100 steel Disk: OFHC copper Load: 100g

V. CONCLUSIONS

(1) As the temperature of lubricants increases, desorption of lubricant molecules leads to the change of interfacial friction conditions and to severe plowing.

(2) The experimental data and the calculations based on the proposed plowing model support the thoery that plowing by hard asperities and wear particles is the predominant friction mechanism in boundary lubricated sliding.

(3) At temperatures above the transition temperature, undulated surfaces maintain low friction even with additive-free lubricants. While surface undulations do not change the transition temperature of lubricants and the interfacial friction conditions, they eliminate plowing by wear particles, thereby keeping the friction coefficient at a low value.

APPENDIX

Plowing by Spherical Wear Particles

For a spherical wear particle of radius r (Figure 8), the elemental normal load, dL, and the elemental friction force, dF, acting on an elemental area dA at an angle β are given by

$$dL = p \cos\beta \, dA \tag{A1}$$

$$dF = p \sin\beta \cos\gamma \, dA + s \sin\gamma \, dA \tag{A2}$$

where $dA = r^2 \sin\beta \, d\beta \, d\gamma$, and p and s are respectively the interfacial normal pressure and shear stress. Intergrating Equations (A1) and (A2) over the front half of the spherical surface,

$$L = \frac{\pi}{2} p r^2 \left[2\left(\frac{h}{r}\right) - \left(\frac{h}{r}\right)^2\right] \tag{A3}$$

$$F = p r^2 \left\{\sin^{-1}\left[2\left(\frac{h}{r}\right) - \left(\frac{h}{r}\right)^2\right]^{1/2} - \left[2\left(\frac{h}{r}\right) - \left(\frac{h}{r}\right)^2\right]^{1/2}\left[1 - \left(\frac{h}{r}\right)\right]\right\} + 2 s r^2 \left(\frac{h}{r}\right) \tag{A4}$$

where L is the normal load and F the friction force, and the ratio (h/r) represents the extent of penetration of the wear particle. Let $\sigma(r)$ and $\varphi(h/r)$ be frequency distribution functions of radius r and the ratio (h/r), respectively. Then the total normal load, L_t, and the total friction force, F_t, are given by

$$L_t = \int_0^{r_{max}} \int_0^{\left(\frac{h}{r}\right)_{max}} L \, \sigma(r) \, \varphi\left(\frac{h}{r}\right) \, dr \, d\left(\frac{h}{r}\right) \tag{A5}$$

$$F_t = \int_0^{r_{max}} \int_0^{\left(\frac{h}{r}\right)_{max}} F \, \sigma(r) \, \varphi\left(\frac{h}{r}\right) \, dr \, d\left(\frac{h}{r}\right) \tag{A6}$$

Assuming that radius r and the penetration depth h are independent, the radius r and the ratio h/r are also independent. Then Equations (A5) and (A6) can be further written as

$$L_t = A \int_0^{r_{max}} r^2 \sigma(r)\, dr \tag{A7}$$

$$F_t = B \int_0^{r_{max}} r^2 \sigma(r)\, dr \tag{A8}$$

where

$$A = \frac{\pi}{2} p \int_0^{(\frac{h}{r})_{max}} \left[2(\frac{h}{r}) - (\frac{h}{r})^2\right] \varphi(\frac{h}{r})\, d(\frac{h}{r}) \tag{A9}$$

$$B = p \int_0^{(\frac{h}{r})_{max}} \left\{\sin^{-1}\left[2(\frac{h}{r}) - (\frac{h}{r})^2\right]^{1/2} - \left[2(\frac{h}{r}) - (\frac{h}{r})^2\right]^{1/2}\left[1 - (\frac{h}{r})\right] + \frac{2s}{p}(\frac{h}{r})\right\} \varphi(\frac{h}{r})\, d(\frac{h}{r}) \tag{A10}$$

Thus the friction coefficient μ can be expressed as

$$\mu = \frac{F_t}{L_t} = \frac{B}{A} \tag{A11}$$

i.e.,

$$\mu = \frac{2 \int_0^{(\frac{h}{r})_{max}} \left\{\sin^{-1}\left[2(\frac{h}{r}) - (\frac{h}{r})^2\right]^{1/2} - \left[2(\frac{h}{r}) - (\frac{h}{r})^2\right]^{1/2}\left[1 - (\frac{h}{r})\right] + \frac{2s}{p}(\frac{h}{r})\right\} \varphi(\frac{h}{r})\, d(\frac{h}{r})}{\pi \int_0^{(\frac{h}{r})_{max}} \left[2(\frac{h}{r}) - (\frac{h}{r})^2\right]^{1/2} \varphi(\frac{h}{r})\, d(\frac{h}{r})} \tag{A12}$$

Assuming that the normal pressure p is approximately equal to six times the shear strength of the soft materials and that N measurements of the ratio (h/r) are available, Equation (A12) can be approximated as

$$\mu = \frac{2\sum_{i=1}^{N}\left\{\sin^{-1}\left[2\left(\frac{h}{r}\right)_i - \left(\frac{h}{r}\right)_i^2\right]^{1/2} - \left[2\left(\frac{h}{r}\right)_i - \left(\frac{h}{r}\right)_i^2\right]^{1/2}\left[1 - \left(\frac{h}{r}\right)_i\right] + \frac{s}{3s_m}\left(\frac{h}{r}\right)_i\right\}}{\pi\sum_{i=1}^{N}\left[2\left(\frac{h}{r}\right)_i - \left(\frac{h}{r}\right)_i^2\right]^{1/2}} \qquad \text{(A13)}$$

When $s/s_m=0$, Equation (A13) represents the friction coefficient due to pure plowing. Therefore, Equation (13) can be rewritten as the sum of the sliding component of friction, μ_s, and the plowing component of friction, μ_p, i.e.

$$\mu = \mu_p + \mu_s \qquad \text{(A14)}$$

where

$$\mu_p = \frac{2\sum_{i=1}^{N}\left\{\sin^{-1}\left[2\left(\frac{h}{r}\right)_i - \left(\frac{h}{r}\right)_i^2\right]^{1/2} - \left[2\left(\frac{h}{r}\right)_i - \left(\frac{h}{r}\right)_i^2\right]^{1/2}\left[1 - \left(\frac{h}{r}\right)_i\right]\right\}}{\pi\sum_{i=1}^{N}\left[2\left(\frac{h}{r}\right)_i - \left(\frac{h}{r}\right)_i^2\right]^{1/2}} \qquad \text{(A15)}$$

$$\mu_s = \frac{2\sum_{i=1}^{N}\frac{s}{3s_m}\left(\frac{h}{r}\right)_i}{\pi\sum_{i=1}^{N}\left[2\left(\frac{h}{r}\right)_i - \left(\frac{h}{r}\right)_i^2\right]^{1/2}} \qquad \text{(A16)}$$

The indentation diameter w and the penetration depth h are the two parameters that have been obtained from the profiles of worn surfaces in the present investigation. Then the ratio (h/r) was determined from the relations

$$r^2 = (r - h)^2 + \left(\frac{w}{2}\right)^2 \qquad \text{(A17)}$$

$$2\left(\frac{h}{r}\right) - \left(\frac{h}{r}\right)^2 = 4\left[\left(\frac{2h}{w}\right) + \left(\frac{w}{2h}\right)\right]^{-2} \qquad \text{(A18)}$$

REFERENCES

[1] Bowden, F.P., and Tabor, D., "Mechanism of Boundary Lubrication," Chap. X, *The Friction and Lubrication of Solids*, Oxford University Press, pp200-227 (1950).

[2] Tabor, D., "Effect of Temperature on Lubricant Films," *Nature*, **145**, p308 (1940).

[3] Frewing, J.J., "The Influence of Temperature on Boundary Lubrication," *Proc. Roy. Soc.*, **A181**, pp23-42 (1942).

[4] Barwell, F.T., and Milne, A.A., "The Lubrication of Rough Steel Surfaces by a Series of Metallic Soaps," *Brit. J. Appl. Phys., (Physics of Lubrication)*, No.1, pp44-48 (1951).

[5] Russell, J.A., Campbell, W.E., Burton, R.A., and Ku, P.M., "Boundary Lubrication Behavior of Organic Films at low Temperature," *ASLE Trans.*, **8**, No.1 pp48-58 (1965).

[6] Kapsa, Ph., and Martin, J.M., "Boundary Lubrication Films: A Review," *Tribology International*, **15**, pp37-42 (1982).

[7] Dorinson, A., and Broman, V.E., "Extreme Pressure Lubrication and Wear --- The Chemical Reaction and the Extreme Pressure Action of Two Aliphatic Disulfides," ASLE Trans., 5, N0.1, pp75-90 (1962).

[8] Paleari, C., Girelli, A., and Siniramed, C., "Evaluation of Anti-Seizing and Recovery-from-Seizing Properties of E.P. Lubricants by Four-Ball Machine," *J. Inst. Pet.*, **44**, No4, pp178-181 (1958).

[9] Tian, H., Saka, N., and Suh, N.P., "Boundary Lubrication Studies on Undulated Titanium Surfaces," *ASLE Trans.* (submitted for publication), (1987).

[10] Blok, H., "Theoretical Study of Temperature Rise at Surfaces of Actual Contact under Oilness Lubrication Condition," *Proc. Inst. Mech. Eng. General Lubrication Discussion*, Group IV, pp429-441 (1937).

[11] Archard, J.F., "The Temperature of Rubbing Surfaces," *Wear*, **2**, No6, pp438-455 (1959).

[12] Ling, F.F., and Pu, S.L., "Probable Interface Temperatures of Solids in Sliding Contact," *Wear*, **7**, pp23-34 (1964).

[13] Tabor, D., "Friction and Wear," *Proc. International Symposium on Lubrication and Wear*, eds. Muster, D., and Sternlight, B., Houston, Texas, pp703-765 (1963).

[14] Komvopoulos, K., Saka, N., and Suh, N.P., "The Mechanisms of Friction in Boundary Lubrication," *Journal of Tribology, ASME Trans.*, **107**, pp452-462 (1985).

DRY SLIDING OF UNDULATED SURFACES

Summary

Sliding tests were performed on flat and undulated OFHC copper and cast iron samples under various loads. Under relatively light normal loads the friction coefficient was lower with the undulated surfaces than with the flat surfaces. When the normal load was increased, however, due to excessive sub-surface deformation in OFHC copper and fracture of the undulated pattern in cast iron, the undulated surfaces did not reduce friction.

I. INTRODUCTION

In recent years, it has become increasingly evident that plowing by wear particles is an important, in some cases the dominant, friction and wear mechanism [1]. In the past, tribologists have devised many schemes to reduce friction and wear, in effect by decreasing the impact of plowing. Lubrication, hard coatings, fiber-reinforced composites are but a few examples. All these methods have found wide applications and will continue to be used. Nevertheless, there are many instances in which a proper application of a lubricant is not possible and it is not desirable to change the material structure or composition.

For example, many machine elements may be located in positions where the access is difficult for changing the lubricant or rubbing parts may have to operate in vacuum. In such cases, it may be desirable to find methods to reduce friction and wear without using a lubricant. Moreover, during the start and stop periods, when a hydrodynamic film is absent between the sliding surfaces, the friction and wear of journal bearings may be appreciable and need to be reduced. Furthermore, in many cases, using different materials, composites and coatings, etc. may not be possible because other design requirements may necessitate the bulk properties of a certain material. For instance, due to light weight requirements, materials such as aluminum or titanium may have to be used, or due to thermal and electrical conductivity requirements, copper may be the choice material.

The idea of using surfaces with microgrooves to trap wear particles, i.e., the undulated surfaces was initially proposed for the control of electrical contact resistance [2-3]. It was found that the contact resistance rises for two reasons: due to the oxidation of the wear particles which act as insulators and due to the reduction in the contact area because of the wear debris entrapped between the surfaces. It was shown [3] that the undulated surfaces entrap the oxidized wear particles and thus the contact resistance does not rise with continuing operation. Later, the same idea was extended to dry [4] and boundary lubricated sliding [5], and it was shown that friction and wear of undulated surfaces are lower than those of flat surfaces due to the reduction of plowing by wear particles.

In this study, the dry sliding of undulated surfaces was further analyzed for various normal loads and the effect of ductility on the performance of undulated surfaces was investigated. Experimental results

obtained with two different materials (OFHC Copper and cast iron) and various normal loads are presented and discussed.

II. EXPERIMENTAL

Sliding Geometry and Sample preparation

The basic sliding geometry consists of a 15 cm diameter disk and a sample which has a 2.5 cm^2 apparent contact area (Figure 1.a). The sliding surface of the sample is curved to conform the circular perimeter of the disk [6]. All surfaces of the sample are heat-insulated except for the sliding surface and the opposite surface which is in contact with the sample holder. The sample holder is made of aluminum and is cooled by circulating water. Thus the flow of frictional heat is approximately one-dimensional.

A schematic side view of the surface undulations is shown in Figure 1.a. The area fraction of the surface voids is 0.375. The undulated surface was made by precision machining of the surface with a dedicated apparatus on a vertical milling machine. (Figure 2). The sample was mounted on a rotary table and positioned such that its curved surface coincides exactly with a 15 cm diameter imaginary circle with respect to the rotary table. The undulations were cut with a 150 μm thick circular saw. After each cut, the sample was rotated by 0.3° angular intervals and another cut was made. Following this procedure, a total of about 96 parallel microgrooves were cut on the sample surface.

After machining the microgrooves on the surface, the machining marks and burrs were removed by 600 grit emery papers followed by polishing with 0.3 and 0.05 μm alumina slurries. After the polishing process, the samples were ultrasonically cleaned in acetone to remove any remaining particles inside the microgrooves.

Experimental set-up

Two different set-ups were used depending on the load requirements. The light-load apparatus shown in Figure 3 is a conventional friction tester. The normal load was applied by dead weights and the

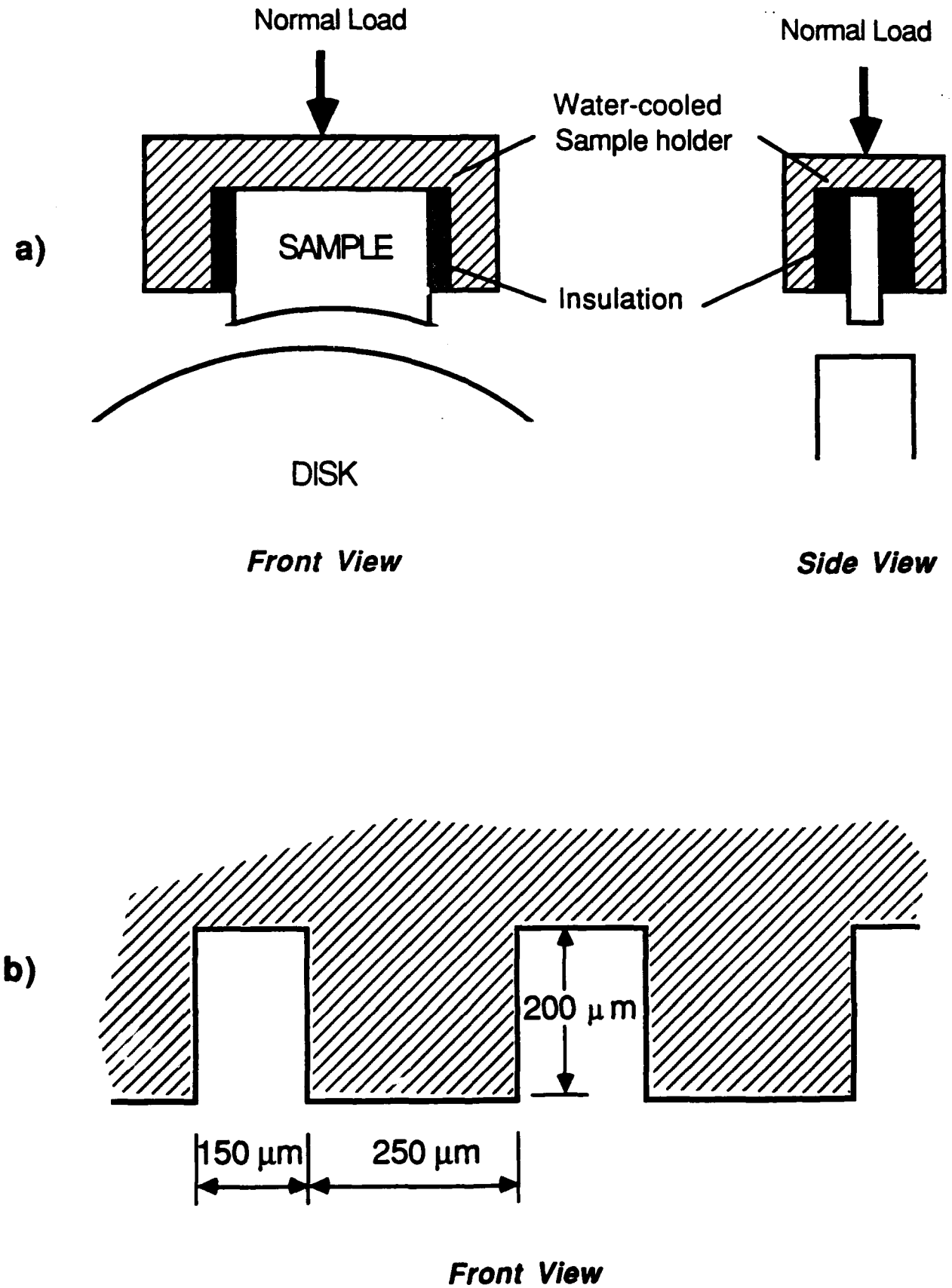

Figure 1. a) Pad-on-disk sliding geometry, b) Geometry of undulations.

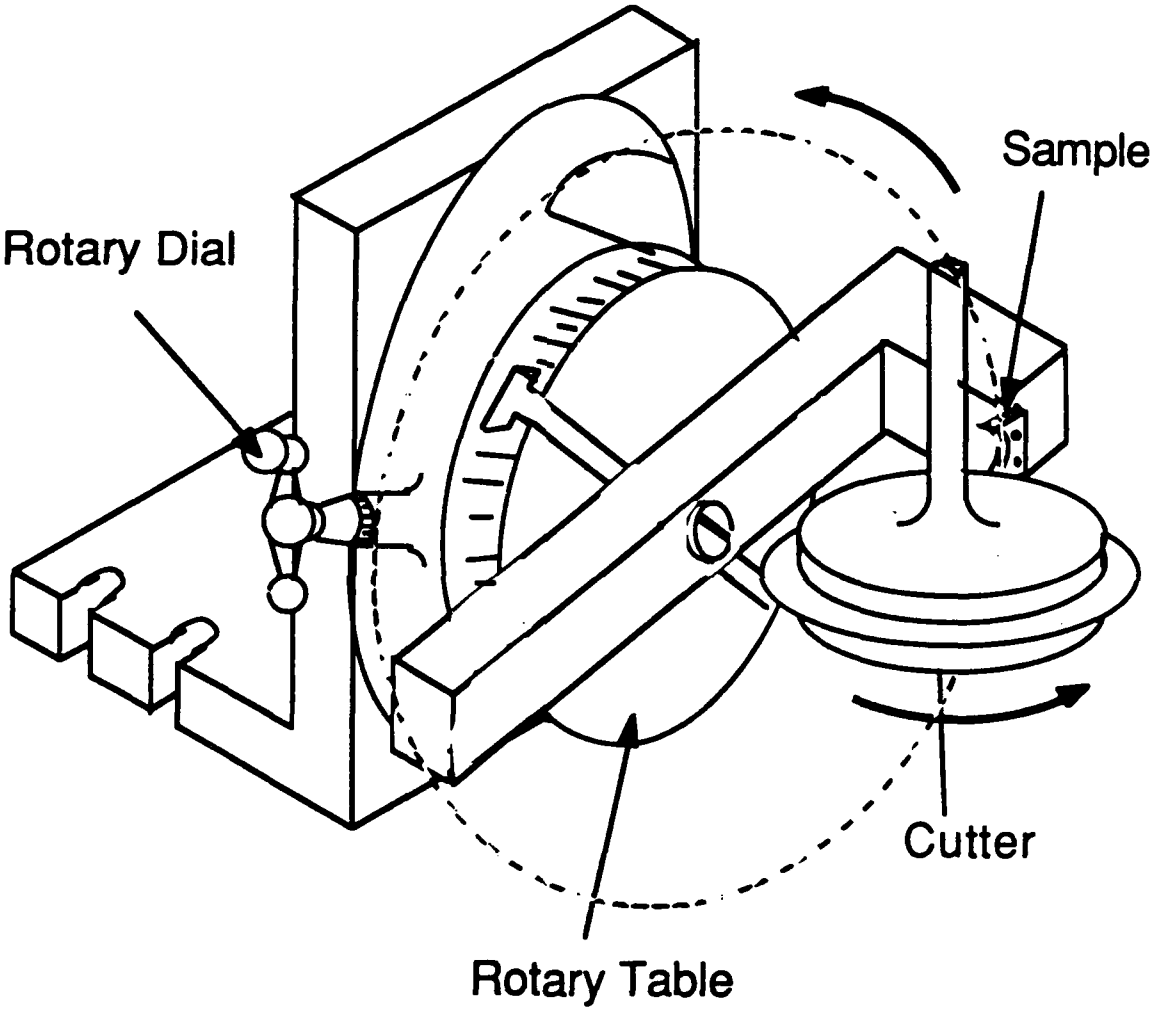

Figure 2. a) Apparatus used for cutting microgrooves on the sample surface.

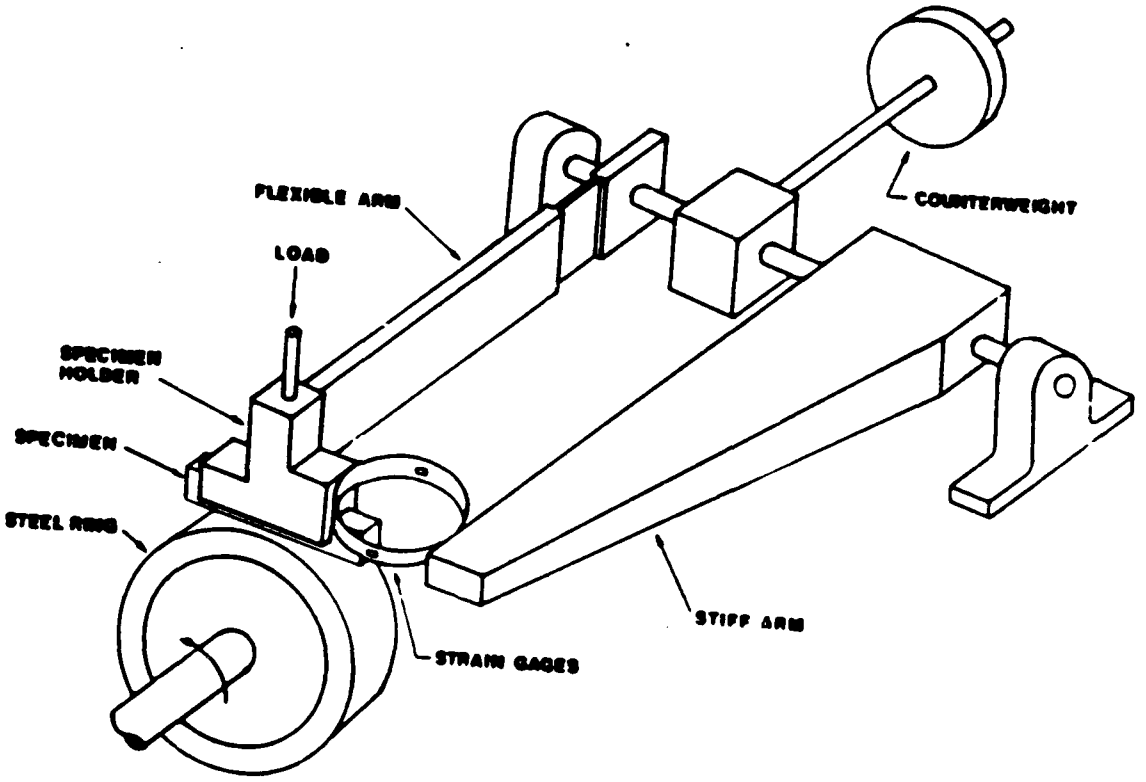

Figure 3. Friction and wear tester used in the light load range.

tangential force was measured with a strain ring. This apparatus was successfully used for normal loads less than 10 N, above which the strain ring deformed plastically and the measurements were unreliable.

A second apparatus was designed and built especially for heavy loads. The apparatus is shown in Figure 4. A pneumatic cylinder was used to apply the normal load because it could provide loads as high as 500 N very easily and occupied a relatively small space. However, it could not provide loads under 50 N because its breakaway pressure limited the minimum load. The main part of the apparatus is the loading arm assembly, which consists of the sample holder, load cells, two ball bearings, linear-displacement shafts and a connecting bar. The loading arm assembly was supported by two linear bearing and could move back and forth to load and unload the sample. The normal load was set by changing the gas pressure in the pneumatic cylinder.

The sample was mounted in a sample holder which had a self-aligning feature. It could rotate with respect to the rest of the loading arm assembly so that the sample could perfectly conform itself to the disk surface even in the presence of severe vibration. The disk was mounted on a shaft which was supported by two ball bearings. The shaft was driven by a variable-speed DC motor, whose rotational speed could be adjusted between 0-100 rpm. The exact rotational speed was measured by an optical tachometer and a reflective tape mounted on the shaft.

The normal and tangential forces were measured with strain gages mounted on the aluminum load cell. The data were acquired by a Metrabyte DASH-8 data acquisition board in combination with a EXP-16 amplifier-multiplexer and recorded in real-time with a personal computer for later processing.

Experimental Materials

Preliminary experiments showed that the performance of the undulated surfaces were very much dependent on the sliding material properties. It was also observed that the ductility of the undulated surfaces was very important in that it determined the extent of subsurface plastic deformation, fracture of the undulations, and so on. Consequently, OFHC copper, which is a typical ductile material, and cast iron, which is a brittle material were chosen for experimental study. Both materials were slid against hardened 4340 steel disks.

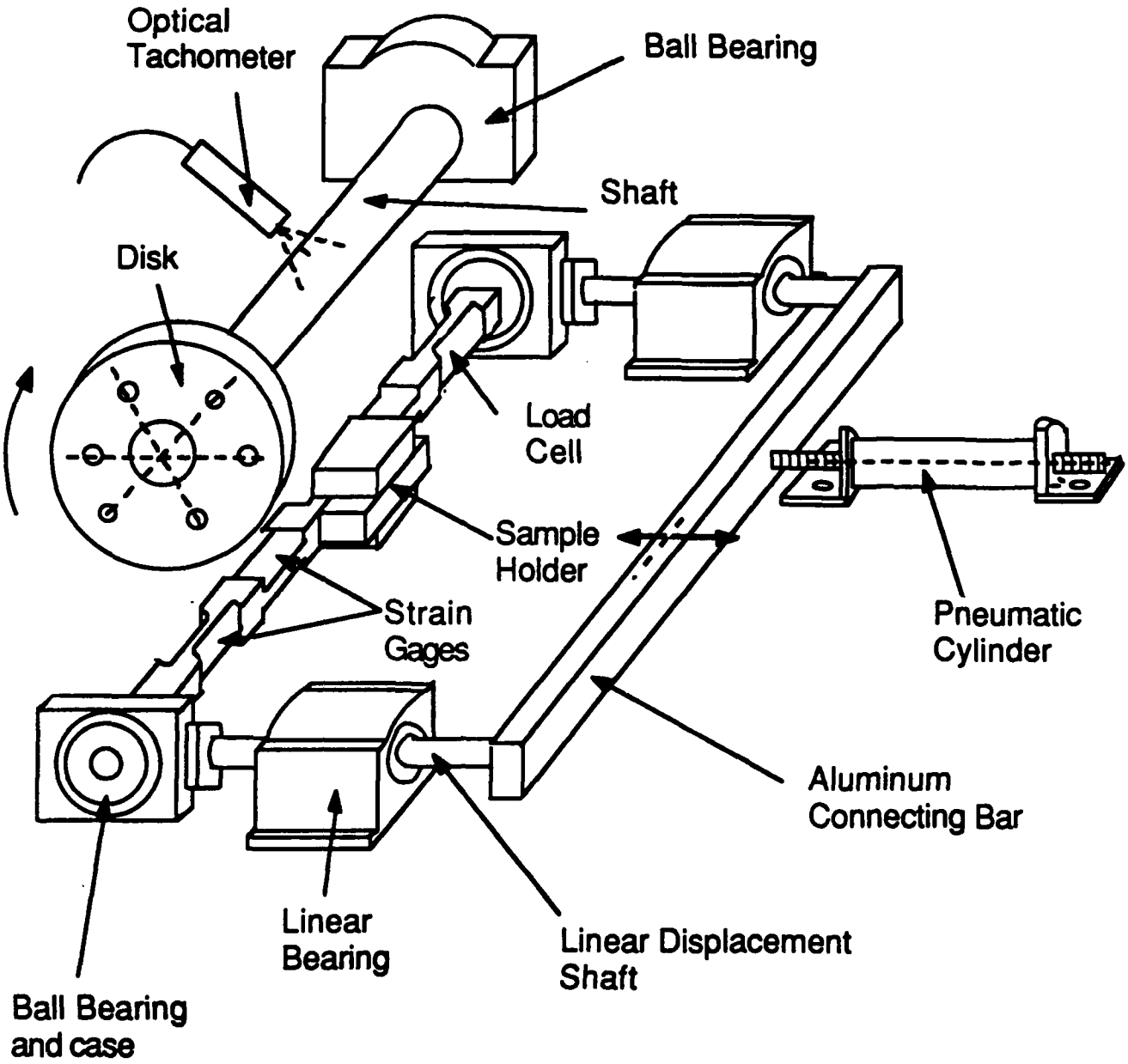

Figure 4. Friction and wear tester used in the heavy load range.

III. RESULTS AND DISCUSSION

OFHC Copper vs. 4340 Steel

A set of experiments were conducted on the sliding of OFHC copper vs. 4340 steel under the normal loads of 5, 50 and 100 N. The experimental conditions are listed in Table 1. Figure 5 shows the plots of the friction coefficient of flat and undulated surfaces, both for 5 N normal load. These experiments were conducted using the apparatus shown in Figure 3. The friction coefficient of the undulated surface was lower, both initially, 0.5 and in the steady state, 0.98, than that of the flat surface. On the other hand, the initial friction coefficient of the flat surface was 0.68 and the steady state value was 1.18.

Figure 6 shows the plots of the friction coefficients of the flat and undulated surfaces under 100 N load. The experiments were conducted on the apparatus shown in Figure 4. As opposed to the results of the experiments under 5 N normal load, the steady state friction coefficients of the flat and undulated surfaces were not markedly different, both being around 0.6. The initial friction coefficients were different in each case: 0.55 for the flat surface and 0.40 for the undulated surface.

Figures 7 and 8 are the optical micrographs showing the top and side views of the undulated surfaces after 1000 m of sliding against the 4340 steel disks, respectively. In each figure, the micrograph (a) shows the undulated surface before the test; (b), (c) and (d) show the surfaces after tests under 5, 10, 50 and 100 N, respectively. The undulated surface tested under 5 N load did not deform plastically. The microgrooves were still capable of trapping wear particles after the test. The contacting peaks of the undulated surfaces were covered with a black and blue oxide film and some plowing grooves were present (Figure 9.a). After sliding, many wear particles were present inside the grooves of the undulations (Figure 9.b), indicating that the undulated surface efficiently removed the loose wear particles.

However, the undulated surfaces tested under 10 N, 50 N and 100 N normal loads underwent a substantial surface and subsurface deformation. Some microgrooves were partially clogged and lost their capability to trap wear particles (Figure 7.d). In some cases, the entire peaks of the undulations were bent and deformed and microcracks appeared around the valleys of the undulations (Figure 8.d). Futhermore, the plowing

Table 1. Experimental Conditions

Load	5 -100 N
Sliding Speed	0.5 m/s
Sliding Distance	250 -1000 m
Ambient Temperature	295 K
Relative Humidity	10-20 %
Environment	Laboratory Air

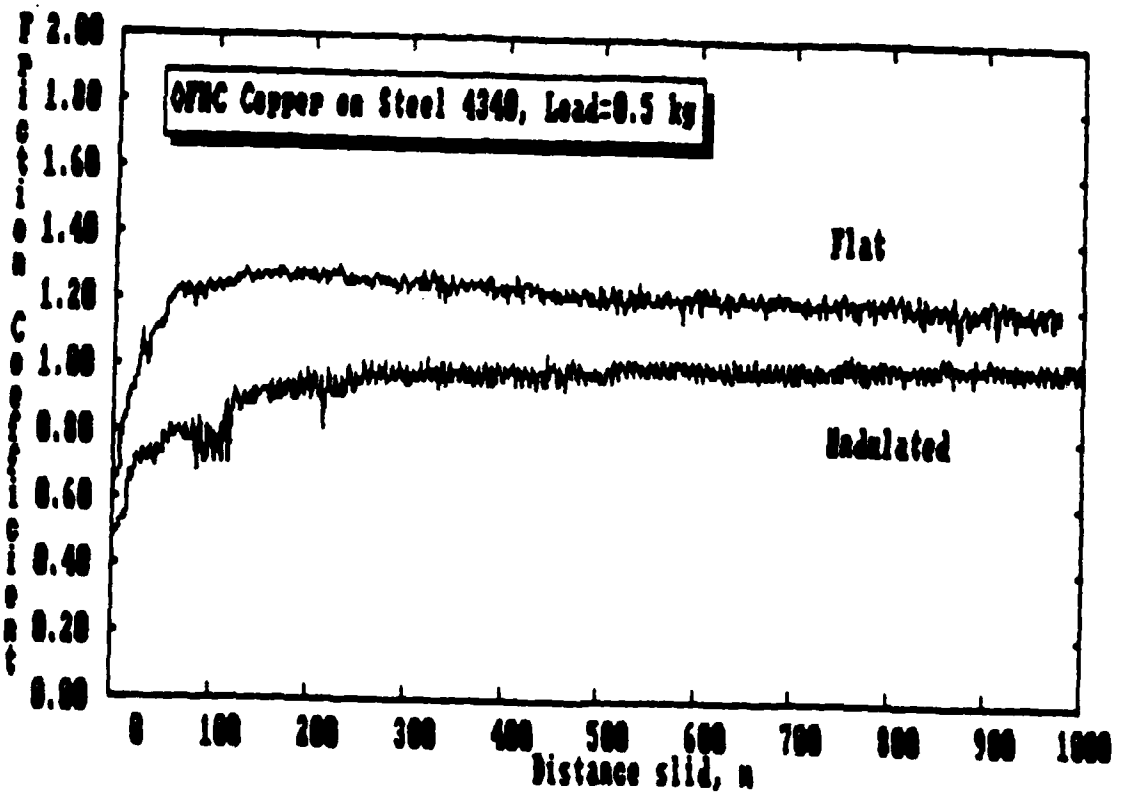

Figure 5. Friction coefficient vs. sliding distance for flat and undulated samples of OFHC copper at 5N normal load.

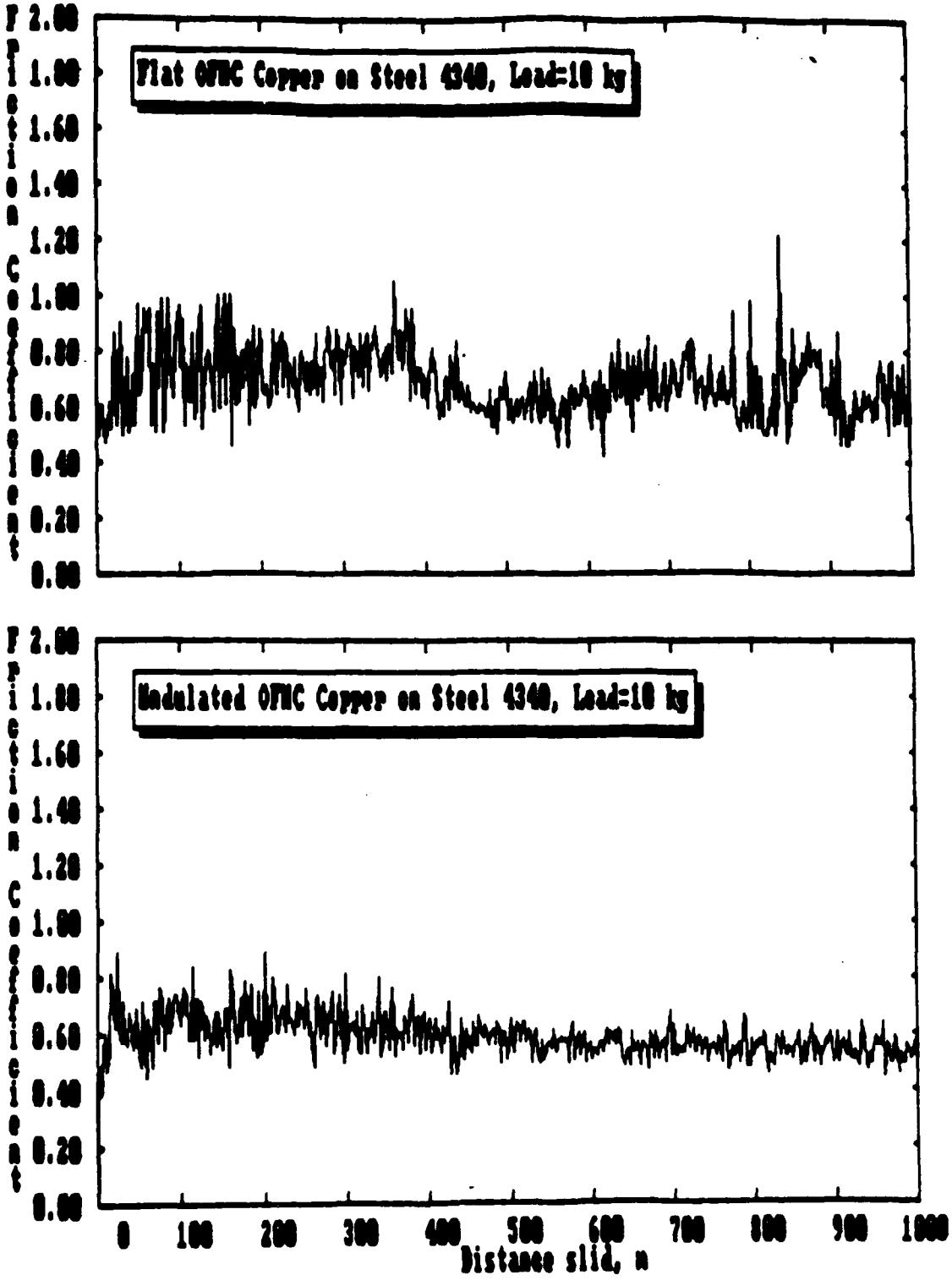

Figure 6. Friction coefficient vs. sliding distance for a) flat, and b) undulated OFHC copper at 100 N normal load.

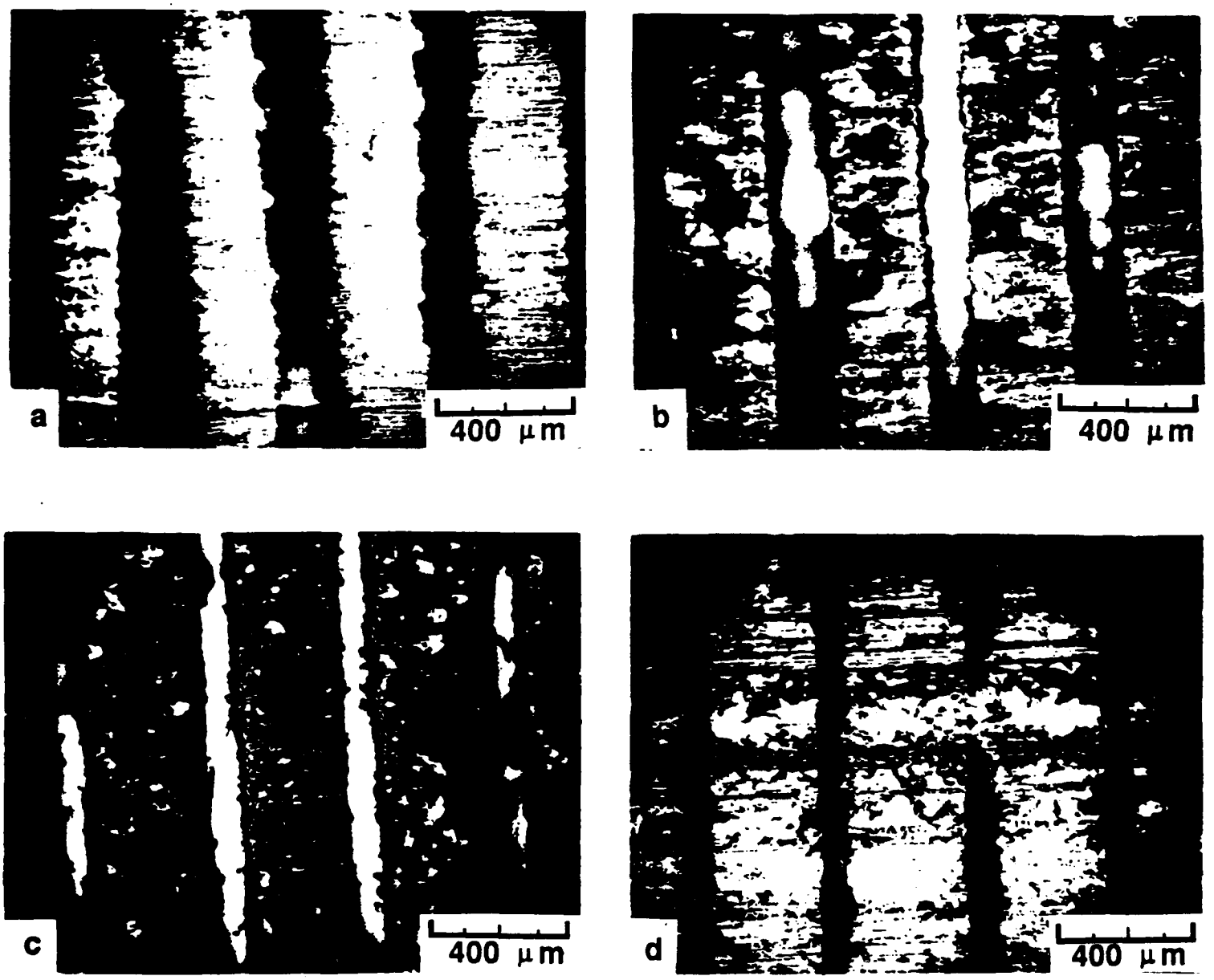

Figure 7. Top view micrographs of the undulated surfaces, a) before sliding, and after sliding at b) 5 N, c) 50 N, and d) 100 N normal loads.

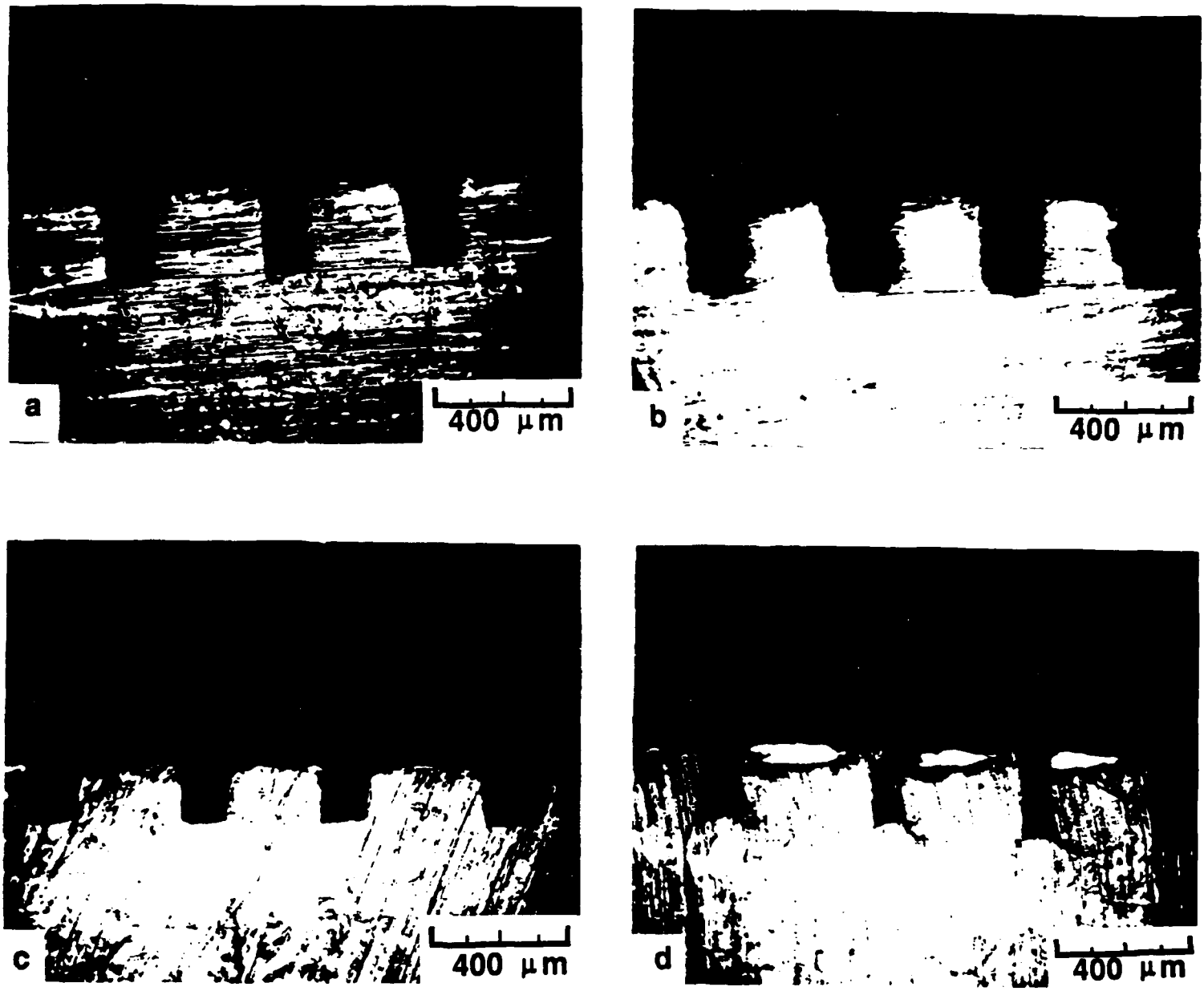

Figure 8. Side view micrographs of the undulated surfaces, a) before sliding, and after sliding at b) 5 N, c) 50 N, and d) 100 N normal loads.

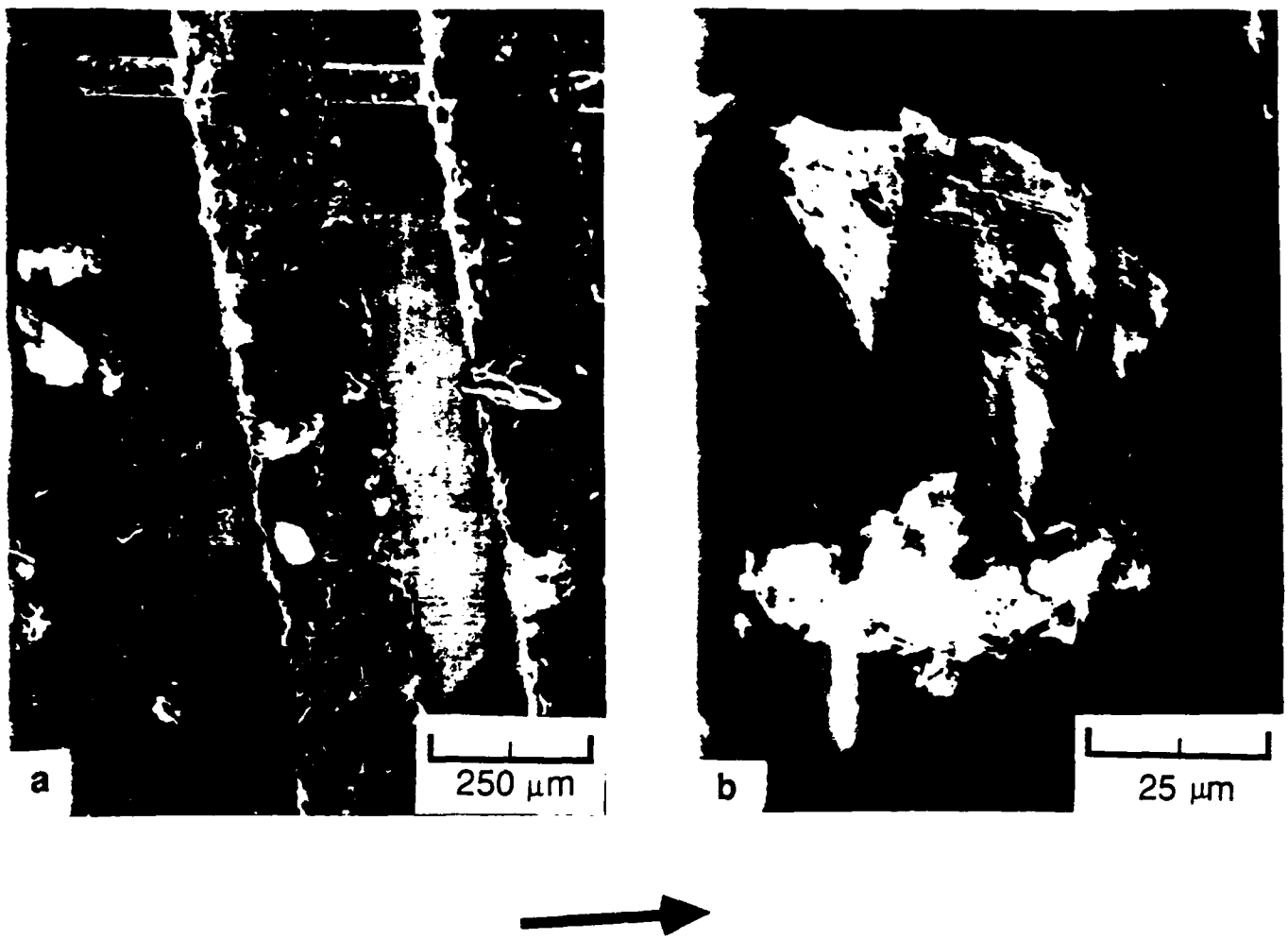

Figure 9. (a) Plowing grooves and wear particles on an OFHC copper sample after 1000 m sliding at 5 N load, (b) A higher magnification SEM micrograph of the wear particles. (The arrow indicates the sliding direction.)

grooves that are seen in the samples slid at 5 N of normal load were absent in this case. Rather the surface was covered with small pits and potholes (Figure 10.a). No loose wear particles were found inside the grooves. Instead, some wear sheets which are still connected to the plateaus of the undulations were noticed (Figure 10.b).

A similar situation was observed by several authors in the sliding of loosely sintered iron-based materials [7,8]. It was found that at relatively light loads, the pores in sintered iron acted as sites of wear particles entrapment and decreased the friction coefficient and wear rate. However, at heavier loads, the pores were clogged and were no longer effective in reducing friction and wear.

The wear sheets and the substantial sub-surface deformation observed at relatively heavy loads are characteristics of the delamination type of wear [9, 10]. As the load was increased from 5 N, the dominant wear mechanism shifted from plowing to delamination. When the dominant wear mechanism is other than plowing, the undulated surfaces do not reduce the friction coefficient and the wear rate. First of all, there are very few loose wear particles being generated at the interface to be trapped by the microgrooves. The sliding action produces displaced material rather than loose wear particles. *In fact even after ultrasonic* cleaning of the undulated samples tested at 100 N load, the measured weight loss was very small, furher confirming the observation that very few loose wear particles were generated. Consequently, the use of the undulated surfaces reduced the friction coefficient and wear when the dominant wear mechanism was plowing by loose wear particles. On the other hand, when the load was increased, the dominant wear mechanism was delamination and the use of undulated surfaces did not make a considerable difference.

Cast Iron vs. 4340 Steel

Experiments similar to those conducted on OFHC samples were also run with cast iron specimens. However, the total sliding distance was 250 m for the cast iron samples because especially at 100 N normal load, this sliding distance was large enough to wear out the undulated pattern. After the undulated pattern was completely removed, the the friction and wear behavior was the same as that of the flat surfaces. Therefore the sliding tests on cast iron specimens were terminated at shorter sliding distances.

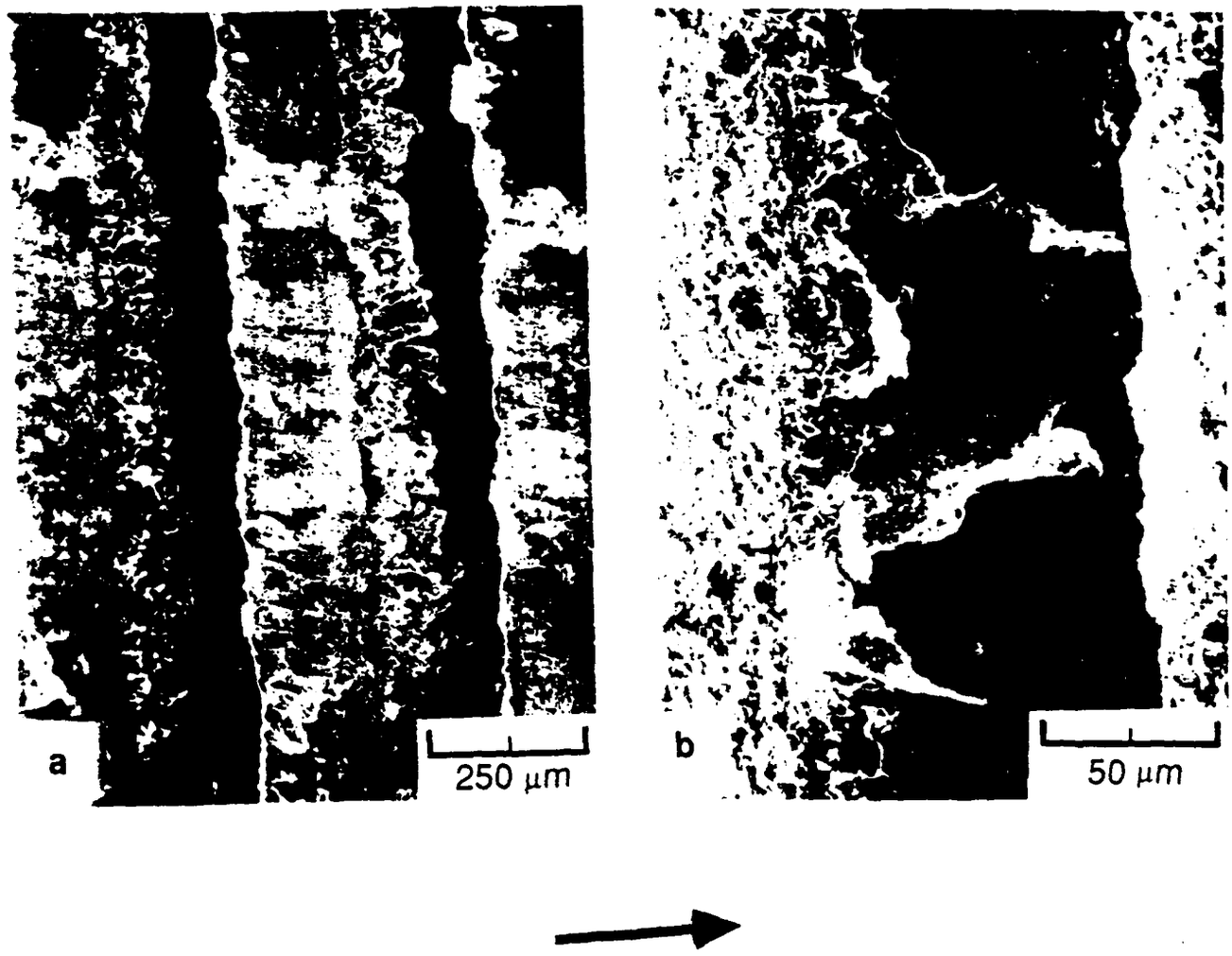

Figure 10. (a) Potholes and wear sheets on an OFHC copper sample after 1000 m sliding at 10 N load, (b) A higher magnification SEM micrograph of the wear sheets. (The arrow indicates the sliding direction.)

Figure 11 shows the plots of the friction coefficients of flat and undulated cast iron samples at 5 N normal load. The friction coefficient of the flat surfaces was 0.52 initially and rose up to about 1.2. On the other hand, the friction coefficient of the undulated surface was lower during the entire sliding test; 0.18 initially and about 1.0 after 150 m of sliding.

Similar experiments conducted on cast iron with a heavier load, i.e., 100 N produced different results (Figure 12). The initial friction coefficient was still lower, 0.22, for the undulated surface compared with that for the flat surface, which was 0.53. However, the friction coefficients in both cases increased first with the sliding distance, then dropped to about 0.5 and remained constant during the rest of sliding. During the first period of rising friction, significant amount of wear was observed. The wear particles during this period were collected and are shown in Figure 13 for both flat and undulated surface tests. The wear particles obtained from the undulated surfaces were considerably larger, in fact close to the size of the undulations. This observation suggests that during sliding, the undulations underwent a brittle fracture process (Figure 14).

IV. CONCLUSIONS

1. When the normal load is relatively small (5 N), the friction coefficient of the undulated surfaces was lower than that of the flat surfaces under the same experimental conditions due to the entrapment of the wear particles.

2. Under heavier normal loads, e.g. 50-100 N, the friction coefficients of the undulated and flat surfaces were not significantly different.

3. The undulations on the OFHC samples were plastically deformed in the heavily loaded cases. Under 100 N normal load, the microgrooves were mostly clogged with deformed material and became ineffective in trapping the wear debris.

4. The cast iron undulated surfaces underwent a brittle fracture process. After a short sliding period, all the undulations were removed by fracture.

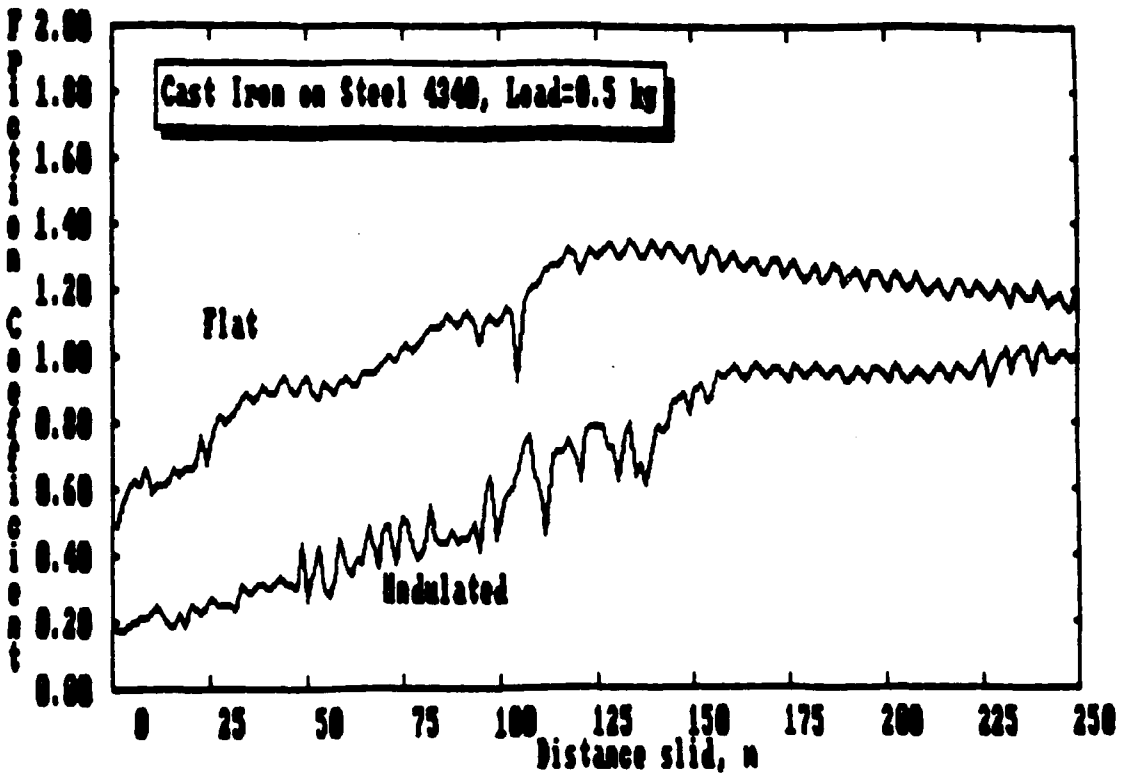

Figure 11. Friction coefficient vs. sliding distance for flat and undulated samples of cast iron at 5N normal load.

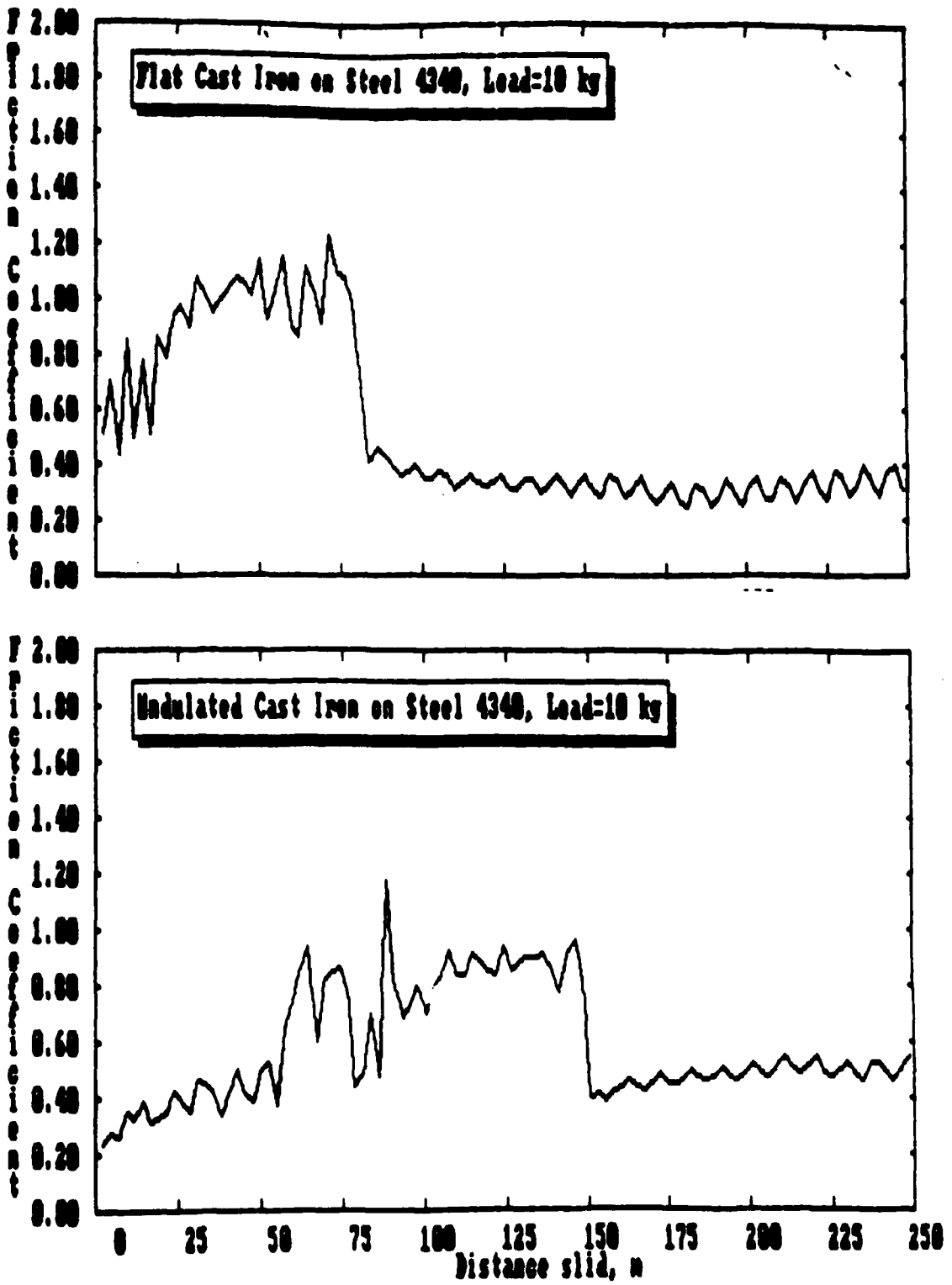

Figure 12. Friction coefficient vs. sliding distance for a) flat, and b) undulated cast iron at 100 N normal load.

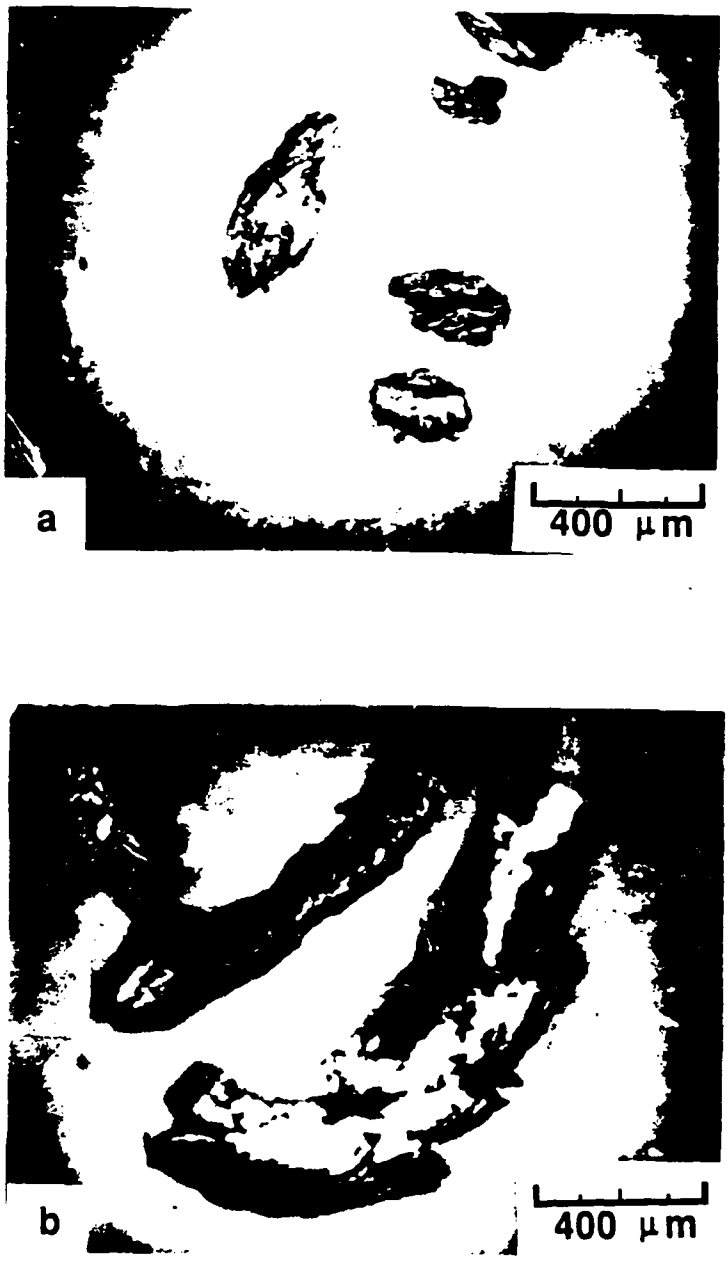

Figure 13. Loose cast iron particles collected after sliding 250 m distance at a) 5 N and b) 100 N normal load.

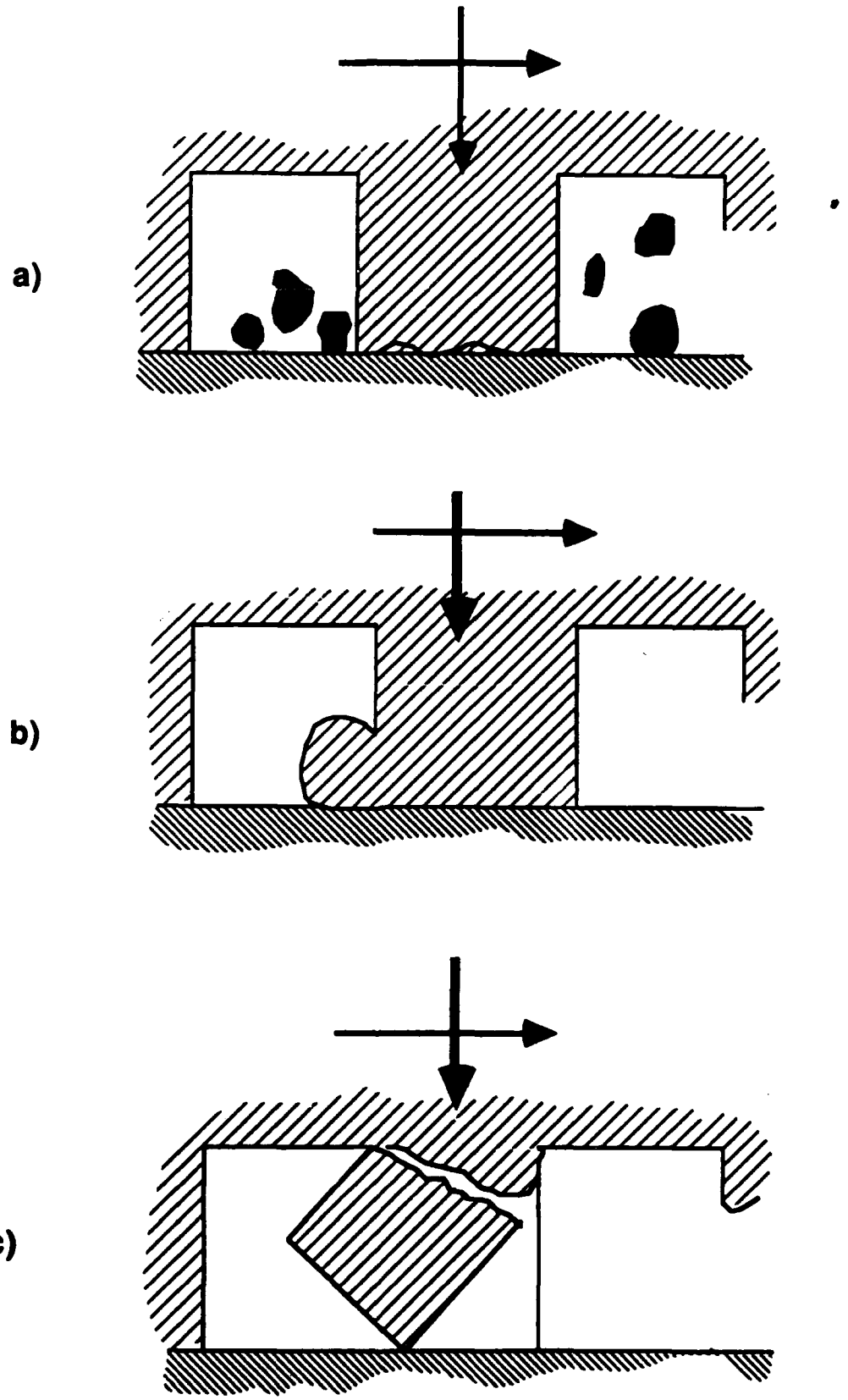

Figure 14. Schematic representations of the deformation patterns of undulated surfaces; a) lightly loaded undulated surfaces, b) heavily loaded OFHC copper, and c) heavily loaded cast iron.

REFERENCES

1. Komvopoulos, K., Saka, N., and Suh, N. P., "Plowing Friction in Dry and Lubricated Metal Sliding", *Transactions of the ASME, Journal of Tribology*, Vol.108, 1986, pp. 301-313.

2. Saka, N., Liou, M. J., and Suh, N. P., "The Role of Tribology in Electrical Contact Phenomena", *Wear*, Vol. 100, 1984, pp. 77-105.

3. Suh, N. P., Saka, N., and Liou, M. J., "Improved Design for Electrical Contacts", U.S. Patent 4,687,274, August 18, 1987.

4. Suh, N. P. and Saka, N., "Surface Engineering", *Annals of the CIRP*, Vol. 36, 1987, pp. 403-408.

5. Tian, H., Saka, N., and Suh, N. P., "Boundary Lubrication Studies on Undulated Titanium Surfaces", *STLE Paper* No. 88-AM-IE-2.

6. Ling, F. F., "Measurement of Pointwise Juncture Condition of Temperature at the Interface of Two Bodies in Slidng Contact", *Transactions of the ASME, Journal of Basic Engineering*, Vol. 85, 1963, pp. 481-487.

7. Gopinath, K., "The Influence of Speed on the Wear of Sintered Iron-based Materials", *Wear*, Vol.71, 1981, pp. 161-178.

8. Lim, S. C., and Brunton, J. H., "The Unlubricated Wear of Sintered Iron", *Wear*, Vol. 113, 1986, pp. 371-382.

9. Pamies-Teixeira, J. J., Saka, N., and Suh, N. P., "Wear of Copper-based Solid Solutions", *Wear*, Vol. 44, 1977, pp. 65-75.

10. Jahanmir, S., Suh, N. P., "Mechanics of Sub-surface Void Nucleation in Delamination Wear", *Wear*, Vol. 44, 1977, pp. 17-38.

A COMPARATIVE STUDY OF FRICTION AT THE PISTON/BORE INTERFACE OF SMOOTH AND UNDULATED CYLINDERS

SUMMARY

In this study, the feasibility of using undulated cylindrical surfaces for reciprocating engines is investigated. It is proposed that the surface undulations serve to trap or eliminate the wear particles at the piston/bore interface, thereby preventing the particles from clogging and causing catastrophic failures. Dry sliding friction force at the piston/bore interface was investigated using a modified engine motored at low speeds. The undulated cylinder resulted in longer running time without excessive increase in friction compared with the smooth cylinder. It is suggested that future cylinder surface design for IC engines be optimized with respect to local lubrication conditions along the piston stroke, for example by the use of undulated topography in the poorly lubricated regions.

I. INTRODUCTION

It has long been recognized that the optimal performance of internal combustion (IC) engines largely depends on the frictional losses, or the state of lubrication, at the piston-ring/cylinder-bore interface. Friction problems specific to the IC engines primarily arise from varying speeds (over several orders of magnitude from dead-centers to mid-stroke), alternating loads and high operating temperatures. Problems encountered due to the inadequacy of lubrication include: piston ring scuffing [1], excessive bore wear at the top dead-center (TDC), and high friction at the ring/bore interface.

Scuffing, a severe plowing phenomenon of the surfaces by large wear particles, often leads to catastrophic failure of the engine. Excessive wear at the TDC, experienced by a wide variety of engines, is largely due to the momentary evaporation of the lubricant and high ring pressure during the combustion stage. Continuous preferential wear near the TDC gradually spreads along the entire bore as shown in Figure 1 [2], and leads to decreased fuel efficiency of the engine.

As for friction, it has been shown in several studies that piston and ring friction is the major cause of energy dissipation in the IC engines. For example, studies by Rogowski [3] have shown that piston assembly friction accounts for as much as 75 percent of the mechanical power loss of the entire engine, and friction at the piston-ring/cylinder-bore interface in turn is

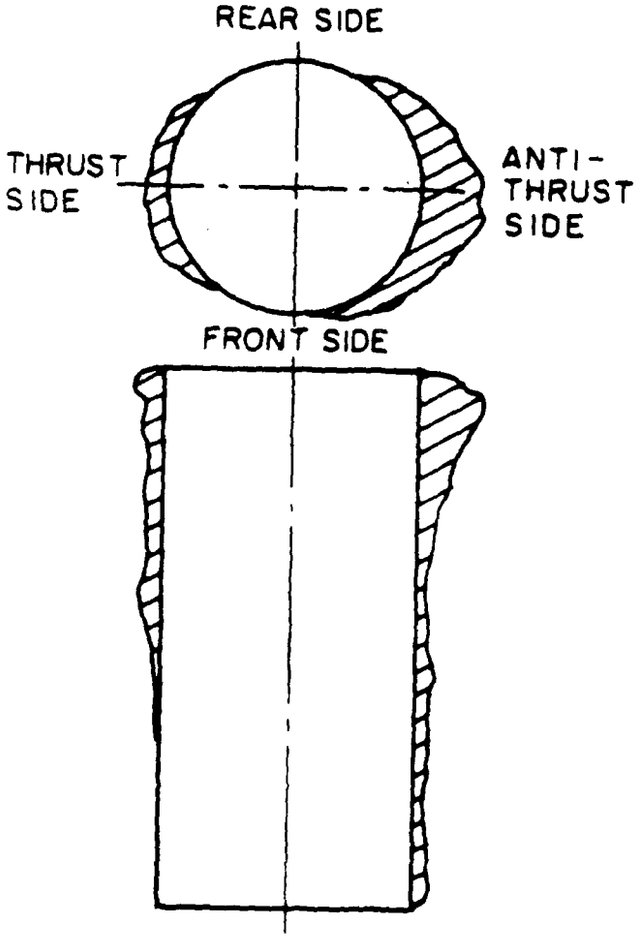

Fig. 1 - Cylinder liner wear pattern (from ref. 2).

responsible for as much as 75 percent of the piston assembly friction. Other investigators have also reported similarly high power losses due to piston ring friction in IC engines [4-7].

During the past decade, much has been published on the causes and remedies of problems related to the performance of internal combustion engines. Such interest and concern were motivated by unexpected failures experienced with heavy-duty and high-performance engines during critical operations and the pressing need to improve fuel economy. Basically, two approaches were tried to tackle the friction problems. One was to improve the performance of the piston ring through an optimization of its profile geometry as well as the surface finish of the cylinder [8-11]. The other was the development of lubricants which would provide effective lubrication for a greater portion of the piston stroke [12,13]. Despite extensive investigations along these lines, problems continue to plague the operation of many internal combustion engines, especially the heavy-duty engines.

A major reason for the lack of significant improvements is the conflicting functionality of piston rings. While piston rings should provide favorable lubrication conditions for a greater part of the stroke, providing effective sealing is an equally important functional requirement. Sliding conditions experienced by the rings during a single stroke is schematically shown in Figure 2 [14]. They range from dry sliding to hydrodynamic lubrication, depending on the ring pressure, lubricant viscosity, and speed of the piston as it advances along the cylinder wall. Consequently, at best only marginal improvements can be expected from the

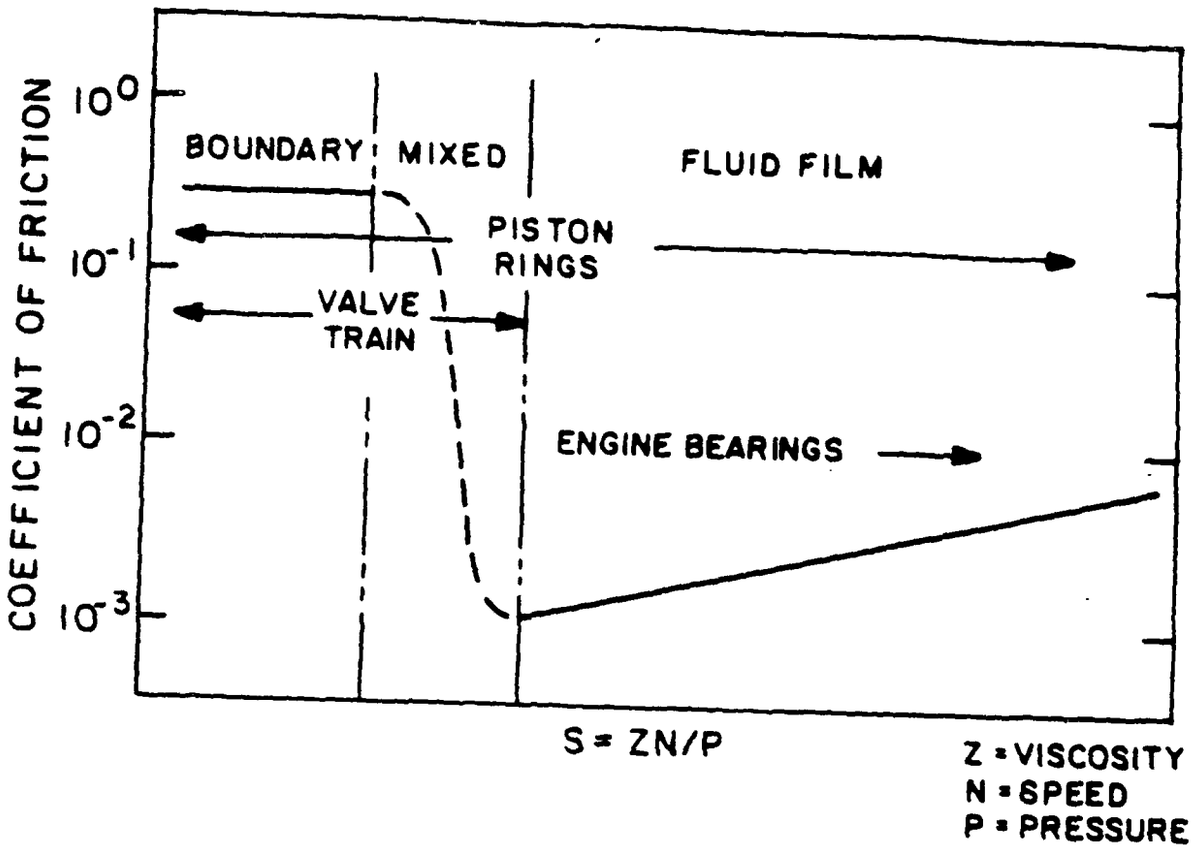

Fig. 2 - Streibeck diagram showing friction modes of engine components (from ref. 14).

optimization of ring geometry and lubricant chemistry.

In this report, modification of cylinder surface design to best accomodate the varying lubrication conditions along the piston stroke is presented as a solution to friction problems of IC engines. For example, a type of surface, namely undulated surface, that can provide low friction even under dry sliding conditions may be used selectively at areas along the bore that experience poor lubrication. Undulated metal surfaces have been shown to have low friction coefficients in dry friction experiments [15]. One reason for such low friction is that wear debris present at the sliding interface which causes plowing, a major mechanism of friction, can be eliminated by trapping them in the valleys of the undulations. Therefore, by undulating the bore surface, large wear debris particles generated from plowing action may be eliminated from the sliding interface, thus preventing the particles from causing further damage. Also, friction at the TDC where sliding is momentarily dry, should be significantly reduced.

The purpose of this study is to investigate the feasibility of using undulated cylinders to maintain satisfactory operating performance of reciprocating engines regardless of the lubrication at the piston ring and cylinder interface. The results of this investigation will aid in the design of future cylinder surface topography that would provide favorable sliding along the entire piston stroke rather than just in the mid-section. Results of the experimental investigation of piston friction in dry sliding for undulated as well as smooth cylinders are presented and discussed.

II. EXPERIMENTAL SETUP

One of the initial concerns was the design of an appropriate apparatus that would permit a proper comparison of sliding friction force between the two type of bore surfaces, i.e., smooth and undulated. Since severe problems in internal combustion engines stem form local lubrication deficiency, dry sliding test seemed appropriate for simulating the worst possible conditions. It was decided therefore that while maintaining the features of the crank mechanism of reciprocating engines, dry sliding of piston by motoring at low speeds would be adequate for a comparative study.

The major considerations in designing the apparatus are: ease of replacement of cylinder sleeve and piston rings and piston friction should be the only force transmitted to the force sensors. A 2 3/8 in stroke engine was modified to satisfy such requirements. A cylinder block into which different sleeves could be pressed in and out, and which itself could be detached from the engine assembly, provided the ease with which both the sleeves and the pistons could be replaced. In order to isolate the piston friction force, a structure where the cylinder block could be separated from the crank case was used. A schematic of the test apparatus is illustrated in Figure 3 and the photographs in Figure 4.

Strain gages in full bridge configuration were used as friction force sensors. The gages were mounted on one of the dual symmetric beams that supported the cylinder block which was isolated from the rest of the equipment. Consequently, the

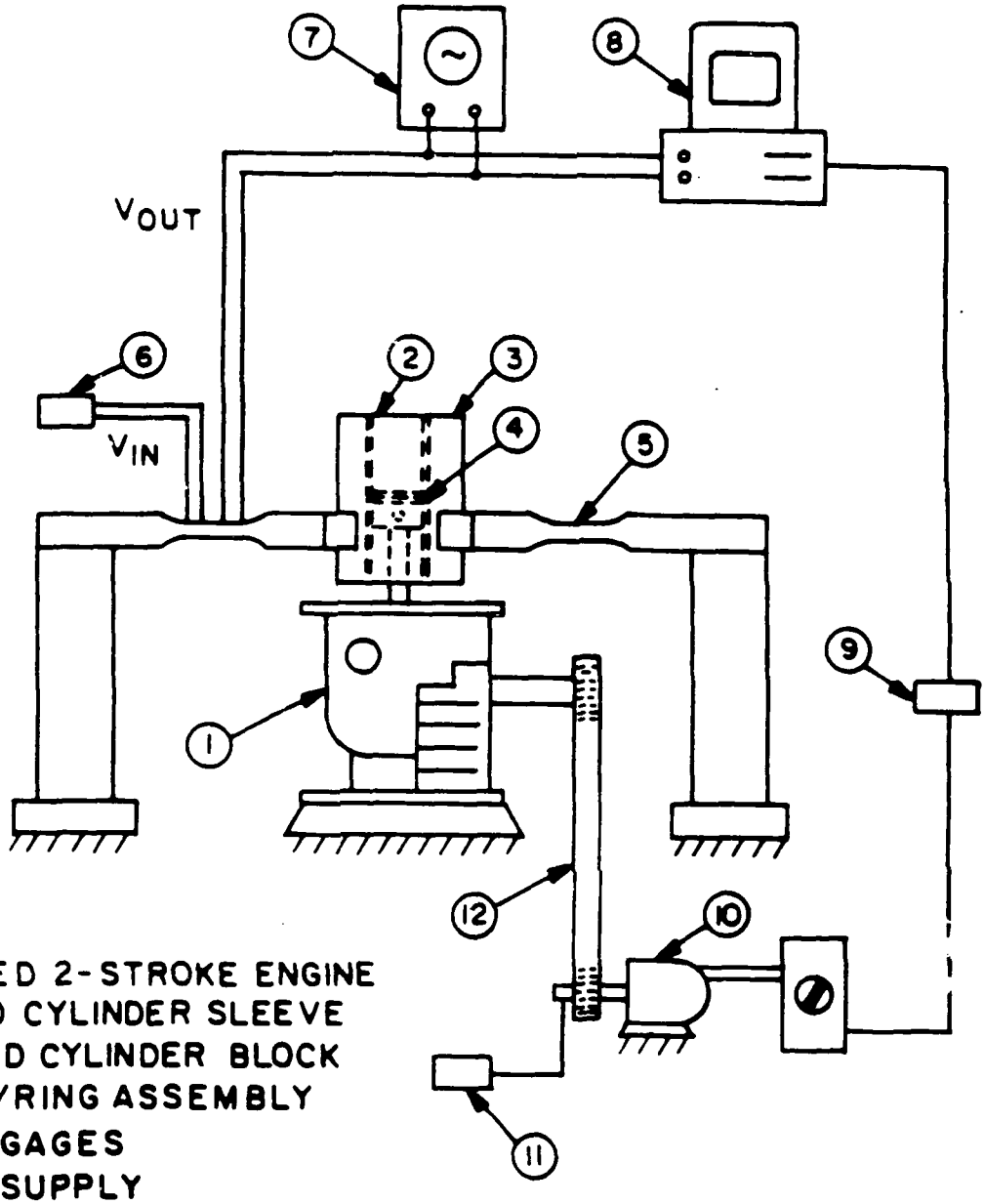

1. INVERTED 2-STROKE ENGINE
2. PRESSED CYLINDER SLEEVE
3. ISOLATED CYLINDER BLOCK
4. PISTON/RING ASSEMBLY
5. STRAIN GAGES
6. POWER SUPPLY
7. OSCILLOSCOPE
8. DATA ACQUISITION SYSTEM
9. MOTOR ON/OFF RELAY
10. VARIABLE SPEED DC MOTOR
11. TACHOMETER
12. TIMER BELT

Fig. 3 - Schematic of the experimental set-up.

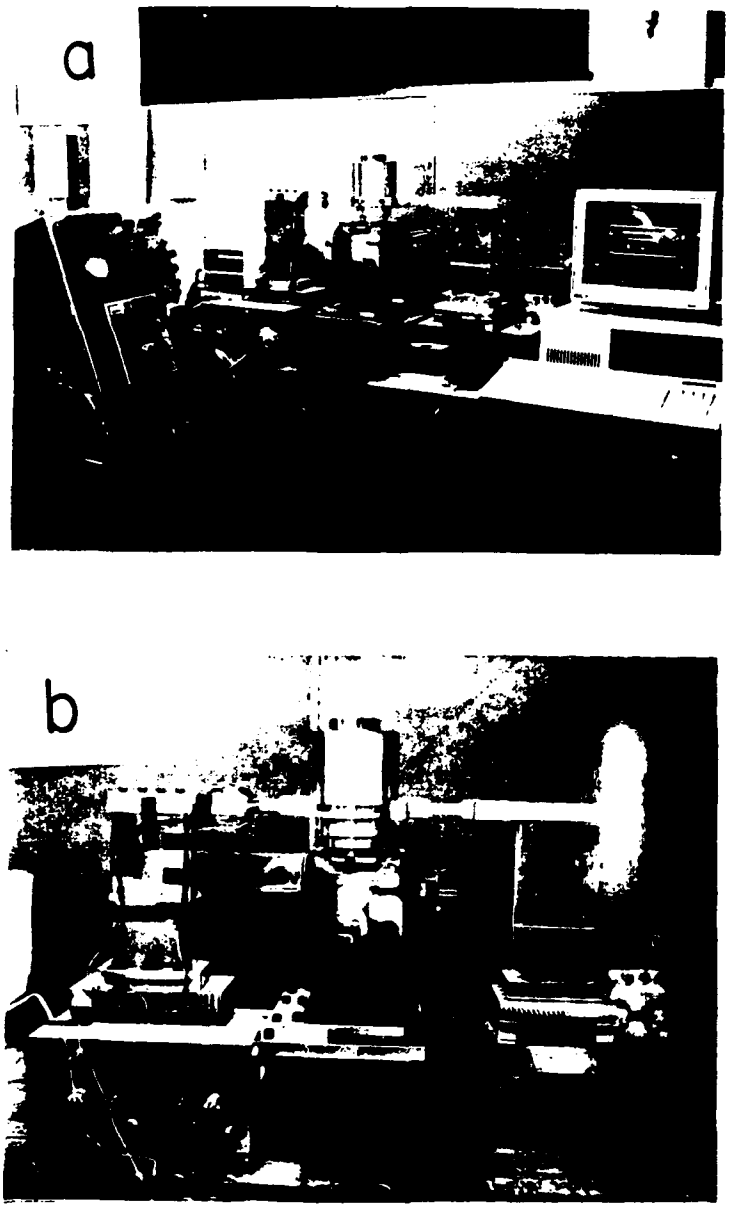

Fig. 4 - (a) Overall view of the apparatus and (b) view of the cylinder block and the supporting beams.

friction force at the piston/bore interface could be obtained directly from the output of the strain gage bridge which was calibrated with known loads prior to each test. The strain gage output was recorded by a microcomputer-based data acquisition system and was also observed by an oscilloscope. The oscilloscope was mainly used during force calibration and for detailed scanning of piston friction force, while the microcomputer aided in automatic data acquisition for long duration tests and data analyses.

III. PREPARATION OF CYLINDER SURFACE AND PISTON RINGS

The piston rings and cylinder sleeves were obtained from manufacturers of engine components. Cast iron Badger cylinder sleeves, 2 3/8 in in diameter, and matching piston sets were used. The sleeves were acquired in a rough machined form and the desired bore surfaces were prepared by following the guidelines observed in the industry. Fabrication steps for the undulated cylinder are as follows:

(a) the cylinder sleeve was pressed into an aluminum block,

(b) the block was mounted on a lathe and centered with respect to the outside diameter,

(c) the sleeve surface was finished with a carbide boring tool to 2.368 in diameter,

(d) a sharp carbide threading tool was used to create fine undulations on the cylinder surface in the

form of a helix (92 undulations/in; depth of cut of 0.003 in), and

(e) the bore was honed using a 64 grit stone to a final diameter of 2.371 in.

Similar procedure was followed to fabricate the smooth cylinder but for the internal threading operation. Scanning electron micrographs of the smooth and undulated cylinder surfaces with crosshatch honing marks are shown in Figure 5. The width of the valley is about 80 m and the plateau of about 160 m.

The piston assembly was used as obtained from the suppliers, but only the top ring was used. The rings were made of cast iron and were electroplated with chromium. The contact width of the rings was 0.08 in and the radial thickness was 0.09 in. A photograph of the disassembled cylinder/piston assembly is shown in Figure 6.

IV. EXPERIMENTAL PROCEDURE

Dry sliding friction tests were conducted at low speeds in order to avoid the inertial effects due to the crank mechanism. With the cylinder head open to the atmosphere, the only force transmitted to the strain gage force sensors was that of piston friction. Since dry sliding friction is in general independent of velocity, the results of tests performed at low speeds are acceptable. After a few trials a speed of 25 revolutions per minute was identified as appropriate for the tests. At this speed the inertial effects could be neglected and the data

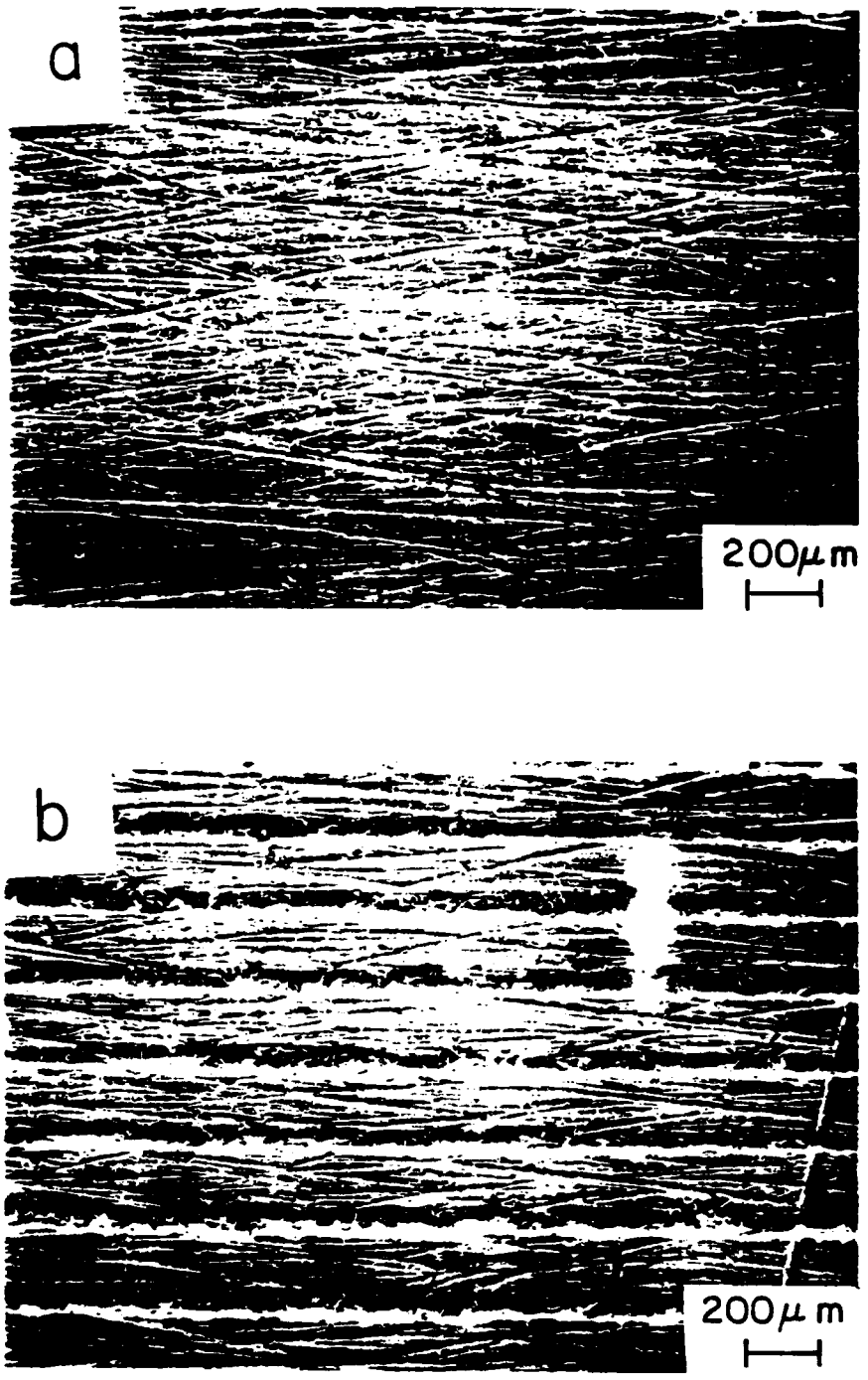

Fig. 5 - SEM micrographs of (a) smooth and (b) undulated cylinder surfaces.

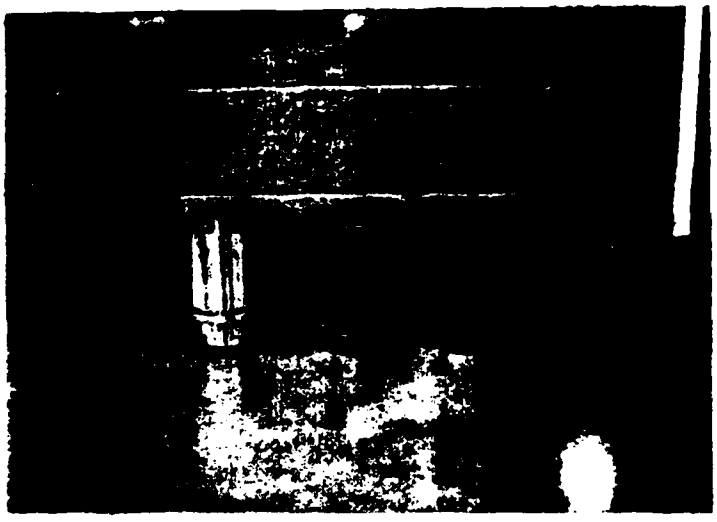

Fig. 6 - Disassembled cylinder/piston assembly: cylinder block, cylinder sleeve, piston, and piston ring.

acquisition electronics provided adequate temporal resolution for tracing the friction force during each stroke.

Before each test the bore surface and the rings were run-in by operating the modified engine with lubrication at 150 to 200 rpm for 10 to 24 hours. The run-in procedure was necessary to obtain a smooth even surface and to eliminate microburrs of the undulated cylinders. The duration of run-in was determined by inspecting the color of the lubricant which indicated the amount of wear that had taken place. Run-in was considered adequate when fresh engine oil retained its original color for about two hours of operation. After the run-in procedure, the cylinder/ piston parts were disassembled and the sliding surfaces were thoroughly cleaned. The cylinder liner, piston, and the rings were degreased with detergent and cold water, and cleaned with acetone and isopropyl alcohol. The parts were then dried in air and reassembled.

A force calibration was performed prior to each test. The procedure involved observing the voltage output from the strain gages at different loads. Dead weights of 5, 10, and 15 lbf were placed on the cylinder and the outputs were noted. The strain gage output to the applied load was approximately linear. The voltage output for upward force was also verified by checking the reading while the cylinder was being pulled up with different loads.

The tangential force, or the friction force, exerted on the bore by the piston was obtained for the duration of about one and a half cycles at ten minute intervals. The tests were

automatically terminated when the friction force exceeded 30 lbf. Since 30 lbf was more than three times the friction force observed at the beginning of sliding, it seemed unnecessary to carry on the experiment beyond this level. That is, friction force of 30 lbf was a sufficient indication that the engine was about to experience a catastrophic failure or seizure. The performance of smooth and undulated cylinders were compared by noting the sliding distance to reach the limiting friction force of 30 lbf.

V. RESULTS AND DISCUSSION

(A) Frictional Force

A typical continuous trace of the friction force observed by an oscilloscope as a function of crank angle at 25 rpm is shown in Figure 7. The shape of friction trace resembles roughly a square wave indicative of the change in sliding direction of the piston. Discretized output obtained from the data acquisition system for the same trace is also shown in the figure for comparison. Although the resolution of the digital output did not provide detailed local description of the force, it was sufficient to measure the average piston friction force as a function of sliding distance. Nevertheless, the oscilloscope was also used during the experiments for checking the digital output.

As expected, the friction tests on the smooth cylinders resulted in early failures. The friction force increased to 30 lbf in about 1,000 m of sliding. As for the undulated

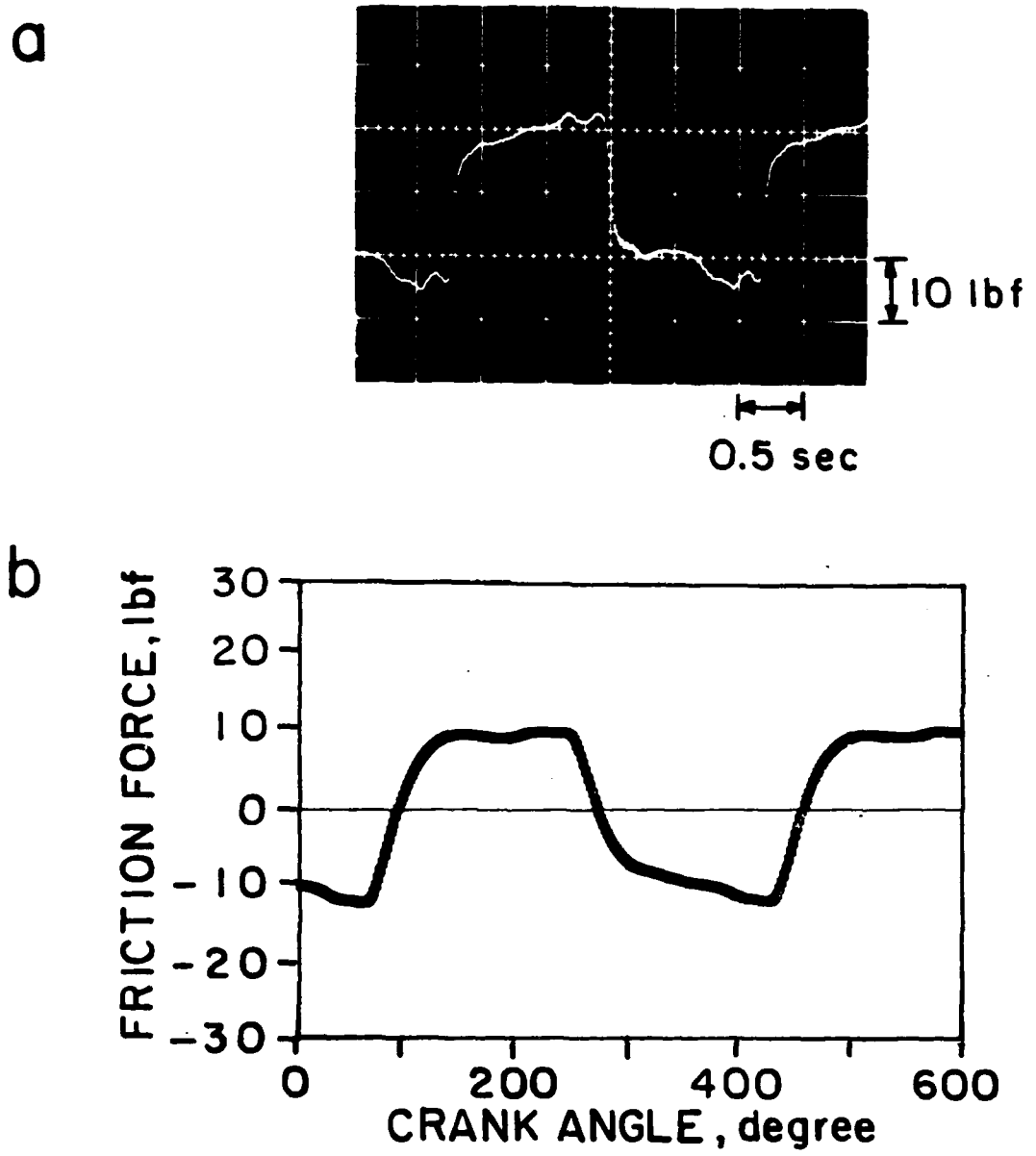

Fig. 7 - Typical friction force observed as a function of crank angle obtained by (a) oscilloscope and (b) data acquisition.

cylinders, the increase in friction force was much more gradual and the sliding distance up to failure was about 3,000 m. Figure 8 summarizes the results of the friction experiments. It should be mentioned, however, that repeatable results were difficult to obtain with the undulated cylinder. In certain trials the undulated cylinder failed as early as the smooth cylinder. The main reason for the variation was that uniform surface preparation was very difficult to produce. Also, the dimensions of the undulations may have not been optimal. It is believed, however, that if the undulations of identical spacing and depth can be fabricated with consistency, similarly consistent friction force output as a function of sliding distance should be realized.

As far as the optimization of the dimensions of the undulations is concerned, further investigation is necessary. However, as a first measure of determining the ideal dimensions, the following two factors were considered:

(a) the depth and width of the undulations should be of the order of the diameter of the largest wear particle, and

(b) the width of the undulations should be at least an order of magnitude smaller than the thickness of the piston ring.

Considering the common thickness of piston rings, which is about 0.08 in or larger, the second criterion can be easily satisfied. Therefore, despite the helical geometry of the undulations, blowby of the compressed gas in firing engines would not be a

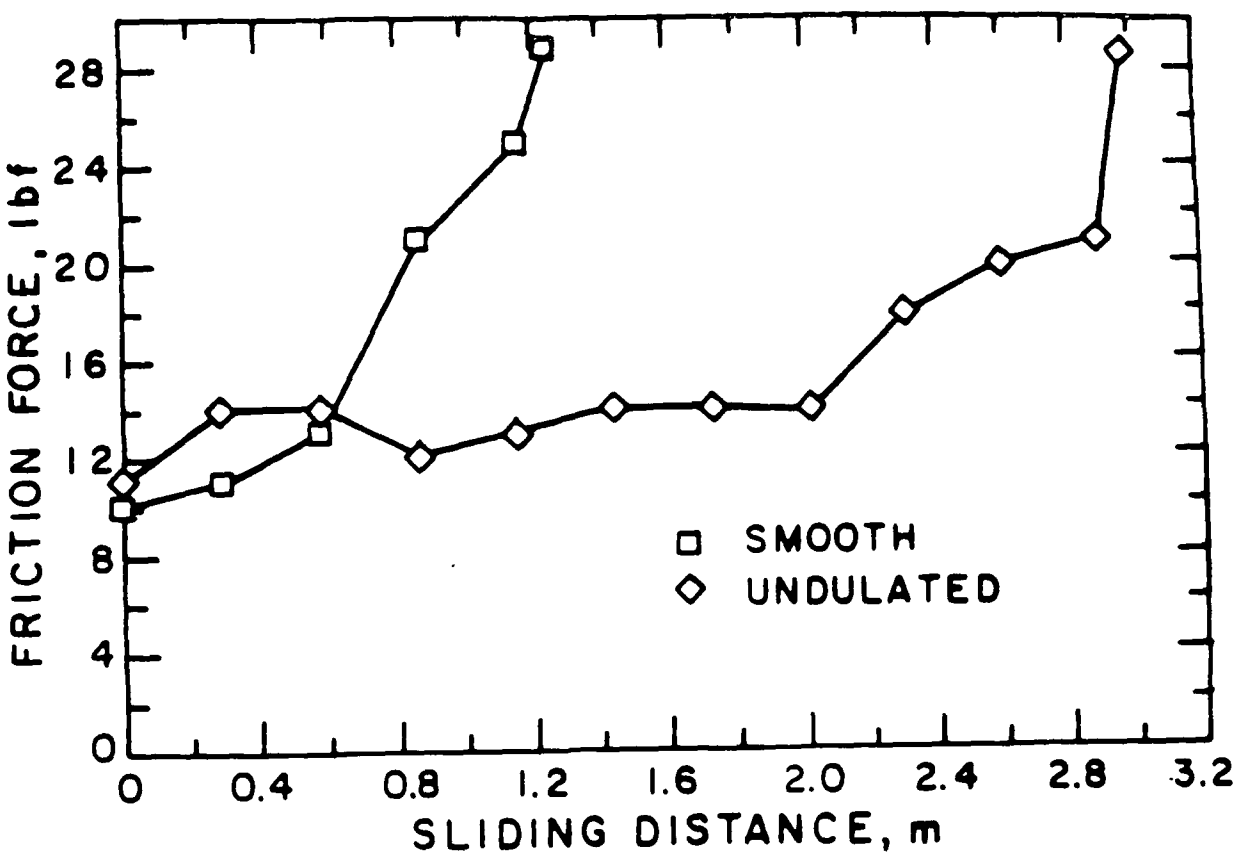

Fig. 8 - Average friction force at the piston/bore interface as a function of sliding distance.

problem. The first criterion, however, is more difficult to satisfy. The rationale for this criterion is that in order to minimize the plowing component of friction, the wear particles must be trapped within the valleys of the undulations as mentioned earlier. Since larger particles tend to do more damage to the surface than the smaller ones, the undulations should be large enough to trap the lager particles. SEM micrographs of wear particles sampled from experiments on smooth cylinders showed that the particles produced were in the submicron range (Figure 9). Indeed, such small wear particles generated from the cylinder makes cast iron an attractive material for cylinders of modern heavy-duty IC engines. Nevertheless, undulations should be large enough to trap large chunks of debris that sometimes form as a result of wear particle agglomeration and piston scuffing. The dimensions chosen for the undulations in this study were mainly limited by the fabrication technique. Poor machinability of cast iron made it very difficult to fabricate finer undulations, but other surface prepartion techniques (e.g. laser grooving, chemical etching) may be more appropriate.

(B) Estimation of the Friction Coefficient

A difficulty faced in the calculation of friction coefficients in this study was that the normal force could not be directly measured. In firing engines the gas pressure behind the rings accounts for much of the normal pressure applied to the bore. The other contributions to normal load are the elastic force of the rings and the side thrust of the piston body against

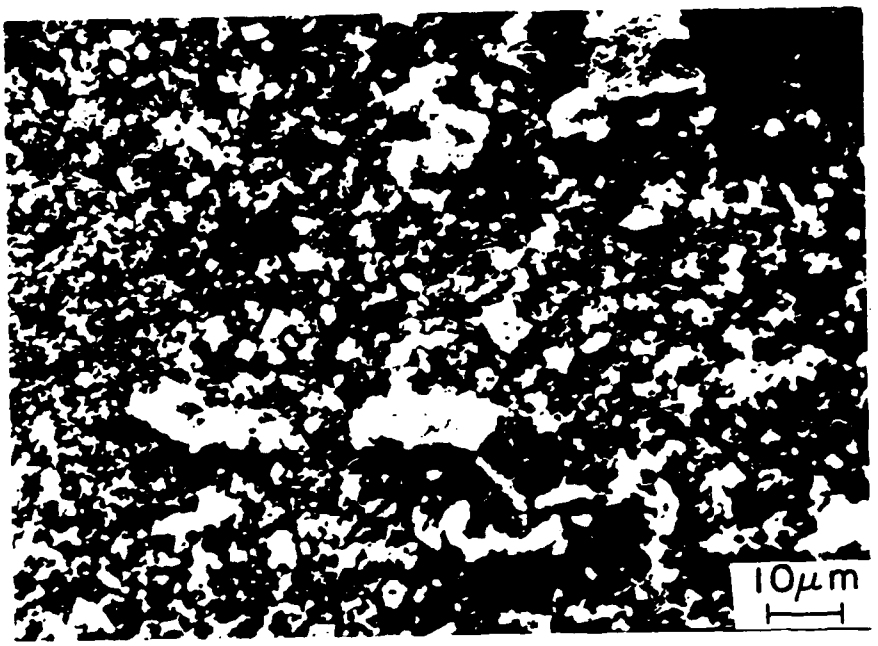

Fig. 9 - SEM micrograph of clusters of submicron range wear particles.

the cylinder wall. In the apparatus used here, the elastic force of the ring was assumed to be the only normal force applied to the cylinder wall. Under this assumption, the friction coefficient calculated was about 0.5 in the early stages of sliding for both the undulated and the smooth cylinders, and the friction coefficient rose to about 1.5 by the time the experiments were terminated. High values of friction coefficients suggest that significant plowing was taking place towards the end of the experiments.

(C) Causes for Increase in Friction

By observing the wear marks on both the smooth and the undulated cylinder surfaces, as well as the rings, areas which experienced high friction were identified. Surprisingly, very few wear marks could be found along the surface of the cylinder. Comparison of profilometer traces of the surfaces before and after the friction test also indicated little sign of wear (Figure 10). SEM micrographs of the cylinder surfaces after the sliding tests, shown in Figure 11, indicate that plowing marks are more evident with the smooth cylinder. In both cases the original crosshatch honing marks are removed and the surfaces became slightly polished and smoother. As for the rings, some plowing wear tracks as well as polished areas were found as shown in Figure 12 for both the smooth and undulated cylinder tests.

Evolution of friction increase along the cylinder was observed in detail with the oscilloscope. Oscilloscope traces of continuous friction force at the piston/bore interface were

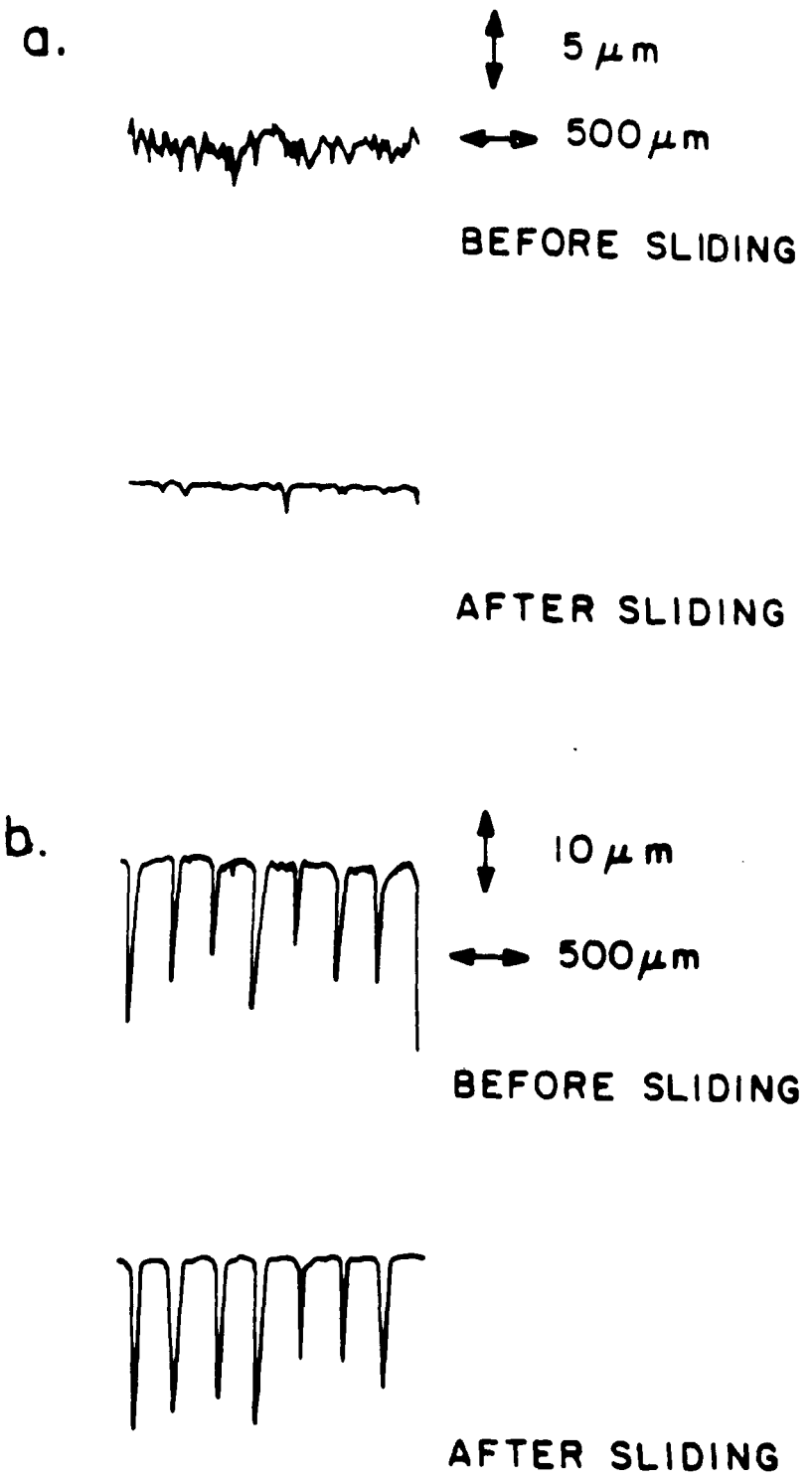

Fig. 10- Profilometer trace of (a) smooth and (b) undulated cylinder surfaces before and after sliding tests.

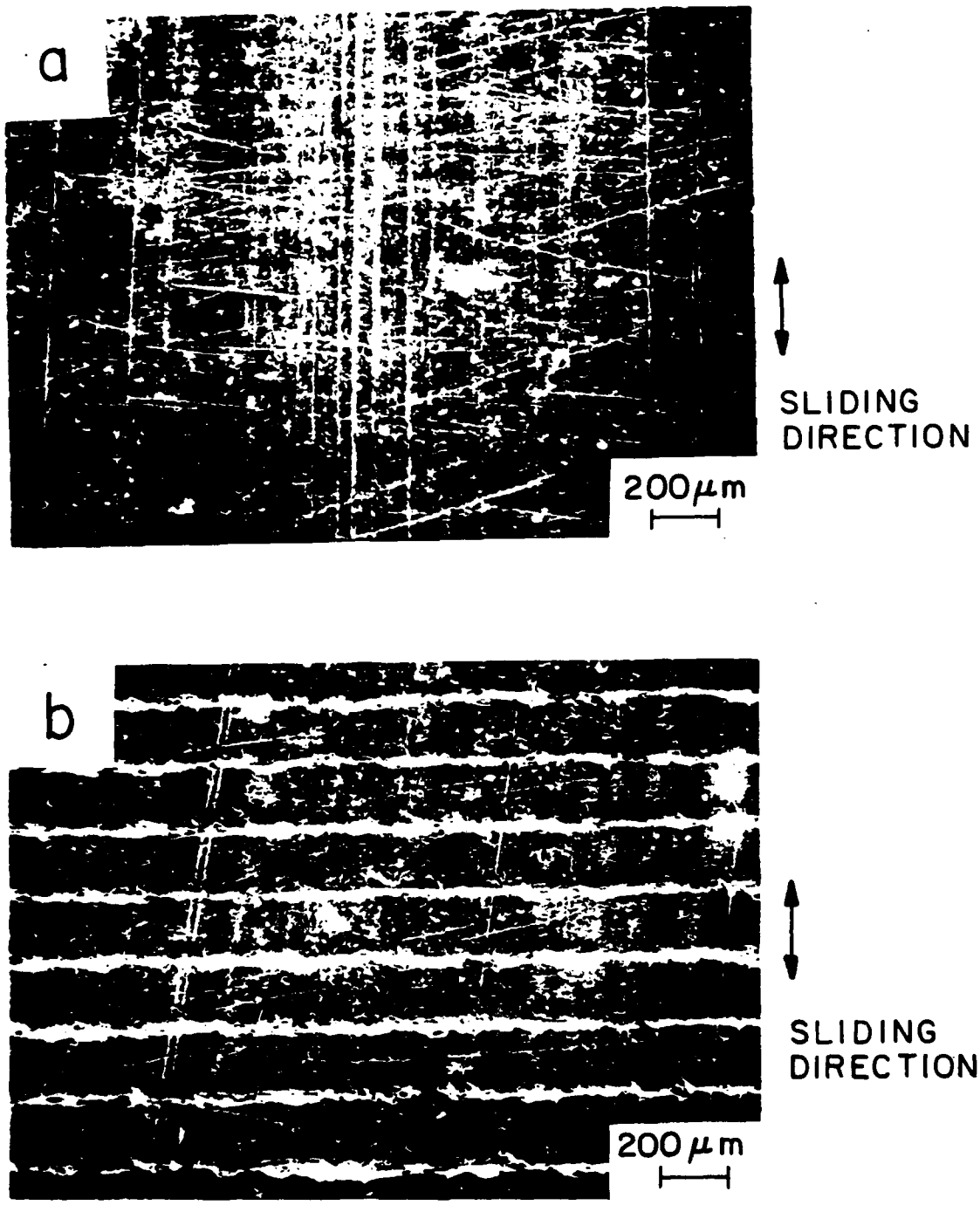

Fig. 11- SEM micrographs of (a) smooth and (b) undulated cylinder surfaces after sliding tests.

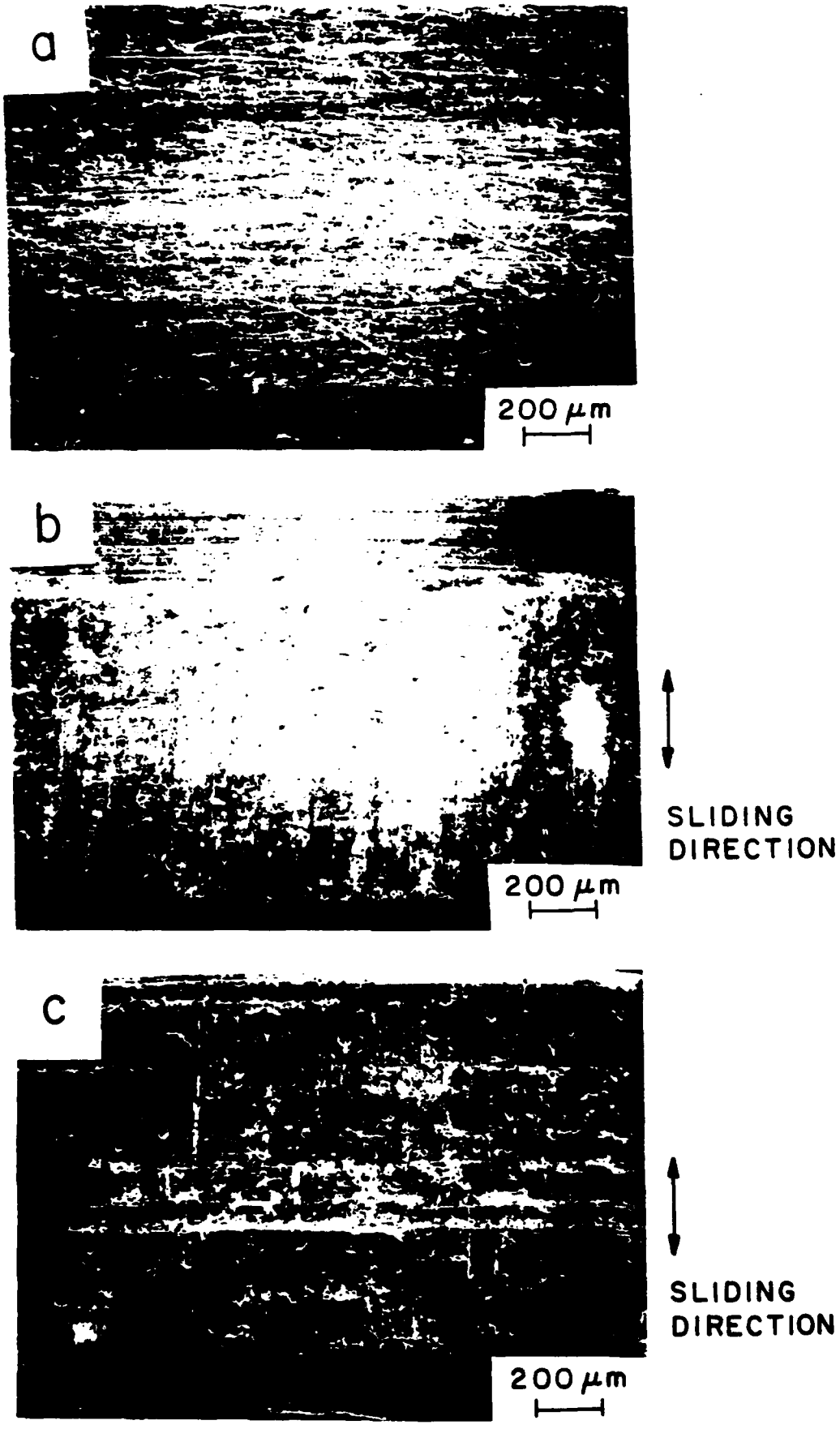

Fig. 12- SEM micrographs of piston ring surfaces (a) before and after sliding against (b) smooth and (c) undulated cylinders.

taken at various sliding distances. As shown in Figure 13, there were locations along the stroke where the friction force increased gradually for both the smooth and undulated cylinders, although in the case of the undulated cylinder, the increase was more gradual.

By observing the friction behavior as a function of the crank angle, it became evident that piston skirt contact with the cylinder was partly responsible for the increase in the measured friction force. The wear scars on the piston were found to be concentrated at the bottom, toward the main thrust side. Plowing wear tracks were also found on both the smooth and the undulated bore surfaces where the sliding locations of the piston scars matched.

In conclusion, two independent phenomena may have been responsible for the increase in friction contributed by piston skirt contact. The first is that the asperities of the hard cylinder plow the softer aluminum piston causing damage to the piston surface. Continuation of plowing would cause further damage to the surface as indicated by the increase in friction. The second phenomenon is attributed to piston cocking. Piston cocking results from slight rotational motion of the piston during motoring due to the fact that the diameter of the piston top is less than the bottom by about 0.005 in. The difference in diametral dimensions is to compensate the difference in thermal expansion between the top and bottom of the piston during the actual operation of IC engines. In the experiments, the cocking phenomena was further aggrevated by the absence of

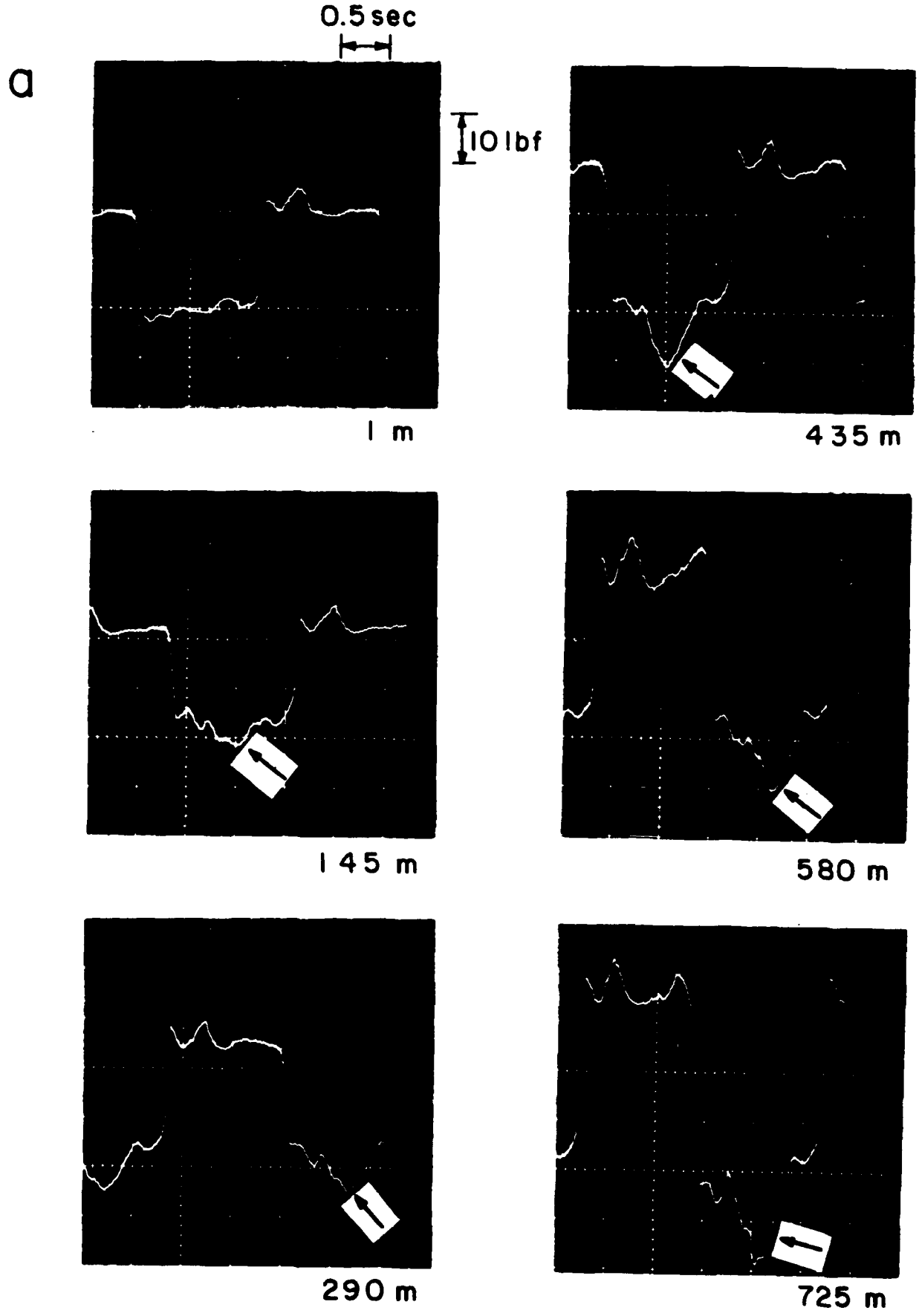

Fig. 13- Stages of local friction increase observed by an oscilloscope for (a) smooth and (b) undulated cylinders.

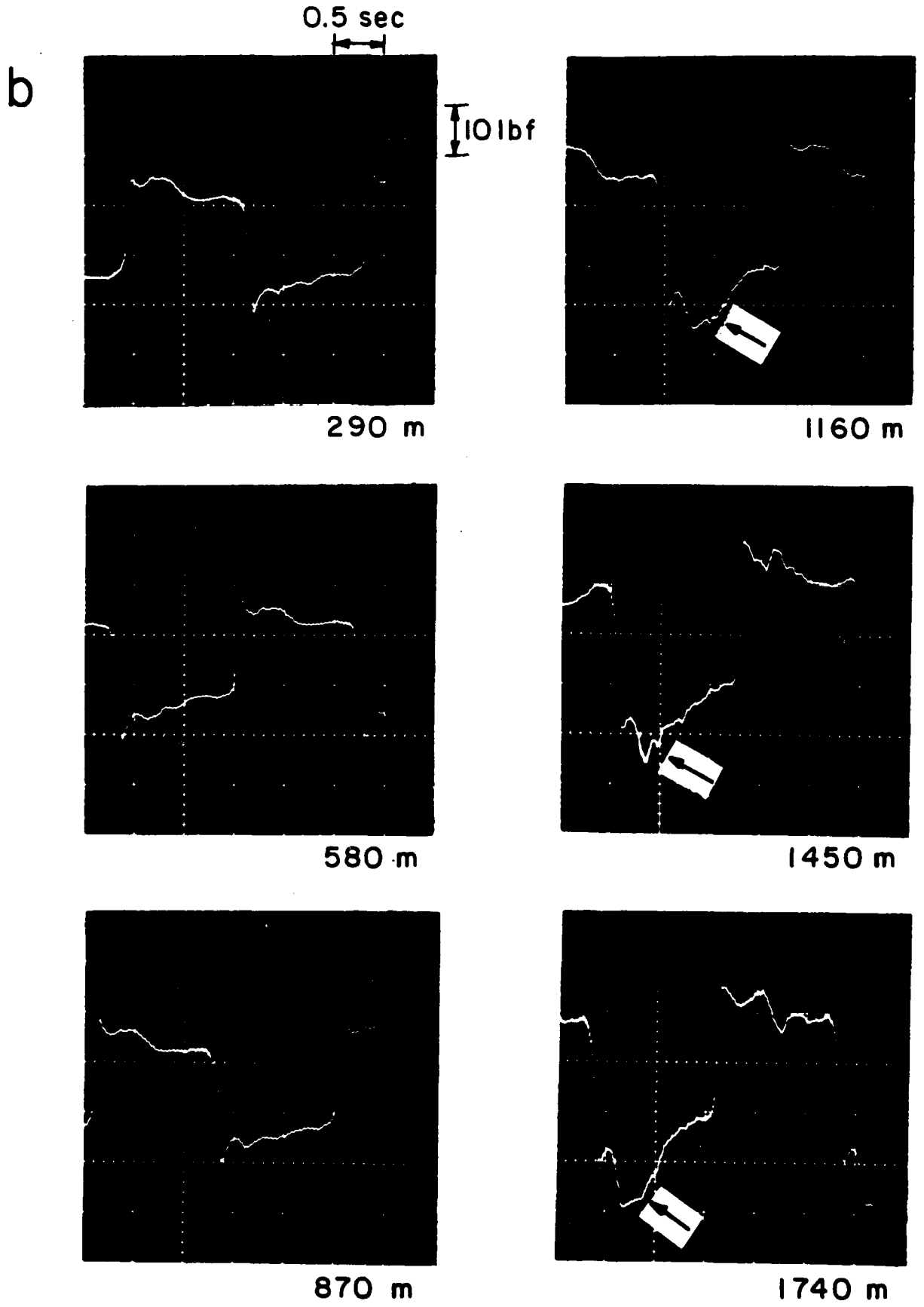

Fig. 13 cont.

any lubricant.

Using the motoring set-up, the effect of piston cocking could be tested by either reducing the piston skirt to the dimension of its top and using a cylinder of corresponding bore size or by maintaining the appropriate temperature difference between the top and bottom of the piston. As for the increase in friction due to piston plowing by asperities, surface hardening of the piston is a possible remedy. The other possibility is to increase the run-in time in order to eliminate the micro-asperities. It is believed that the undulated cylinder would give much more favorable results than the ones presented here, if problems such as piston skirt friction and plowing by asperities can be eliminated by any or all of the methods described above.

VI. PROPOSED SURFACE TOPOGRAPHY FOR FUTURE ENGINES

The approach taken in this work to improve the performance of IC engines is a novel one. Engine research in this area has traditionally focused on maintaining hydrodynamic lubrication between the piston rings and the bore. However, this approach may not be appropriate for the optimization of piston/cylinder systems since mixed, boundary lubricated as well as dry sliding conditions also operate during each stroke. In the future, surface preparation of the cylinder should be optimized with respect to lubrication condition as a function of crank angle for best engine performance. For example, undulations would be

desirable near the two ends of the piston stroke, where lubrication fails to be hydrodynamic, while smooth surface can be used in the mid-stroke region of the cylinder as illustrated in the following analysis.

In order to effectively utilize the undulated topography in IC engines, the lubrication behavior along the piston stroke must be clearly understood. Lubrication at the ring/bore interface may be roughly predicted by noting the magnitude of the bearing parameter

$$(nu/pb)^{0.5}$$

where n = viscosity

u = piston speed

p = pressure behind the ring

b = ring thickness

as a function of the crank angle. It has been shown empirically that lubrication fails to be mixed or hydrodynamic in regions where $(nu/pb)^{0.5} < 2x10^{-3}$ [7]. Such regions, where lubrication is poor or friction is high, would be most appropriate for the undulated topography.

The variables in the bearing parameter can be determined for a given engine operating at a certain rpm from geometric relations and empirical data. Figures 14a to 14d illustrate the functional relations between the variables and the crank angle for a chosen engine. Here, the viscosity of the oil was assumed to vary linearly along the two dead-centers reflecting the

a.

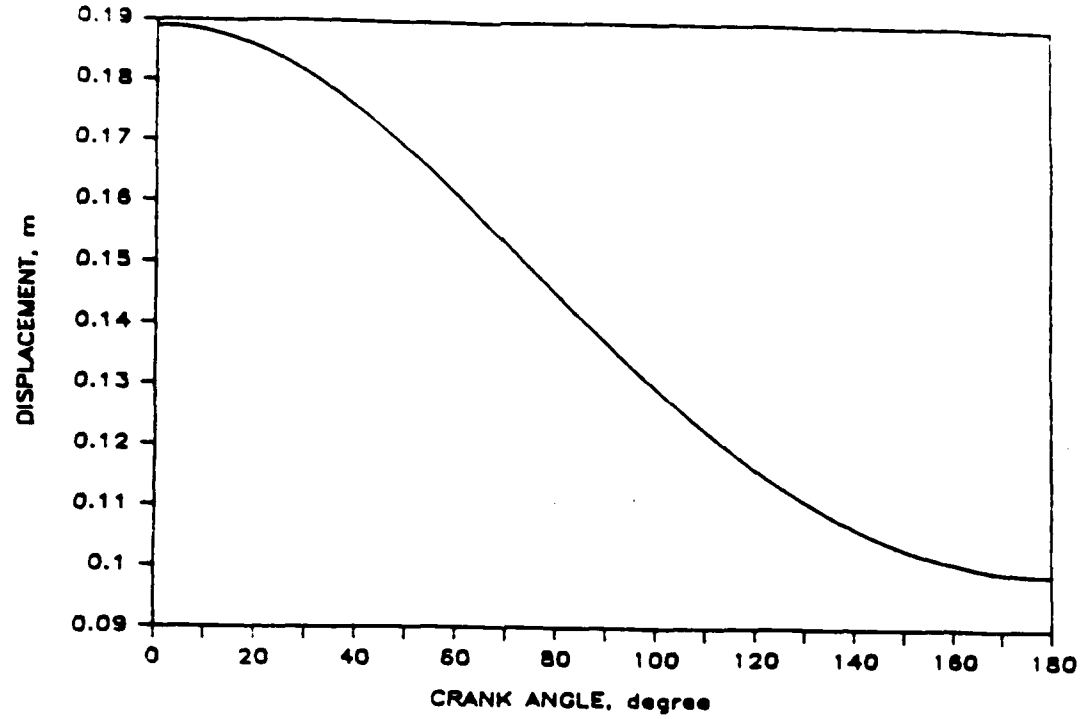

b.

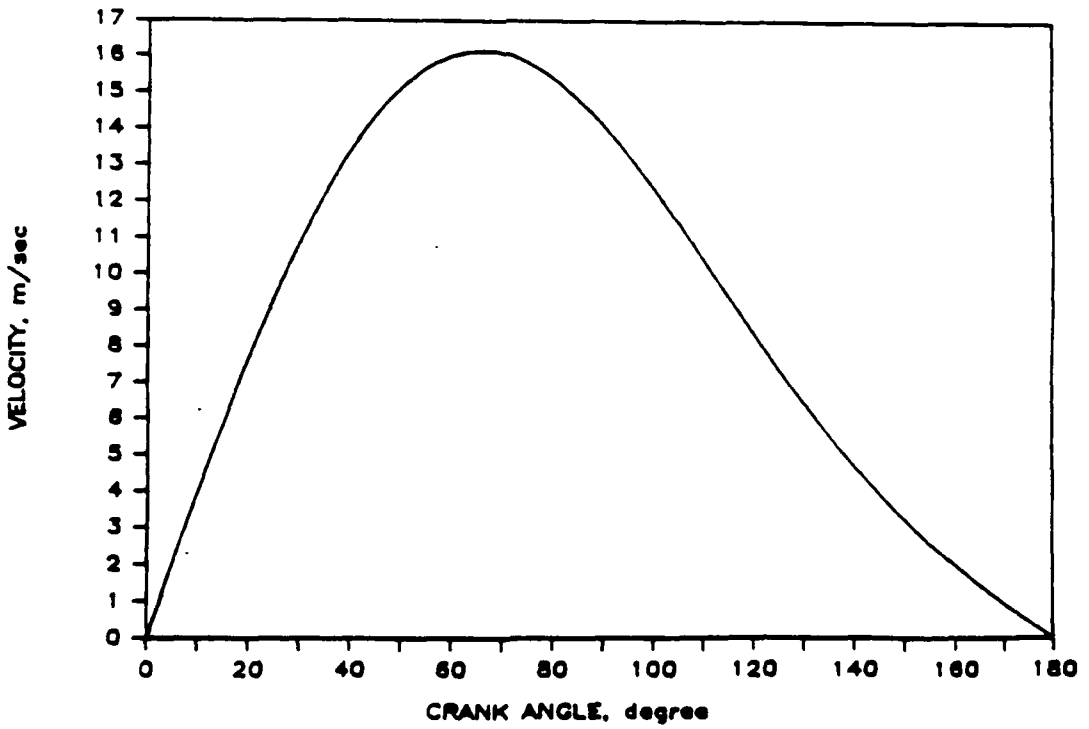

Fig. 14- (a) Piston displacemnt, (b) speed, (c) oil viscosity, (d) chamber pressure, and (e) bearing parameter as functions of crank angle (for 3.88 in bore, 3.53 in stroke, 5.65 in connecting rod, .125 in ring thickness, and at 3000 rpm).

c.

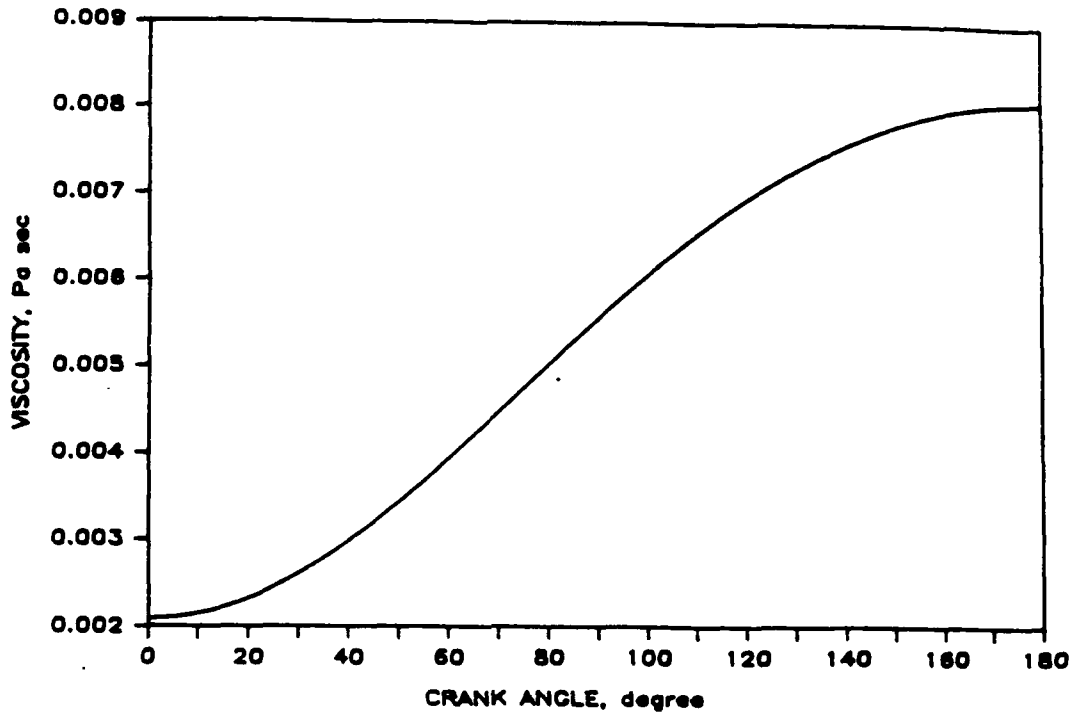

d.

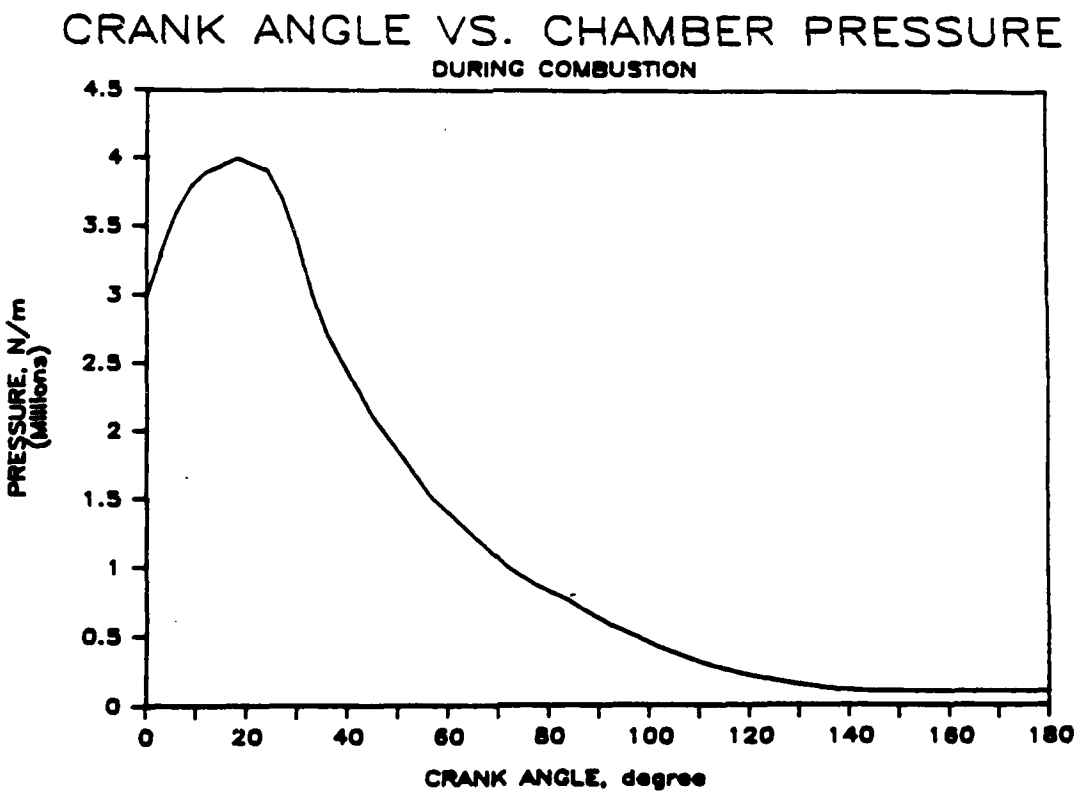

Fig. 14 cont.

e.

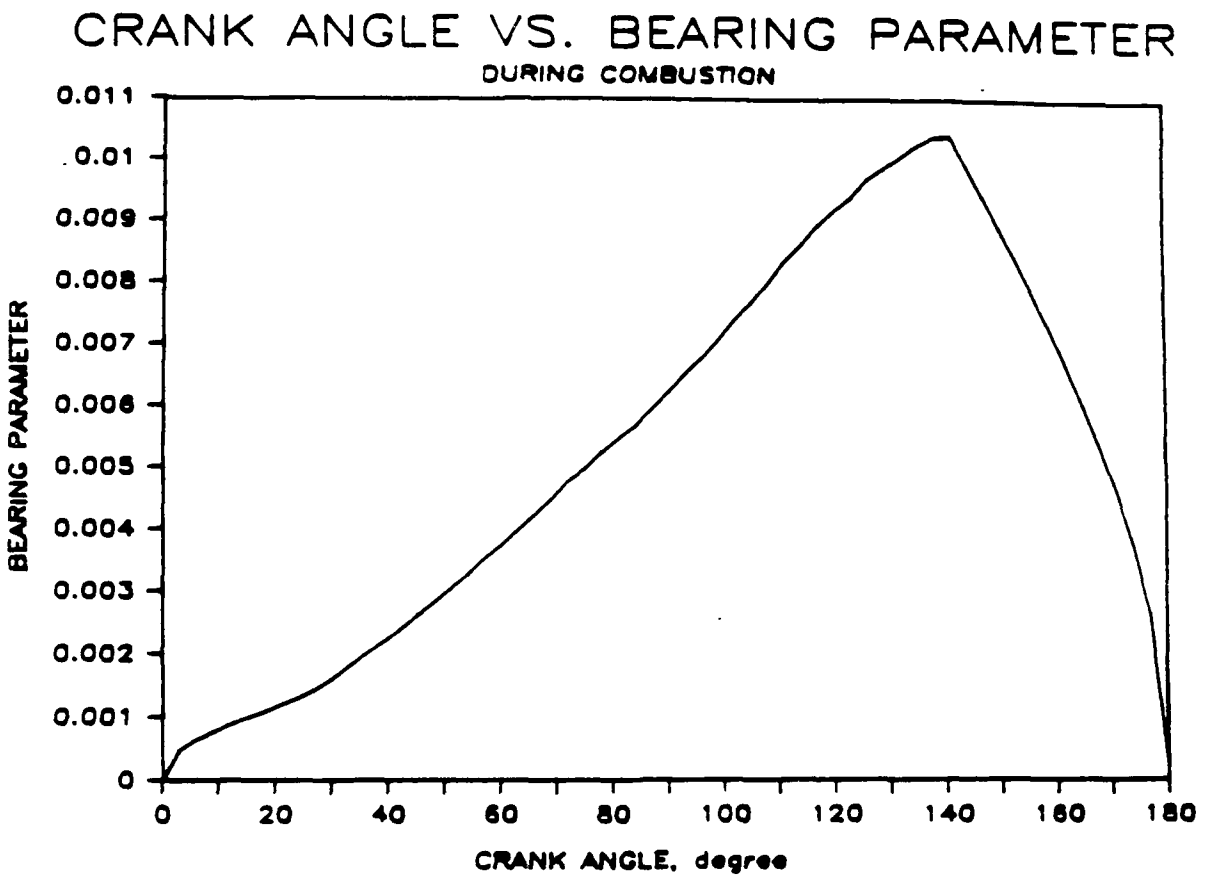
CRANK ANGLE VS. BEARING PARAMETER
DURING COMBUSTION
BEARING PARAMETER
0.011
0.01
0.009
0.008
0.007
0.006
0.005
0.004
0.003
0.002
0.001
0
0
20
40
60
80
100
120
140
160
180
CRANK ANGLE, degree

Fig. 14 cont.

variation in the oil temperature. As for the chamber pressure, which is effectively the pressure that is exerted behind the top ring, a typical profile observed experimentally during the combustion stroke was obtained from reference [16]. The combustion stroke is investigated because of the high chamber pressure experienced during this stroke.

The plot given in Figure 14e indicate that for crank angles between 0° - 35° and 175° - 180°, the bearing parameter is below the critical value of $2x10^{-3}$. This suggests that the appropriate regions for the undulations would correspondingly be at about 10% of the stroke from the TDC and 3% of the stroke from the BDC as schematically illustrated in Figure 15.

The procedure used in this excercise to determine the optimum location for the undulations may be used as a first approximation only. Better understanding and more rigorous treatment of the lubrication and wear behavior would ensure proper utilization of undulated surfaces in future IC engines.

VII. CONCLUSIONS

Experimental investigation of friction force at the piston/bore interface of a modified reciprocating engine was compared between undulated and smooth cylinder surfaces. The advantage sought from using undulated cylinders is to accomodate the varying lubrication condition along the entire piston stroke, and reduce the dependence of engine performance on hydrodynamic lubrication. Such approach will help eliminate the

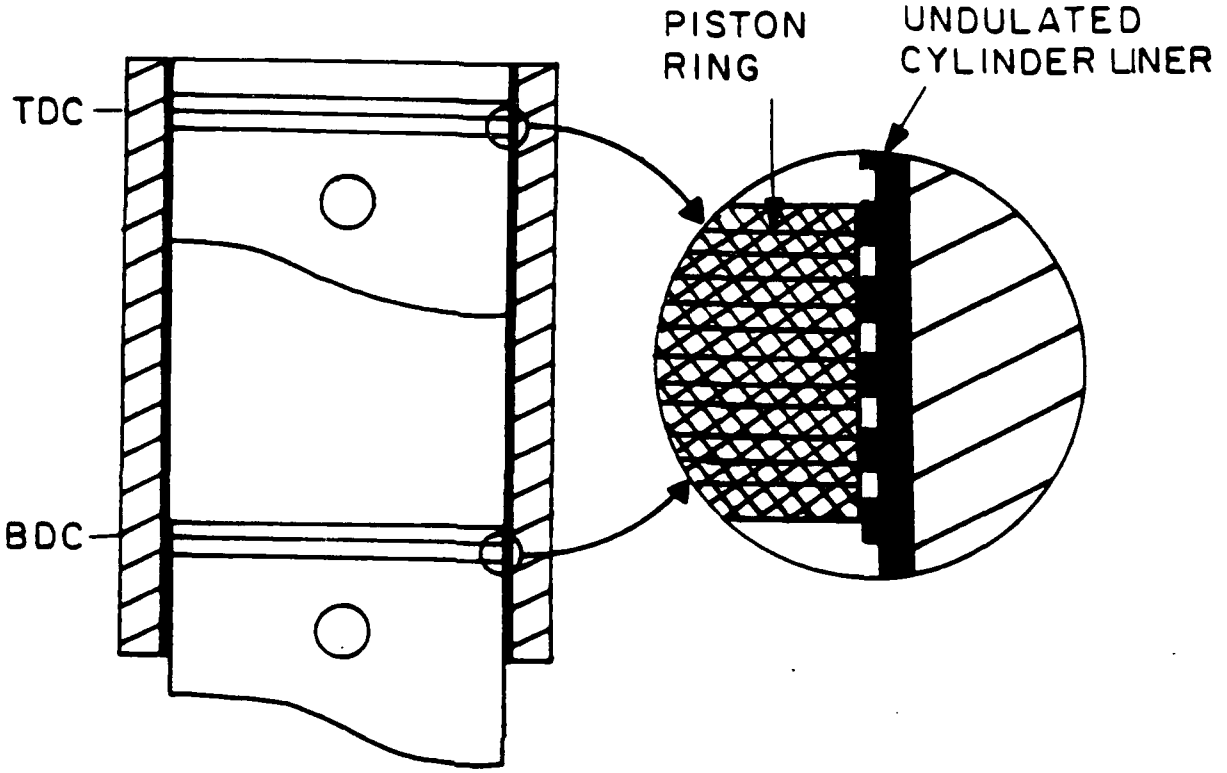

Fig. 15- Schemetic of the proposed design for future IC engine cylinder surface.

commmon problems of modern IC engines that occur as a consequence of lubrication failure along the stroke of the piston. In dry sliding, the undulated cylinders operated for significantly longer sliding distances without excessive increase in friction than the smooth cylinders. However, consistent results were difficult to obtain due to the difficulty of reproducing undulated cylinders of exact dimensions. A fabrication technique which would allow for the production of consistent undulating geometry is thus desirable. Also, for best engine performance, optimization of cylinder surface design with respect to varying lubrication conditions is proposed.

REFERENCES

(1) Carver, D.P. and Johnson, K.A., "The Effect of Bore Finish on Piston Ring Scuffing," Piston Ring Scuffing, Mechanical Engineering Publications Limited for the Institution of Mechanical Engineers, London (1975).

(2) Ishizuki, Y., Sato, F. and Takase, K., "Effect of Cylinder Liner Wear on Oil Consumption in Heavy Duty Diesel Engines," SAE Paper No. 810931, pp. 2794-2803 (1982).

(3) Rogowski, A.R., "Method of Measuring the Instantaneous Friction of Piston Friction of Piston Rings in a Firing Engine," SAE Paper 379F (1961).

(4) Cleveland, A.E. and Bishop, I.N., "Several Possilbe Paths to Improve Part-Load Economy of Park-Ignition Engines," SAE Paper 150A (1960).

(5) Bishop, I.N., "Effect of Design Variables on Friction and Economy," SAE Paper 812A (1964).

(6) Ricardo, H. and Hempson, J.G., The High Speed Internal Combustion Engine," Blackie, London (1968).

(7) McGeehan, J.A., "A Literature Review of the Effects of Piston and Ring Friction and Lubricating Oil Viscosity on Fuel Economy," SAE Paper No. 780673, pp. 2619-2638 (1979).

(8) Curtis, J.M., "Piston Ring Dynamics and Its Influence on the Power Cylinder Performance," SAE Paper No. 810935, pp. 2822-2837 (1982).

(9) Dueck, G.E. and Newman, B.A., "Piston Ring Development Trends in Europe for Off-Highway Applications," SAE Paper No. 810934, pp. 2812-2821 (1982).

(10) Rhode, S.M., Whitaker, K.W. and McAllister, G.T., "A Study of the Effects of Piston Ring and Engine Design Variables on Piston Ring Friction," Energy Conservation Through Fluid Film Lubrication Technology: Frontiers in Research and Design, ASME Publication (1979).

(11) Furuhama, S., Takiguchi, M. and Tomizawa, K., "Effect of Piston Ring Designs on the Piston Friction Forces in Diesel Engines," SAE Paper No. 810977, pp. 3018-3030 (1982).

(12) Daskivich, R.A., "Sensitivity of New-Engine Oil Economy to Cylinder Bore Characteristics," Surface Roughness Effects in Hydrodynamic and Mixed Lubrication, ASME Publication (1980).

(13) Olsen, D.H. and Pullen, G.A., "Engine Wear Protection of SAE 5W-30 Oils," SAE Paper No. 852075, pp. 484-495 (1986).

(14) Rhode, S.M., "A Mixed Friction Model for Dynamically Loaded Contacts with Application to Piston Ring Lubrication," Surface Roughness Effects in Hydrodynamic and Mixed Lubrication, ASME Publication (1980).

(15) Suh, N.P. and Saka, N., "Surface Enginerring," Annals of the CIRP, Vol. 36, pp. 403-408 (1987).

(16) Parker, D.A., Stafford, J.V., Lendrick, M. and Graham, N.A., "Experimental Measurements of the Quantities Necessary to Predict Piston-Cylinder Bore Oil Film Thickness and the Oil Film Thickness Itself in Two Particular Engines," Piston Ring Scuffing, Mechanical Engineering Publications Limited for the Institution of Mechanical Engineers, London (1975).